LONG-TERM ENVIRONMENTAL MONITORING PROGRAM:

2018 SAMPLING RESULTS AND INTERPRETATIONS

JAMES R. PAYNE, PH.D.
WILLIAM B. DRISKELL

AUGUST 2019

PWSRCAC Contract No.
951.19.04

CONTENTS

Cover image – Bountiful intertidal landscape (with 8 species); Disk Island. Photo by William Driskell.

LIST OF FIGURES

LIST OF TABLES

ABBREVIATIONS

Stations:

AMT	Alyeska Marine Terminal, Saw Island, Port Valdez
AIB	Aialik Bay, west of Seward
COH	Constantine Harbor, Hinchinbrook Entrance, PWS (no longer sampled)
DII	Disk Island, Knight Island Group, western PWS
GOC	Gold Creek, Port Valdez
JAP	Jackson Point, Port Valdez
KNH	Knowles Head, eastern PWS
SHB	Sheep Bay, eastern PWS
SHH	Shuyak Harbor, Kodiak
SLB	Sleepy Bay, Latouche Island, western PWS
WIB	Windy Bay, outer Kenai Peninsula
ZAB	Zaikof Bay, Montague Island, central PWS

ABL	Auke Bay Laboratory, NOAA/NMFS, Juneau, Alaska
AHC	Aliphatic hydrocarbons (same as saturated hydrocarbons – SHC)
ANS	Alaska North Slope
APDES	Alaska Pollutant Discharge Elimination System
BTT	Biological Treatment Tank
BWTF	Ballast Water Treatment Facility
cm	Centimeter
DMR	Discharge monitoring report
DW	Dry weight
DWH	*Deepwater Horizon* (oil spill)
EMAP	Environmental Mapping Project, EPA/Cook Inlet Regional Citizens Advisory Council
EMP	Environmental Monitoring Program
EPA	Environmental Protection Agency
EVOS	*Exxon Valdez* oil spill
FSES	Food Safety and Environmental Stewardship, Oregon State University
FT-ICR	Fourier Transform-Ion Cyclotron Resonance mass spectrometer
g	Gram
GC/FID	Gas chromatography/flame ionization detector
GC/MS	Gas chromatography/mass spectrometry
GERG	Geochemical and Environmental Research Group, Texas A&M University
GOA	Gulf of Alaska
GPS	Global Positioning System
KLI	Kinnetic Laboratories, Inc., Anchorage, Alaska
km	Kilometers
L	Liter
LCMS	Liquid chromatography/mass spectrometry
LDPE	Low-density polyethylene
LTEMP	Long-Term Environmental Monitoring Program
m	Meter
MDL	Analytic method detection limit
MGD	Million gallons per day
mL	Milliliter
NIST	National Institute of Standards and Technology
NMFS	National Marine Fisheries Service
NOAA	National Oceanographic and Atmospheric Administration
NPDES	National Pollutant Discharge Elimination System
NRDA	Natural Resource Damage Assessment

OSU	Oregon State University
PAH	Polycyclic (or polynuclear) aromatic hydrocarbons
PECI	Payne Environmental Consultants, Inc., Encinitas, California
PGS	Particle grain size
PSD	Passive sampling device
PWS	Prince William Sound
PWSRCAC	Prince William Sound Regional Citizens’ Advisory Council
QC	Quality control
RL	Reporting level
SAC	Scientific Advisory Committee for PWSRCAC
SHC	Saturated hydrocarbons (same as AHC: n-alkanes + pristane and phytane)
SIM	Selected ion monitoring
SOP	Standard operating procedure
SRM	Standard reference material, NIST
S/T	Sterane/triterpane oil biomarkers
TAS	Triaromatic steroids
TEM	Total extractable materials
TMS	Trimethyl-silane
TOC	Total organic carbon
TPAH	Total PAH
TSHC	Total saturated hydrocarbons (same as total alkanes)
UAF	University of Alaska Fairbanks
UCM	Unresolved complex mixture

RESULTS AND INTERPRETATIONS FROM LTEMP SAMPLING, 2018

EXECUTIVE SUMMARY

The Prince William Sound Regional Citizen's Advisory Council (PWSRCAC) Long-Term Environmental Monitoring Program (LTEMP) was begun in 1993 with the goal of monitoring for environmental impacts from oil transportation activities. The program samples Port Valdez sediments near the Alyeska Pipeline Service Company's Valdez Marine Terminal and at the Gold Creek reference station, as well as intertidal mussel tissues at selected sites in Prince William Sound (PWS) and across the northwest Gulf of Alaska (GOA) region for petroleum hydrocarbon analyses. Within Port Valdez, three stations, Saw Island (AMT) and Jackson Point (JAP) near the terminal, and the Gold Creek (GOC) reference site (6 km across the Port) are sampled annually. Every five years, the Port Valdez stations are augmented by additional mussel sampling along the path of the 1989 *Exxon Valdez* oil spill (EVOS) in Prince William Sound at five stations: Knowles Head (KNH), Sheep Bay (SHB), Disk island (DII), Zaikof Bay (ZAB), and Sleepy Bay (SLB); and along the extended EVOS track at three Gulf of Alaska stations: Aialik Bay (AIB), Windy Bay (WIB), and Shuyak Harbor (SHH). Constantine Harbor (COH) was only sampled for special projects in 2005-2007. This report includes results from the other 11 stations as shown in the table on page two.

LTEMP Station Mussel Samplings*

	Port Valdez			Prince William Sound						Gulf of Alaska		
	AMT	JAP	GOC	KNH	DII	SLB	ZAI	SHB	COH	AIB	WIB	SHH
1993	X		X	X	X	X	X	X		X	X	X
1994	X		X	X	X	X	X	X		X	X	X
1995	X		X	X	X	X	X	X		X	X	X
1996	X		X	X	X	X	X	X		X	X	X
1997	X		X	X	X	X	X	X		X	X	X
1998	X		X	X	X	X	X	X		X	X	X
1999	X		X	X	X	X	X	X		X	X	X
2000	X		X	X	X	X	X	X		X	X	X
2001	X		X	X	X	X	X	X		X	X	X
2002	X		X	X	X	X	X	X		X	X	X
2003	X		X	X	X	X	X	X		X	X	X
2004	X		X	X	X	X	X	X		X	X	X
2005	X		X	X	X	X	X	X	X	X	X	X
2006	X		X	X	X	X	X	X	X	X	X	X
2007	X		X	X	X	X	X	X	X	X	X	X
2008	X		X	X	X	X	X	X		X	X	X
2009	X		X	X	X	X	X	X		X	X	X
2010	X		X	X								
2011	X		X	X								
2012	X		X	X								
2013	X		X	X	X	X	X	X		X	X	X
2014												
2015	X		X	X				X				
2016	X	X	X									
2017	X	X	X									
2018	X	X	X	X	X	X	X	X		X	X	X

*Sediments have been sampled annually at AMT and GOC.

The data are viewed from two perspectives: 1) characterizing the chemical profiles as to the likely source and degradation state of the hydrocarbons, and 2) the concentration of the oil contaminants. There are three groups of petroleum hydrocarbons examined in this data set: polycyclic aromatic hydrocarbons (PAH), saturated hydrocarbons (SHC), and oil biomarkers (sterane/triterpane or S/T). In addition to mussel sampling in 2018, passive sampling devises (PSDs) were deployed by PWSRCAC personnel at the three Port Valdez mussel sites plus Knowles Head and Disk Island. The results from those activities are also presented.

Overall, the petrogenic hydrocarbon (oil) inputs into Port Valdez from the Alyeska Marine Terminal and tanker operations have been declining over the last two decades as reflected in total polycyclic aromatic hydrocarbon (TPAH) concentrations in both mussels and sediments. This trend reflects a combination of reduced Ballast Water Treatment Facility (BWTF) discharge volumes from historically decreased North Slope oil production, the transition to double-hulled tankers with segregated ballast tanks, and improved BWTF efficiency in removing particulate/oil-phase PAH.

As a result, over the last several years, contamination in mussels at AMT has been generally shifting away from the terminal's petrogenic profiles to trace-level background dissolved-phase or pyrogenic (combustion-derived) PAH patterns. A notable exception to this declining trend occurred in September 2017 when an estimated 150 gallons of Alaska North Slope (ANS) crude oil were accidentally released during crude oil loading arm leak testing at Berth 5 of the terminal. As part of the spill monitoring efforts, mussels were collected post-spill from the three Port Valdez LTEMP stations. Pre-spill samples from July 2017 LTEMP collections showed traces of dissolved-phase hydrocarbons and combustion products (TPAH 6-14 nanogram per gram [ng/g] dry weight [DW]) whose signatures could not be attributed to the degraded oil discharges of the terminal's BWTF. In the weeks after the Berth 5 spill event, crude oil was present in the tissues from the adjacent AMT (109-183 ng/g DW) and JAP (21-30 ng/g DW) sites. The reference GOC site across the Port was unaffected (TPAH 4-6 ng/g DW). By December, all three locations had returned to near-background concentrations (2-10 ng/g DW) and patterns, nearly identical to pre-spill profiles.

In June 2018, the tissue hydrocarbon concentrations from all 11 LTEMP stations (from within Port Valdez as well as PWS and the GOA) were all below individual PAH method-detection-limits (MDLs -- in the 0.2-1.0 ng/g DW range) and with TPAH totals reaching all-time lows (TPAH range 4-7 ng/g DW). Except for expected traces of a few combustion products inside Port Valdez at AMT and GOC, the PAH profiles were essentially indistinguishable from laboratory method blanks. At the Gold Creek site, there had been trace evidence of a previous diesel spill in 2016, but in the July 2017 and June 2018 GOC collections there was no evidence of the spill and only trace-level dissolved-phase and pyrogenic profiles were observed. In 2018, the SHC profiles from mussels at all 11 stations showed only biogenic marine plankton and terrestrial plant wax input. These low-level concentrations showed different profiles and were more that 10-times higher than those observed in the corresponding method blanks. Compared to the most recent National Oceanographic and Atmospheric Administration (NOAA) West Coast Mussel Watch data (2004-05) and the more recent 2008-10 Alaska Mussel Watch sites, the 2018 LTEMP mussel-tissue results continue to demonstrate that the sampled region is exceptionally clean. Data from these other studies show 10-1,000 times higher TPAH concentrations than those observed with LTEMP.

The three PSDs deployed at AMT, JAP, and GOC are designed to sample just the more bioavailable, dissolved hydrocarbons. In 2018, all showed a low-level, dissolved PAH profile dominated by heavily-weathered, water-washed naphthalene components plus traces of higher-molecular weight PAH. Alone, they might have suggested an equivocal linkage to the BWTF effluent--as they had in prior 2016 and 2017 collections. However, in 2018, additional PSD deployments outside the Port at Knowles Head and Disk Island returned data with similar levels and profiles. Because KNH is essentially an undisturbed control site and DII is a known residual EVOS oil site, the profiles were expected to be different from the Port samples; however, both profiles were similar to those within Port Valdez. The PSD appear to be acquiring a ubiquitous background of dissolved PAH (i.e., proximity to the BWTF effluent diffuser had little effect on the dissolved PAH patterns). In comparison, the 2018 mussel data, which includes both the particulates as well as dissolved hydrocarbon portions, was also primarily just background level PAH. In summary, the 2018 PSDs and mussel tissues were clean with only background traces of PAH. These concentrations are well below any known toxicity thresholds for sensitive marine organisms and life stages (personal communication, Dr. Sarah Allan).

Results from sediments near the terminal sharply contrasted with the mussel and PSD data as the sediments are still a repository for the BWTF effluent's chronic hydrocarbon inputs. In recent history, Port Valdez sediment TPAH were in a general plateau for 2005-2012, reached all-time, single-digit lows in 2013 and then marginally rebounded in 2016-2018 at both AMT and GOC (around 60 ng/g and 30 ng/g, respectively). The 2016, 2017, and 2018 AMT sediment PAH patterns then shifted from a dominant pyrogenic pattern previously visible in 2011 samples to a mix of pyrogenic and weathered BWTF petrogenic components. Even at these low TPAH levels, the sediment biomarkers (hydrocarbons that are highly resistant to degradation) confirm that from 2011 through 2018, the contaminant source is the BWTF effluent. From the SHC profiles, the terminal's 2018 sediments show a not surprising mixture of marine and terrestrial biogenic components along with higher-molecular-weight (C_{31}-C_{40}) petrogenic waxes at levels seen in 2016 and 2017. Based on these sediment PAH and SHC signatures, the patterns suggest variable or increased low-level inputs of weathered ANS oil plus combustion products from local vessel traffic, runoff, or aerial deposition.

At the GOC reference site, sediment PAH profiles since 2000 have shown a combustion (pyrogenic) pattern with little or no contribution from the BWTF discharge and with concentrations consistently 4-10 times lower than those observed at the terminal. The PAH patterns also differ, dominated by ubiquitous low-level naphthalenes and combustion products. The 2018 sediment PAH patterns and concentrations are essentially identical to the 2016-2017 data. The SHC profiles in GOC sediments continue to be biogenic, reflecting only background inputs of marine biota and terrestrial plant waxes. From the more extensive biomarker data reported in 2016, 2017, and 2018, it appears that, in addition to natural background biomarkers, low-level traces of some ANS-derived biomarkers are accumulating in the GOC sediments, particularly in 2016 and 2017 with a slightly weaker signal in 2018. However, despite the trace levels of ANS-derived biomarkers, there is no evidence of BWTF-derived PAH or SHC accumulation at that site.

In an unfunded pilot project with Bigelow Lab (Maine) using another analytic method, oxygenated hydrocarbons have, for the first time, been documented in the BWTF effluent. These compounds represent the next step in natural degradation of oil. Oxygenation weathering can be either photo-chemically or microbially effected. The microbial process likely dominates in this situation as the BWTF's Biological Treatment Tank (BTT) is operated to optimally facilitate the microbial process. As a result, the effluent appears to have more single- and double-oxygenated hydrocarbons than non-oxygenated SHC and PAH combined. Toxicity of these compounds is mostly unknown but is the subject of ongoing research, particularly following the 2010 *Deepwater Horizon* spill event. We suggest analysis of these compounds in future LTEMP monitoring.

INTRODUCTION

PROJECT HISTORY

The Long-Term Environmental Monitoring Program (LTEMP) data serve to monitor and provide independent quality-control for Alyeska Marine Terminal and tanker operations throughout the Prince William Sound (PWS) and Gulf of Alaska (GOA) region. The primary goal of this on-going Prince William Sound Regional Citizens' Advisory Council (PWSRCAC) program is to monitor impacts from oil transportation activities on the environment at selected sites from PWS and GOA for "as long as the oil flows."

At Alyeska's terminal, the Ballast Water Treatment Facility (BWTF) treats and discharges oil-contaminated ballast water offloaded from tankers utilizing the terminal, so two stations have been traditionally sampled to assess impacts from the effluent: at Alyeska Marine Terminal adjacent to the offshore BWTF discharge diffusers near Berth 4 for sediments and at Saw Island near Berth 5 for mussels (AMT), and at Gold Creek (GOC), a reference station 6 km across the Port (Figure 1) for both sediment and mussels. Another station, Jackson Point (JAP), was added in 2016 near Berth 3, towards the opposite end of the terminal. Currently measured variables include levels of polycyclic aromatic hydrocarbons (PAH) and saturated hydrocarbons (SHC), as well as oil biomarkers in mussel (*Mytilus trossulus*) tissues from the three stations within the Port. Eight additional stations, comprising the geographic reach of the *Exxon Valdez* oil spill (EVOS), are now sampled every five years (2018 was sampled and reported herein) between Valdez and Kodiak (Figure 2).

Sediment samples collected from the two Port stations are analyzed for PAH, SHC, particle grain size, and total organic carbon content, with oil biomarkers added in recent years to confirm petrogenic sources. Sampling and analytical methods are modelled after the protocols developed by the National Oceanic and Atmospheric Administration (NOAA) Status and Trends Mussel Watch Program as fully detailed in previous annual monitoring reports prepared by Kinnetic Laboratories, Inc. (KLI), the Geochemical and Environmental Research Group (GERG), and Payne Environmental Consultants, Inc. (PECI).

Following the first five years of the program, the collective results from the KLI/GERG team were reviewed in a synthesis paper (Payne et al., 1998). At that time, sampling was more extensive and identification of weathered sources was important (Table 5-1 in Payne et al. 1998). The results effectively documented higher background oil levels while identifying hot spots and both large and small spill events. Subsequently, the PWSRCAC reduced the scope of the program from triannual to just spring and summer sampling of regional mussel tissues and Port Valdez sediments. Fall mussel sampling (without sediments) was then re-added just in Port Valdez (AMT and GOC) to better track the terminal's discharge. Mussel-tissue SHC analyses that were dropped from the original program in 1995 (due to results being confounded by lipid interference) were reinstated in 1998 using improved laboratory methods.

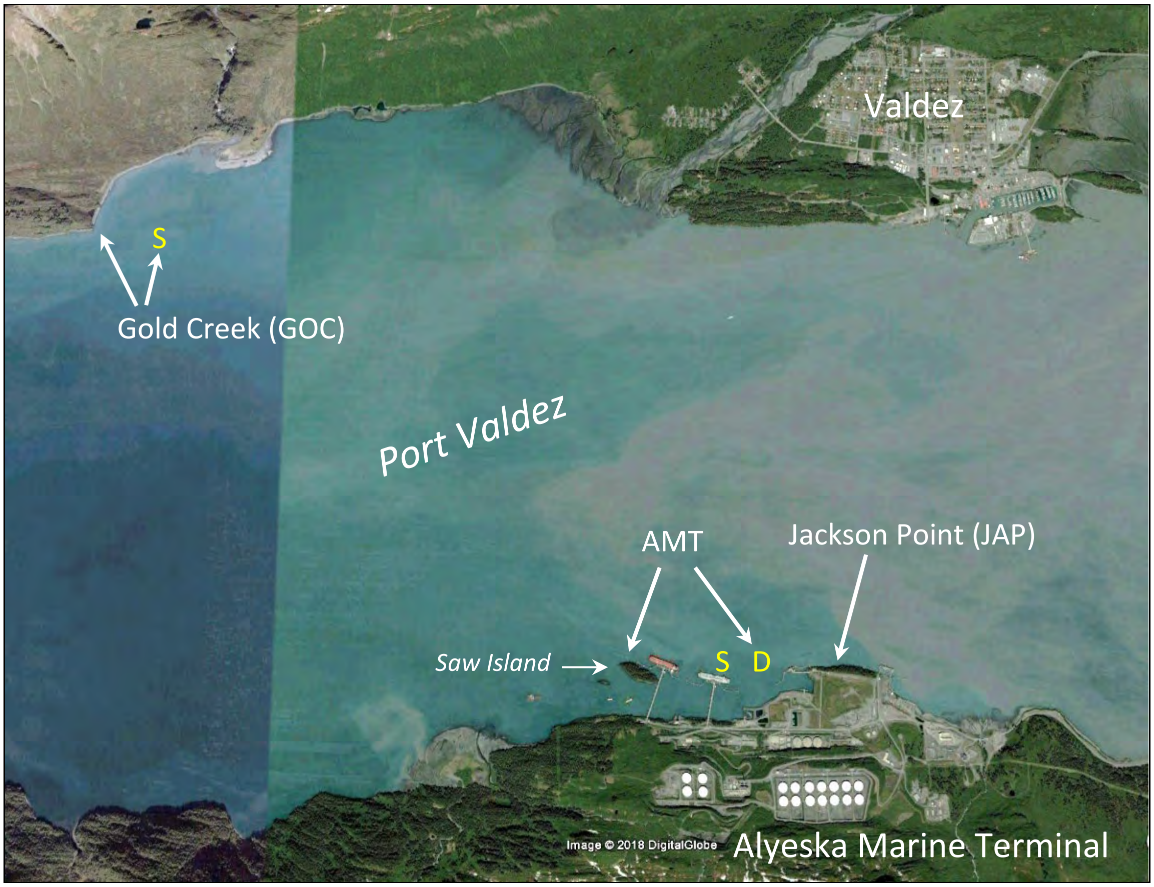

Figure 1. LTEMP sampling stations in Port Valdez adjacent to (AMT and JAP) and 6 km northwest (GOC) of the Alyeska Marine Terminal. This Google Earth image shows tankers docked at both Berth 4 and 5. The yellow "D" denotes the offshore location of the BWTF Biological Treatment Tank diffuser; yellow "S" indicates sediment grab locations at AMT and GOC. The JAP station was added in summer 2016.

In 2001, another comprehensive data evaluation and synthesis was completed on just the Port Valdez sites' LTEMP results (Payne et al., 2001). From AMT and the GOC reference site, Alaska North Slope (ANS) crude oil residues from the terminal's BWTF were shown to accumulate in the intertidal mussels. However, the sediment and tissue (and the estimated water-column) PAH and SHC levels were very low.

More importantly, the pattern and trend of signatures suggested a novel transport/exposure mechanism; discrimination of particulate (oil droplet) and dissolved-phase signals in the water column correlated with seasonal uptake in Port Valdez mussels (Payne et al., 2001). Stratified waters formed during the milder seasonal winds of late-spring/summer kept the discharge plume's particulate oil-phase droplets from the surface but dissolved-phase components could be observed in the intertidal mussels. The wind-mixed, non-stratified waters of fall/winter allowed some portion of the plume's particulate/oil phase to surface, which was then visible in the mussel tissues. The results suggested a surface microlayer mechanism may be responsible for seasonal transport of ANS weathered oil residues from the BWTF diffuser to intertidal zones across the fjord. Combined with other study results showing toxic absorption in herring eggs at trace levels, the authors warned that the potential for photo-enhanced toxicity of concentrated contaminants in a surface microlayer should be considered in future impact investigations (Payne et al., 2001, 2003a, 2003b, 2005c).

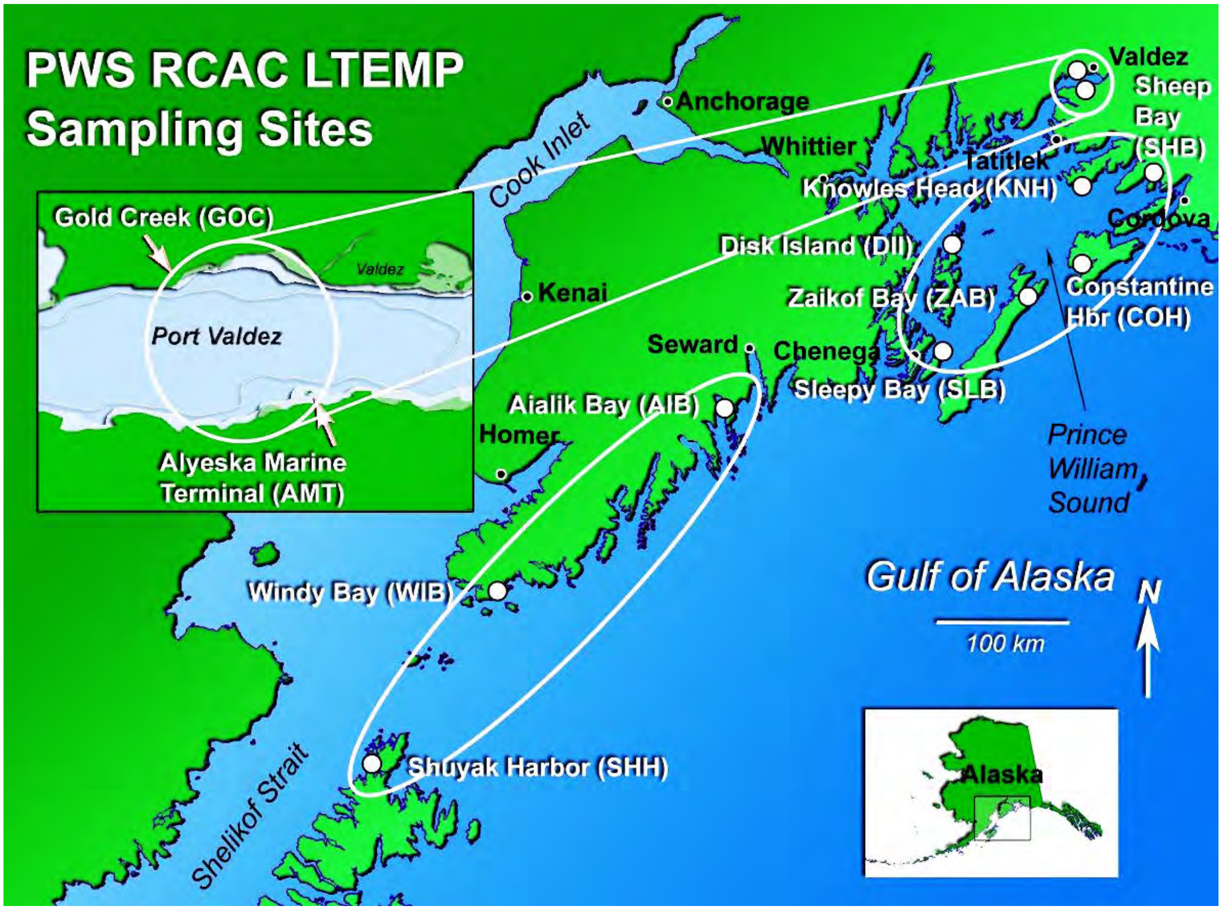

Figure 2. Map of the LTEMP sites. Circled regions represent sites with similar hydrocarbon signatures and events.

In July 2002, PECI and the NOAA/National Marine Fisheries Service (NMFS) Auke Bay Laboratory (ABL) began collecting and analyzing the LTEMP samples. Changing laboratories can be problematic; detailed discussions of the transitional 2002/2003 LTEMP samples and inter-laboratory comparisons of split samples and Standard Reference Materials (SRMs) analyzed by both GERG and ABL are presented in Payne et al. (2003b). The results from the 2003/2004 LTEMP and a comprehensive review and synthesis of all analyses completed since the beginning of the program are available in Payne et al. (2005a, 2006, 2008a). Results and discussion of the program through 2006 were also published in *Marine Pollution Bulletin* (Payne et al., 2008b).

The program again changed analytical services in 2016 when ABL closed its hydrocarbon facilities in Juneau, Alaska. This necessitated a switch to Alpha/NewFields in Mansfield, Massachusetts as the PWSRCAC contract laboratory for LTEMP. Alpha/NewFields was the primary laboratory used by NOAA and other State and Federal Trustees for the 2010-2016 Natural Resource Damage Assessment (NRDA) effort following the BP *Deepwater Horizon* oil spill (Driskell and Payne, 2018a, 2018b; Payne and Driskell, 2017a, 2018a; Stout and Payne, 2016a, 2016b, 2017; Stout et al., 2016a, 2016b). For that event, Alpha/NewFields analyzed ~30 thousand sediment, water, and tissues samples, all with independent, third-party quality control (QC) validation as part of that litigation-sensitive effort. The LTEMP lab transition also involved performance-based round-robin intercalibration programs in which both ABL and Alpha/NewFields participated to demonstrate they were generating comparable data with known precision, accuracy, method detection limits, and representativeness.

Prior to this report, all 10 LTEMP sites were most recently visited in July 2008, April 2009, and then, beginning the reduced effort, 5-year interval scheme, in July 2013 (Executive Summary table, Figure 2). Visits included three northeast sites in or near the Port to monitor terminal and tanker operations, six others to monitor the more remote sites for lingering EVOS impacts, plus Sheep Bay (SHB) which serves as a non-EVOS-impacted control. Initially, to more thoroughly monitor Port operations, LTEMP collections had been taken tri-annually at the two Port sites and nearby Knowles Head (KNH) but efforts were later reduced to annual sampling. Under this modified plan, in 2015, sampling occurred at four of the 10 LTEMP stations: AMT, GOC, KNH, and SHB (Payne et al., 2016). In 2016, another mussel sampling site was added at JAP near the terminal (Figure 1) but east of the active berths and the traditional station at Saw Island (AMT). The JAP site was meant to evaluate a potential PAH gradient to either side of the BWTF outfall and to correlate tissue data with trial passive-sampling devices (PSDs) that were concurrently deployed subsurface at the same terminal locations (Minick and Allan, 2016; Allan, 2018).

In 2018, all three Port Valdez sites were sampled along with additional mussel sampling in Prince William Sound at five stations: KNH, SHB, Disk island (DII), Zaikof Bay (ZAB), and Sleepy Bay (SLB); and outside in the GOA at three stations: Aialik Bay (AIB), Windy Bay (WIB), and Shuyak Harbor (SHH). This report interprets mussel hydrocarbon data from all 11 stations and Port Valdez sediment chemistry from two sites.

Recent years have brought change to both the system and the environment as pipeline throughput has dropped from 85.3 million gallons per day (MGD) at its peak in 1988 to current levels of 21.4 MGD (Table 1). Likewise, tanker regulations have instituted double-hulled tankers with segregated ballast. Aboard segregated-ballast vessels, empty cargo tanks are typically used for supplemental ballast only when operationally necessary (e.g., during winter storms), (i.e., the normal segregated ballast waters are uncontaminated seawater that do not require treatment for hydrocarbons). Treated-ballast water discharges to the Port have also swung from a maximum of around 15 MGD in 1990 to currently only 1.1 MGD (Table 1). Facility operators estimate, and Alyeska's Discharge Monitoring Report (DMR) data confirm, that more than half of the current BWTF effluent discharge in summer is from the terminal's stormwater runoff (Rich Loftin, personal communication, 2016). In summary, less tanker traffic, cleaner ballast, and an improved ballast-water-treatment configuration at the Alyeska terminal have resulted in substantial reductions in detected hydrocarbon concentrations and composition in the field samples. All discharges are made under an Alaska Pollutant Discharge Elimination System (APDES) Permit for which the PWSRCAC submitted detailed reviews during the last three permit renewal cycles (Payne et al., 2003c and 2012, PWSRCAC, 2019).

Table 1. Recent average throughout of Alyeska Pipeline and ballast water treatment.

	2015	2016	2017	2018	
Pipeline throughput	20.6	21.8	22.3	21.4	M gal/day
BWTF throughput	1.10	1.00	0.88	1.11	M gal/day

METHODS

Collection and analytical methods have been described in previous LTEMP reports (Payne et al., 2003b, 2005a, 2006, 2008a, 2010a, 2013, 2015, 2016; Payne and Driskell 2017b, 2018c). Briefly, three replicates of 30 mussels are collected by hand at each site while triplicate sediment samples are collected from the two Port locations (AMT and GOC) using a modified Van Veen grab. Sampling protocols have remained the same but as noted above, Alpha Analytical Laboratory (Mansfield, MA) under the guidance of NewFields Environmental Forensics Practice (Rockland, MA) now provides the analytical services.

The usual hydrocarbon data are reported: polycyclic aromatic hydrocarbons (PAH), sterane/triterpane biomarkers (S/T), and saturated hydrocarbons (SHC). Semi-volatile compounds, the PAH, alkylated PAH, and petroleum biomarkers, are analyzed using selected ion monitoring gas chromatography/mass spectrometry (SIM GC/MS) via a modified Environmental Protection Agency (EPA) Method 8270 (aka 8270M). This analysis provides the concentration of 1) approximately 80 PAH, alkylated PAH homologues, individual PAH isomers, and sulfur-containing aromatics and 2) approximately 50 tricyclic and pentacyclic triterpanes, regular and rearranged steranes, and triaromatic and monoaromatic steroids. Complete lists of PAH, SHC, and biomarker (S/T) analytes are presented in Appendix 1 along with the analyte abbreviations used in figures throughout this report.

Using a modified EPA Method 8015B, SHC in sediments are quantified as total extractable materials (TEM; C_9-C_{44}) and as concentrations of n-alkanes (C_9-C_{40}) and selected (C_{15}-C_{20}) acyclic isoprenoids (e.g., pristane and phytane). A high resolution gas chromatography-flame ionization detector (GC/FID) fingerprint of the sediment samples is also provided. However, due to contractual omissions along with concerns that potential lipid interference and anticipated below analytic method detection limit (MDL) concentration issues might occur with GC/FID, SHC analyses of tissues were not performed by Alpha Analytical on the 2016 and 2017 tissue samples. However, later examination of selected ion monitoring (SIM) plots of *m/z* 85 ions acquired during tissue biomarker analyses demonstrated that the aliphatic hydrocarbons (SHC) actually were present at high enough concentrations to allow GC/FID measurement. SHC analyses using GC/FID were reinstated for tissue analyses with the 2018/2019 Program.

Low-density polyethylene (LDPE) PSDs were deployed for ~30 days and retrieved following protocols used at Oregon State University (OSU) per previous research efforts (Sowers et al., 2008, Huckins et al., 2006, O'Connell et al., 2013). Laboratory handling, sample extraction and analyses of the PSDs followed respective OSU, Food Safety and Environmental Stewardship (FSES) Program Standard Operating Procedures (SOPs).

Analytical chemistry results are presented as bar plot profiles for each analyte; however, the bars for alkylated PAH actually represent the sum of alkylated homologue components. For example, C1-naphthalene, a two-ringed compound with one attached methyl group has two isomer forms that are individually assessed at the lab but reported and plotted as a combined sum; C2-naphthalene (with two attached methyl groups or one ethyl group) has 12 isomers, and C4-chrysene has 1,016 isomers. Each are summed into one value for the bar plots. Also, as described in each figure caption for sample profiles in this report, some appropriate reference (e.g., the summer BWTF-effluent profile or ANS source oil) is depicted as a reference line scaled and overlaid on the selected individual tissue or sediment's profile. MDL overlays are shown for selected time-series data profiles and are shown for all 2018 samples in Appendix 2. Details of our BWTF-effluent sampling and analytical procedures and the importance of differentiating between dissolved and particulate/oil phases are presented in Appendix 2 of Payne and Driskell (2017b).

BIOMARKERS

A recent addition to the LTEMP suite of analytes, petroleum biomarkers are conservative, weathering-resistant, hydrocarbon compounds, unique to each oil formation. For LTEMP, biomarkers can facilitate and confirm detection of AMT-derived, Alaska North Slope crude-oil constituents in Port sediments – even when the PAH are degraded. The objective of using biomarkers is to look at the hydrocarbon signatures using less degradable analytes than the SHC and PAH. In the environment, the SHC are quickly consumed by microbes, giving forensic reviewers a perspective of "freshness" of crude oil patterns while also distinguishing petroleum distillates (diesel vs. fuel oil vs. crude oil, etc.), plus tagging contributions from other (primarily biogenic) sources. PAH compounds are more persistent, weathering slower in predictable patterns and rates, which serve to track longer-term fate, behavior, and mixing with other sources.[1] In contrast, the biomarkers are the hydrocarbon "tattoos," enduring telltales of oil's presence even as the PAH and SHC patterns are weathering and disappearing.

In 2016, 2017, and 2018, biomarkers were analyzed on both sediments and tissues. For routine monitoring, however, mussel tissues biomarkers are generally less effective than in sediments as the mussels regularly purge and, currently, at most LTEMP stations only carry trace-level, dissolved-phase and combustion-derived PAH components (i.e., no biomarkers). Water-insoluble biomarkers would only be detected in tissues when particulate oil was present (e.g., free oil droplets from a recent or chronic release such as the September 2017 Alyeska Berth 5 oil spill) (Payne and Driskell, 2018b).

Multiple approaches have been suggested for interpreting biomarker data, but some degree of expert-guided pattern matching must be employed. Most schemes involve various diagnostic ratios (Stout and Wang, 2016) with several ratios normalized to the highly conservative 17α(H),21β(H)-hopane (also labeled T19 or C30 hopane and herein marked with a golden fill color for visual reference in bar plots). But despite the purported persistence of biomarkers, depending on the local environs and microbial adeptness, all ratios are not equally effective and must be individually evaluated for a given spill/habitat. For interpreting LTEMP data, we initially screen PAH and biomarker results graphically with an ANS reference overlay normalized to the sample's hopane. For biomarkers, the frequently reliable, Ts/Tm and norhopane (T15)/hopane ratios were used to confirm the visual similarities. For this report, we utilize all appropriate and available ratio data and present the overall patterns to facilitate their interpretations.

RESULTS AND DISCUSSION

LABORATORY QUALITY CONTROL

All Alpha/NewFields-analyzed analytes (Appendix 1) are reported on a ng/g dry weight (DW) basis uncorrected for blanks or surrogate recoveries. Surrogates are novel or deuterated compounds added in known amounts to each raw sample in order to assess, by their final percent recovery, the efficiency of extraction and analysis. Surrogate recoveries are considered acceptable if they are between 40% and 120%. A single recovery deviance flags the sample with cautionary remarks; multiple recovery deviations would require batch reanalysis. Surrogate recovery standards were met for all PAH, biomarker and alkane surrogate hydrocarbons analyzed during the 2018 reporting period (Table 2). Laboratory method blanks for each analytic sample batch demonstrated nominally-acceptable (sub-ng/g) laboratory or analytic background PAH interference.

Mussel-tissue hydrocarbon levels are now so low throughout the study region that individual PAH were reported at below-MDL concentrations and patterns in both tissues from all 11 stations and their associated laboratory/method blanks. At these exceptionally low PAH levels, it is not possible to assure that the measured analytes in the field samples actually represent environmental constituents. In addition, some matrix interferents were flagged for two sediment biomarkers, T26 and T32, in their lab qualifiers. As obvious anomalies, they were ignored for sediment data-pattern interpretations. Per our standard forensic reporting practices, the data discussed herein are neither blank-corrected nor surrogate-recovery-corrected and are reported as raw data (with below-MDL values flagged as estimated). All of the PAH, biomarker, and SHC profiles presented in Appendix 2 are shown with their analytical-batch-associated method blanks along with sample-specific MDLs overlaid on the histogram profiles.

---

[1] For readers who are not familiar with oil-spill fingerprinting or forensics, see Appendix 6 in our 2015 LTEMP Report (Payne et al., 2015) for a background primer specific to ANS crude oil, combustion products, and other potential oil sources in Port Valdez and the PWS/GOA region. Additional details are available in Stout and Wang (2007 and 2016).

Table 2. Surrogate recovery statistics by matrix from 2018 Alpha Laboratory analyses.

Matrix	Surrogate	Average (%)	Max	Min	Std Dev	Count
Sediment	Naphthalene-d8	70	79	62	6	9
	Phenanthrene-d10	87	97	81	6	9
	Benzo[a]pyrene-d12	71	84	55	9	9
	5B(H)Cholane	108	111	105	2	9
	ortho-Terphenyl	97	107	91	6	9
	d50-Tetracosane	98	107	93	5	9
Tissue	Naphthalene-d8	85	99	70	7	35
	Phenanthrene-d10	97	103	89	3	35
	Benzo[a]pyrene-d12	95	99	88	3	35
	5B(H)Cholane	110	128	97	9	35

METHOD DETECTION LIMITS

One lab-performance QC measure is the EPA-formulated, statistically-derived, analyte-specific, MDL that EPA defines as “the minimum measured concentration of a substance that can be reported with 99% confidence that the measured concentration is distinguishable from method blank results.” Alpha Analytical Laboratory’s MDLs for hydrocarbons exceed the performance of most commercial labs, falling within the accepted stricter levels for forensic purposes (Table 3).

Table 3. Alpha Analytical MDL target ranges.

Analytes	Sediment (30 g, sample size)	Tissue (15 g sample size)	Water (1 L sample size)	Oil Reporting Level (RL)
PAH and biomarkers	0.1-0.5 ng/g DW	0.2-1.0 ng/g DW	1-5 ng/L	2.0 µg/g
SHC	0.05 µg/g DW	NA	0.8 µg/L	200 µg/g

For data interpretation, there are generally two approaches on use of MDLs: 1) censor all below-MDL data to some pre-decided level (which leads to further issues on how to interpret partially-censored, multi-analyte data sets such as LTEMP) or 2) treat below-MDL data as estimated real values. For reasons described below, it is felt that the second option best serves the purpose of the LTEMP program. For both the readers and our benefit in reviewing data, individual analyte MDLs (adjusted to sample weight) appear as red dotted lines on PAH and SHC plots where appropriate in report figures and in all sample plots presented in Appendix 2.[2]

By definition, EPA’s MDL protocol is designed to control against false positives at the 99% confidence level in an ideal matrix. In other words, MDLs are meant to represent a trustworthy value of low detection, below which, due to expected uncontrolled factors, lower results are not as reliable—the values are estimates of lesser confidence. This reporting bulwark is certainly required when reviewing a crucial single-analyte result (e.g., water arsenic

---

[2] For forensics evaluations, PAH, SHC, and S/T plots in the main body of this report are typically shown with dotted-red-line overlays corresponding to the relevant source oil or BWTF effluent.

concentrations, where the statistically determined MDL value ensures against toxic consequences). There are two differences between this example and the LTEMP dataset.

First, there are no “critical values” involved in the current LTEMP data review; false positives will not affect the overall findings of “PAH are dropping to lower historic lows.” While the MDL procedure is designed to avoid false positives at the 99% confidence level; if a lower confidence level is acceptable, then MDL levels are unnecessarily stringent for the application.

Secondly, because LTEMP data interpretations are based on multi-analyte patterns rather than single values, additional confidence accrues from “pattern expectations.” Conceptually, the more information known about a system or data set, the higher the confidence when seeing recognizable patterns. Such is the case with LTEMP data. Oil weathers predictably (see Appendix 6 in Payne et al., 2015) and if a sample’s PAH profile appears to represent a recognizable pattern, then applying the statistically established, single-analyte MDLs to censure the data would be more conservative than necessary. For example, if a sample’s phenanthrenes/anthracenes (P/As) were reported above MDL levels while dibenzothiophenes and chrysenes (DBTs and Cs) were reported below MDLs but in the same pattern and ratio as the source oil, there would be sufficient confidence in the expected patterns that those detected analytes, albeit below-MDL, were not false positives and that the values had been reasonably estimated. In past LTEMP efforts, this added-confidence attribute was further bolstered in near-trace-level LTEMP data by seeing higher-level patterns of within-site fidelity and regional-wide commonalities that collectively changed between years—which could only occur if the patterns were real and not false positives from lab or procedural artifacts (e.g., see Appendix 3 in Payne et al., 2015). In LTEMP data, MDLs mainly serve to tag when reported values have become, to some degree, estimated. Conversely, when an unrecognizable pattern or anomalous spike appears, it is easily spotted, flagged as an outlier, and closely examined along with any corroborating evidence (e.g., lab QC and field notes) to see if it makes any sense or is indeed a lab, sampling, or field anomaly.

In the 2018 mussel-tissue samples, however, similar trace-level, below-MDL PAH patterns were observed in all the field samples and their batch-associated laboratory method blanks. With these PAH data, source-identifications based on pattern recognition are not possible; it can only be reported that the individual and total PAH (TPAH) concentrations are below a background level.

Alyeska Marine Terminal BWTF Effluent Sampling and Analyses

The primary source of oil contamination in Port Valdez has historically been the partially degraded, ANS crude oil discharged from the Alyeska Marine Terminal’s BWTF. Last analyzed in 2004-2005 prior to current low production levels and the BWTF redesign (Payne et al., 2005b, 2005c), re-sampling the effluent was added as an element to the 2016/2017 program. Sampled during July 2016, the effluent turned out to be nearly 80% freshwater, an unexpectedly low salinity value that reflects the collected runoff from the terminal and smaller treated tanker-ballast volumes during the summer months. Anticipating less runoff and more ballast water in the system during winter operations, effluent samples were again collected in March 2017.

As expected, compared to the summer samples, winter effluent had higher TPAH values (7,605 ng/L vs. 2,885ng/L), and were less weathered and biodegraded relative to initially fresh ANS crude oil (red line overlay in Figure 3). During winter, more frequent and stronger winter storms necessitate additional ballast in the tanker cargo holds and thus, higher volumes and throughput for the BWTF. Also, there is reduced freshwater runoff at the terminal during the colder winter months. In both seasons, however, particulate/oil-phase droplets were present in the effluent (Figure 4) at similar concentrations and with essentially identical degrees of weathering. At the same time, the winter Biological Treatment Tank (BTT) effluent sample had a much higher proportion of bioavailable, dissolved-phase components (Figure 5). It must be cautioned that this profile “snapshot” of the BWTF winter operation occurred as the BTT was recovering from a shutdown from an overnight power outage; the profile may be unknowingly biased as normal conditions were reestablished.

Lower-molecular-weight SHC are subject to both dissolution/evaporation losses and microbial degradation (NAS 1975, 1985, and 2003). In a sample’s profile, microbial degradation processes initially appear as decreases in the more easily assimilated n-alkanes, n-C_{17} and n-C_{18}, relative to the branched-chain isoprenoids, pristane and phytane. In the BWTF’s BTT, particulate/oil-phase SHC are well degraded by the combined abiotic and microbial processes and in summer vs. winter, partially due to the longer summer residence-time within the tank (Figure 4, Table 4). The lower summer BTT throughput actually requires facility operators to retain and recycle a portion of the BTT contents just to keep the biological system active. The two SHC isoprenoids, pristane and phytane, are degraded slower than their straight-chain alkanes, C_{17} and C_{18}. Thus, the reduced n-C_{17}/pristane and n-C_{18}/phytane ratios for the oil-phase droplets in the BTT effluent (Table 4) indicate they have undergone extensive microbial degradation compared to fresh ANS oil.

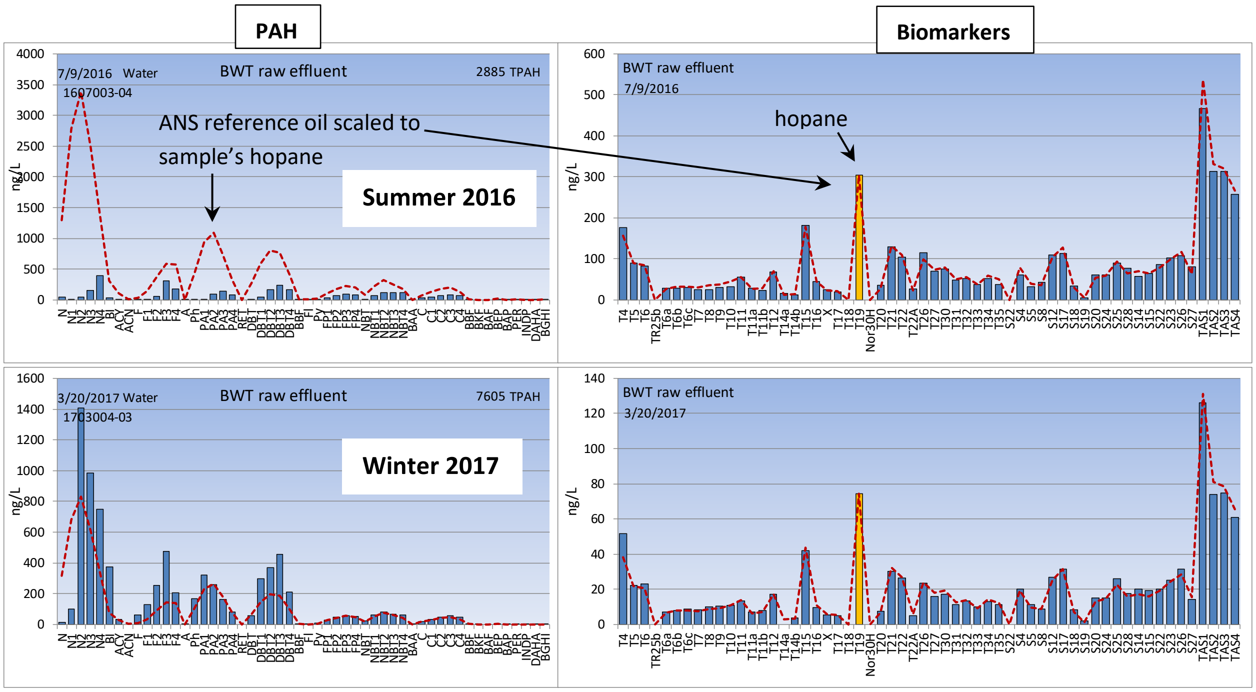

Figure 3. PAH and biomarker profiles (ng/L) of raw (unfiltered) BWTF-BTT effluent samples from July 2016 (upper plots) and March 2017 (lower plots). The dotted red line represents an overlay of fresh ANS crude oil normalized (scaled) to hopane (colored gold in the biomarker profiles). Excess dissolved PAH constituents present in 2017 as analytes above the source reference line.

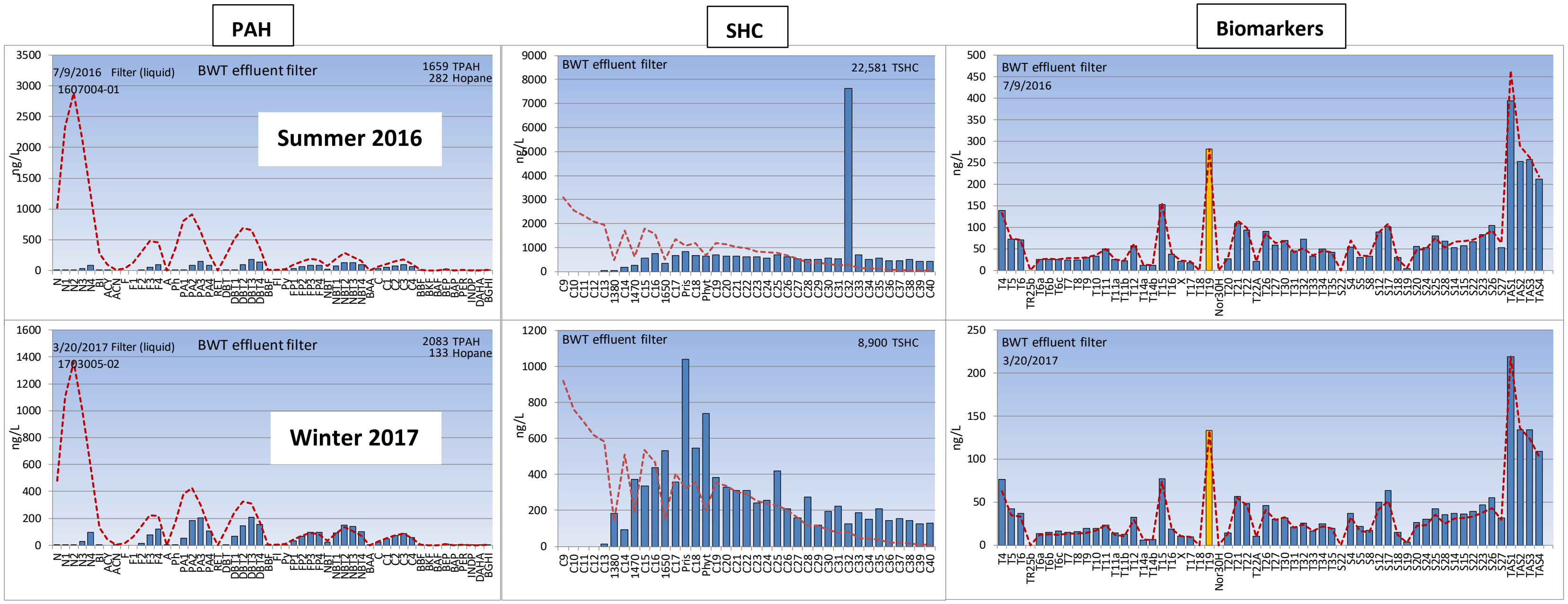

Figure 4. PAH, SHC, and biomarker profiles (ng/L) of the filtered, particulate/oil-phase droplets in the BWTF-BTT effluent. The red line overlay represents fresh ANS scaled to the sample's hopane (colored gold in the biomarker plots). The gaps between the measured PAH and the overlay portray the extent of abiotic (evaporative) and biotic weathering. The TPAH concentrations are very similar but there is additional loss of the higher-molecular-weight (FPs, NBTs, and Cs) due to biodegradation in the summer but not the winter sample. Biomarkers show essentially no degradation relative to fresh ANS (right plots) during either season. SHC show losses of lower-molecular-weight C_9 through C_{15} components (middle plots) due to a combination of evaporation and dissolution processes as well as selective straight-chain n-alkane microbial degradation relative to branched-chain isoprenoids (Table 4). In 2016 SHC, C_{32} is a matrix interferent so the SHC are instead scaled to C_{27}.

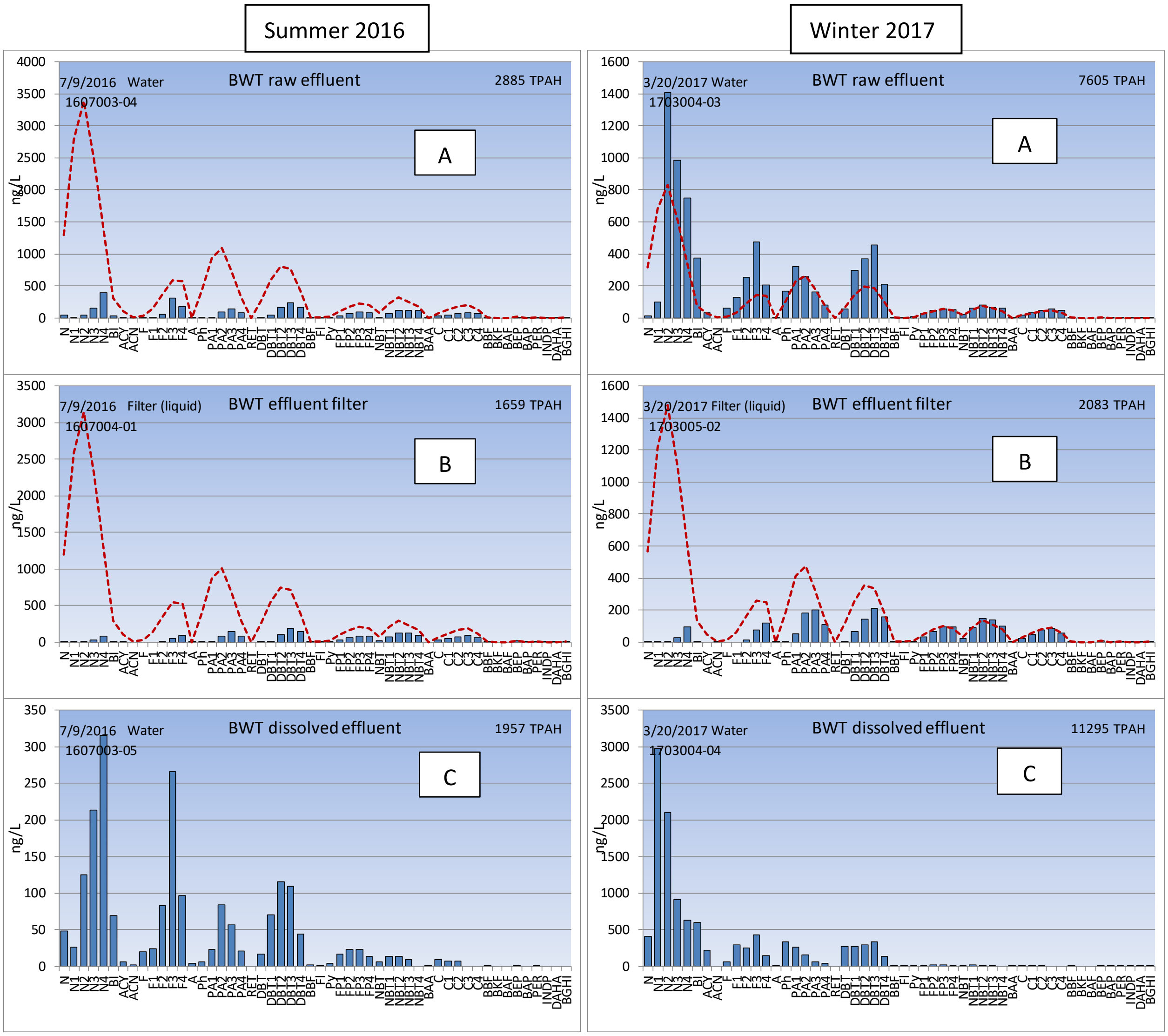

Figure 5. PAH profiles of BTT effluent samples collected under summer (July 2016) and late winter (March 2017) conditions: A) whole unfiltered sample; B) particulate/oil phase trapped on the glass-fiber-filter; and C) dissolved phase. The dotted red line in A and B represents fresh ANS crude oil PAH profile normalized to hopane to show evaporation and dissolution effects on lower-molecular-weight PAH (C is all dissolved and doesn't have a reference pattern overlay on it (i.e., no hopane for scaling)).

Table 4. Ratios of n-C$_{17}$/pristane and n-C$_{18}$/phytane for July 2016 and March 2017 BTT effluent samples (concentrations in ng/L). Lower ratios indicate extent of microbes preferentially degrading the alkanes over the isoprenoids, pristane and phytane.

	n-C$_{17}$	**pristane**	**Ratio**		**n-C$_{18}$**	**phytane**	**Ratio**
ANS Crude Oil	3060	2190	1.40		2710	1410	1.93
July 2016 BTT							
Raw effluent	813	944	0.86		602	662	0.91
Particulate phase	658	836	0.79		682	642	1.06
Dissolved phase	243	0	n.a.		0	0	n.a.
March 2017 BTT							
Raw effluent	1200	1370	0.88		1140	716	1.59
Particulate phase	359	1040	0.35		548	739	0.74
Dissolved phase	0	290	n.a.		500	189	2.65

PORT VALDEZ SEDIMENTS

SEDIMENT TPAH TRENDS 1993-2018

Note that we consider TPAH concentrations to be a very rough proxy of oil contamination (like discussing weather but only talking about the temperature); a truer picture is in the profile interpretations (discussed below). But for historical and trend perspectives, TPAH concentrations are presented. With TPAH levels dropping from historic highs in the hundreds if not thousands of ng/g DW between 1993 and 2004 (including a spike in 1995 from the *Eastern Lion* tanker spill at the terminal), average sediment TPAH concentrations at the 68-72m deep terminal Berth 4 site plateaued at around 50-60 ng/g (DW) from March 2005 through April 2012 (Figure 6). Then in 2013, concentrations dropped further to all-time lows around 10 ng/g. Sediment samples were not collected in 2014 due to a temporary hiatus in the program but in July 2015, the TPAH concentrations at the terminal rebounded slightly to around 30 ng/g and further up to a range of 55 – 80 ng/g between 2016 and 2018 (Table 5 and Table 6). Sediment TPAH trends at GOC have generally tracked with those observed at the terminal (Figure 6), but the concentrations are usually 4-10 times lower, now around 20 ng/g since 2016 (Table 5 and Table 6).

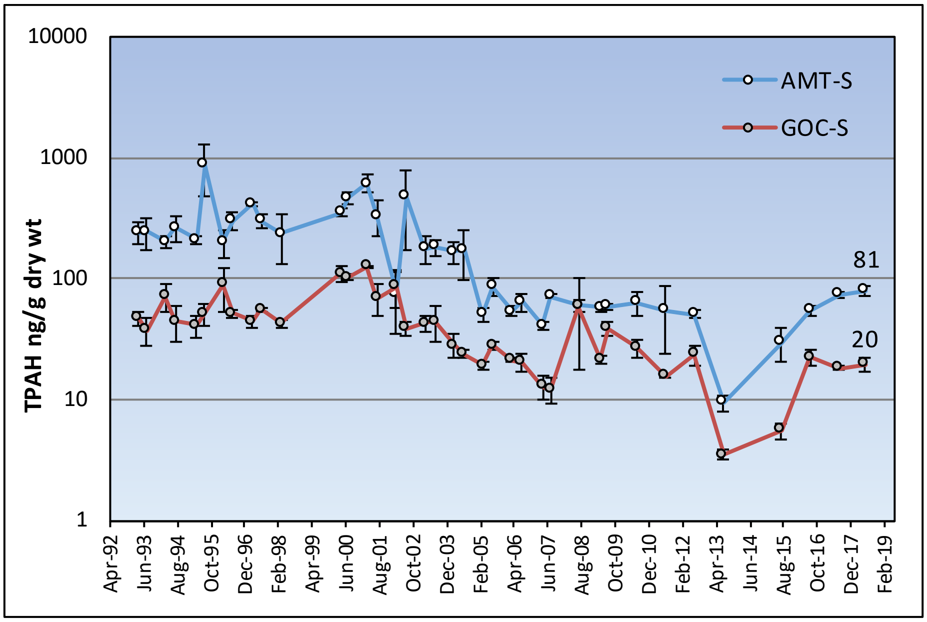

Figure 6. Time series of log (TPAH43) in sediments at AMT and GOC. Error bars are ± SE of means.

Table 5. Summary statistics for 2018 TPAH50 concentrations (ng/g DW).

2018	avg	max	min	count	± SE
AMT-S	80.7	89.7	66.4	3	7.25
GOC-S	19.8	23.6	14.9	3	2.55

Table 6. Historic average sediment TPAH43 values (ng/g DW), 2000-2018.

	AMT-S	GOC-S		AMT-S	GOC-S
Apr-00	353	111	Mar-06	54	21
Jul-00	472	103	Jul-08	61	60
Mar-01	614	126	Apr-09	59	22
Jul-01	335	69	Jul-09	60	40
Mar-02	76	86	Jul-10	64	28
Jul-02	480	39	Jul-11	55	16
Mar-03	179	43	Jul-12	51	24
Jul-03	184	45	Jul-13	9	3
Mar-04	167	28	Jul-15	30	6
Jul-04	175	24	Jul-16	55	23
Mar-05	51	19	Jul-17	74	18
Jul-05	86	28	Jun-18	80	20

SEDIMENT BIOMARKERS

Biomarkers' persistence in the BWTF effluent facilitates tracking ANS signals in the surrounding sediments. Conceptually, as small oil droplets are discharged with the effluent, they readily adsorb onto waterborne suspended particulates (e.g., glacial flour) and eventually settle to the seafloor where microbial degradation and dissolution weathering of the SHC and PAH continue. In an example profile, when the PAH are plotted with a fresh ANS overlay scaled to the sample's hopane (Figure 7, top), the individual components almost completely disappear suggesting nearly complete loss of PAH due to *in situ* weathering during or after sedimentation. And while there is some degradation of the biomarkers as shown by the small gaps between the hopane-normalized ANS profile and the individual components, a sufficient profile exists to still positively assign the signal to the BWTF effluent. The biomarker losses are consistent with microbial degradation and abiotic dissolution weathering/dilution on particulate-phase oil droplets released from the diffusers. Similar losses, including microbial degradation of selected C_{28} and C_{29} tricyclic terpanes, S4 and S5 diasteranes, S14 and S15 steranes, plus (previously unknown) abiotic dissolution losses of the triaromatic steroids (TAS) compounds were observed from particulate-phase oil during transport and sedimentation following the *Deepwater Horizon* blowout in the northern Gulf of Mexico in 2010 (Stout and Payne, 2016b; Payne and Driskell 2015a, 2018a). For illustration, when the PAH and biomarker data are re-scaled to the measured NBT2 rather than the hopane in the sample (Figure 7, bottom plots), an excess of biomarkers appears above the fresh ANS overlay, demonstrating the proportion of accumulated, more recalcitrant biomarkers and the higher-alkylated NBT and chrysene homologues in the near-diffuser sediments over time.

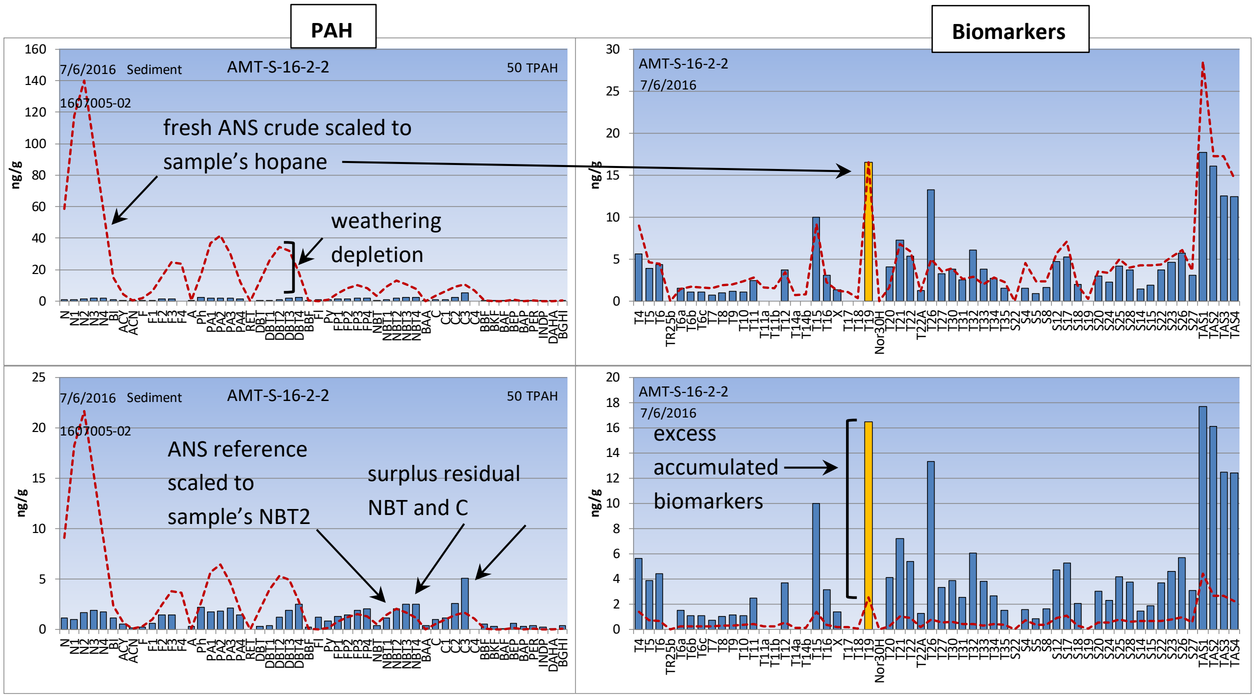

Figure 7. PAH and biomarker profiles of a representative 2016 AMT sediment sample overlaid with fresh ANS crude oil reference (dotted red lines) when alternatively scaled by the highly conservative biomarker, hopane (upper plots), versus the less recalcitrant PAH, NBT2 (lower plots). The lower plot biomarkers exceeding the reference profile (here pointing out hopane, colored gold) demonstrate an accumulated excess relative to the more easily degraded, residual PAH in this sample. There is also an accumulation of the more recalcitrant PAH including higher-alkylated NBT and chrysene homologues.

ALYESKA MARINE TERMINAL SEDIMENTS

Looking at just 2018 AMT sediment replicates, their profile patterns and concentrations were both reasonably tight (Figure 8). There is some variability in chrysene (C0 and C3 homologs) indicating more of a combustion source in replicates 1 and 2 and more of a water-washed petrogenic pattern in replicate 3, but the overall patterns suggest a mixture of combustion-derived and petroleum-sourced PAH. Despite their mixed-source and heavily weathered PAH profiles, the biomarker profiles in all three replicates confirm the presence of ANS crude oil derived from the BWTF effluent. The SHC patterns show a mix of trace-level marine-planktonic alkanes (C_{15}, C_{17}, pristane), odd-carbon numbered terrestrial plant wax components (C_{25}, C_{27}, C_{29}, C_{31}), and residual higher-molecular-weight C_{33}-C_{40} petrogenic waxes (Payne et al., 2015, 2016; Payne and Driskell, 2017b).

More relevant than the minor chrysene shifts noted in the 2018 replicates, the overall changes in the PAH and SHC patterns between 2008 and 2018 reflect different sources and concentration-dependent weathering behavior (Figure 9). Over this period, there has been a shift in PAH profiles from generally petrogenic in 2008 to a mixed pattern where pyrogenic components became more dominant from 2011 through 2015 (not shown; see Payne and Driskell, 2017b for more details). At the same time, the SHC profiles reflected more biogenic input as higher-molecular-weight petrogenic waxes generally disappeared (Figure 9). Specifically, in 2008, the petrogenic PAH patterns were characterized by the parent PAH (PH, FL, PY, C) within each group being generally less than the C-2 or C-3 alkyl-substituted homologues yielding the hump patterns denoted by the red "tents" (Figure 9, top). By 2011, the higher-molecular-weight PAH were almost exclusively pyrogenic as recognized by the dominant parent

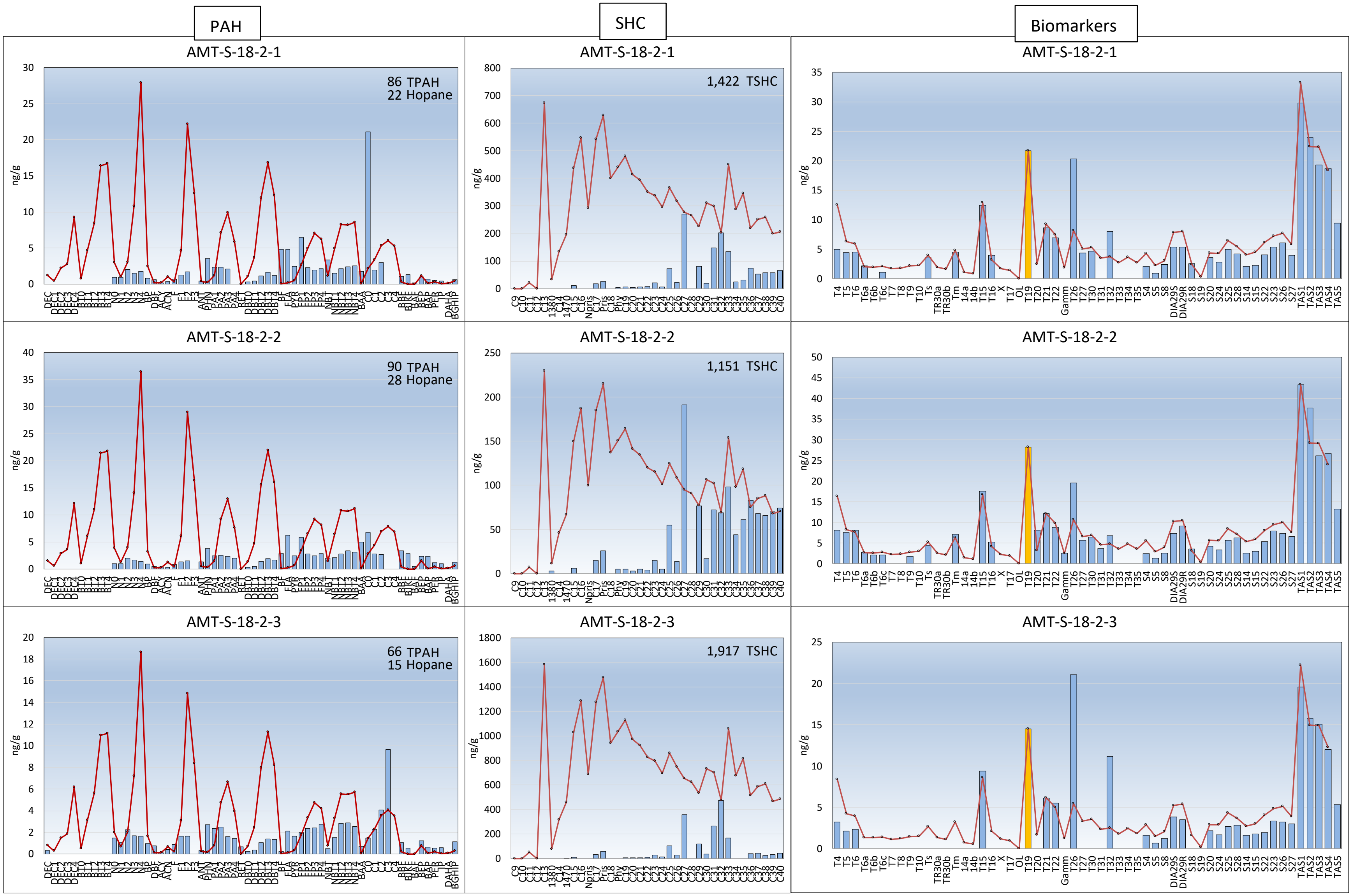

Figure 8. PAH, SHC, and biomarker concentrations and profiles of 2018 AMT sediment replicates with variable combustion- and petrogenic-sourced chrysenes. The dotted red line in the PAH and biomarker profiles is the July 2016 raw BWTF effluent (Figure 3 and Figure 4) normalized against the sample's hopane; SHC ref normalized to C32. Biomarkers confirm the presence of a weathered ANS profile in the PAH.

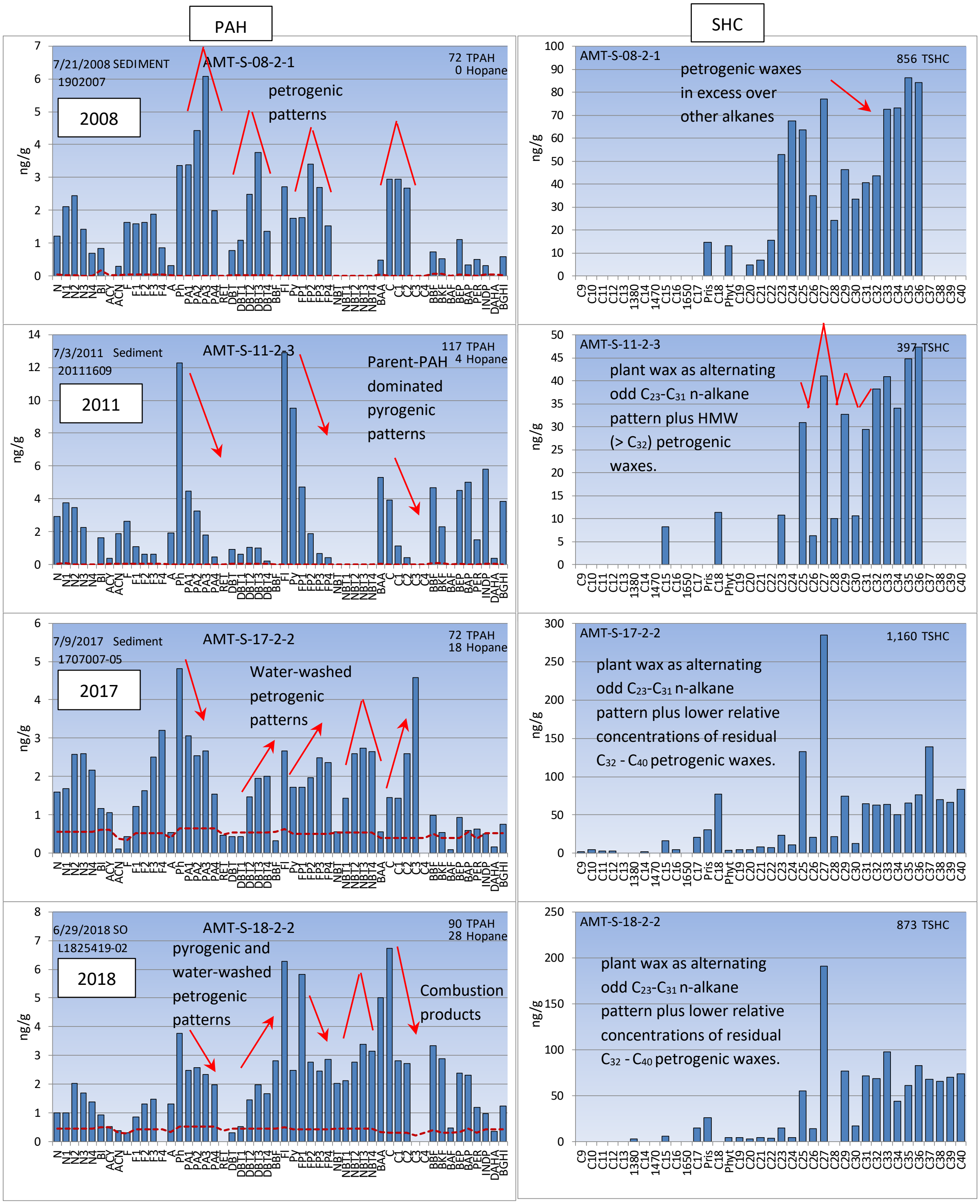

Figure 9. Representative PAH and SHC signatures of sediments at Alyeska terminal between July 2008 and June 2018 showing the progression from a primarily petrogenic to a pyrogenic PAH signature and then a mix of pyrogenic and water-washed petrogenic components with increasing terrestrial biogenic SHC and decreasing higher-molecular-weight n-alkane residuals (petrogenic waxes) through 2018. In July 2017, the PAH pattern became more of a water-washed petrogenic signal with higher relative TPAH concentrations compared to higher-molecular-weight combustion products (BBF through BGHI). In 2018, the pattern was mixed. The 2016 SHC (not shown) was largely biogenic with lower levels of petroleum waxes and this pattern was unchanged in 2017 and 2018.

PAH relative to the alkylated homologues, which decreased in a descending stair-step pattern (note red downward sloping arrows in Figure 9, second panel). In 2017, the majority of the PAH reflected a water-washed petrogenic source while in 2018 the signal is more mixed with variable combustion-derived chrysenes (Figure 8 and Figure 9, bottom two panels).

In the SHC plots, the 2008 alkanes were dominated by higher-molecular-weight petroleum waxes (Figure 9, top right panel) but, by July 2011, the SHC exhibited a mix of biogenic n-alkanes and higher-molecular-weight C_{32}-C_{36} petroleum waxes (Figure 9, second right panel). The 2017 and 2018 AMT SHC patterns were very similar and reflect lower relative contributions of high-molecular-weight petrogenic waxes compared to 2008 and 2011.

Considering the very low but higher-trending (and above-MDL) TPAH levels since 2013 (Figure 6), the transitions from petrogenic to pyrogenic patterns between 2008 and 2015 and then back to petrogenic or mixed petrogenic/combustion sources in 2017 and 2018 presumably reflect a dynamic balance between variable PAH loads from BWTF effluent and accumulation of soot. Because background combustion product or soot accumulation at GOC is over two-times lower (see next section), tanker and workboat exhaust while at or maneuvering near the berths is the likely source of the pyrogenics. The biomarker patterns over this timeframe (Figure 10) show a continued accumulation of BWTF-derived ANS components even as the PAH patterns reflect extensive weathering and the variable introduction of additional combustion sources.

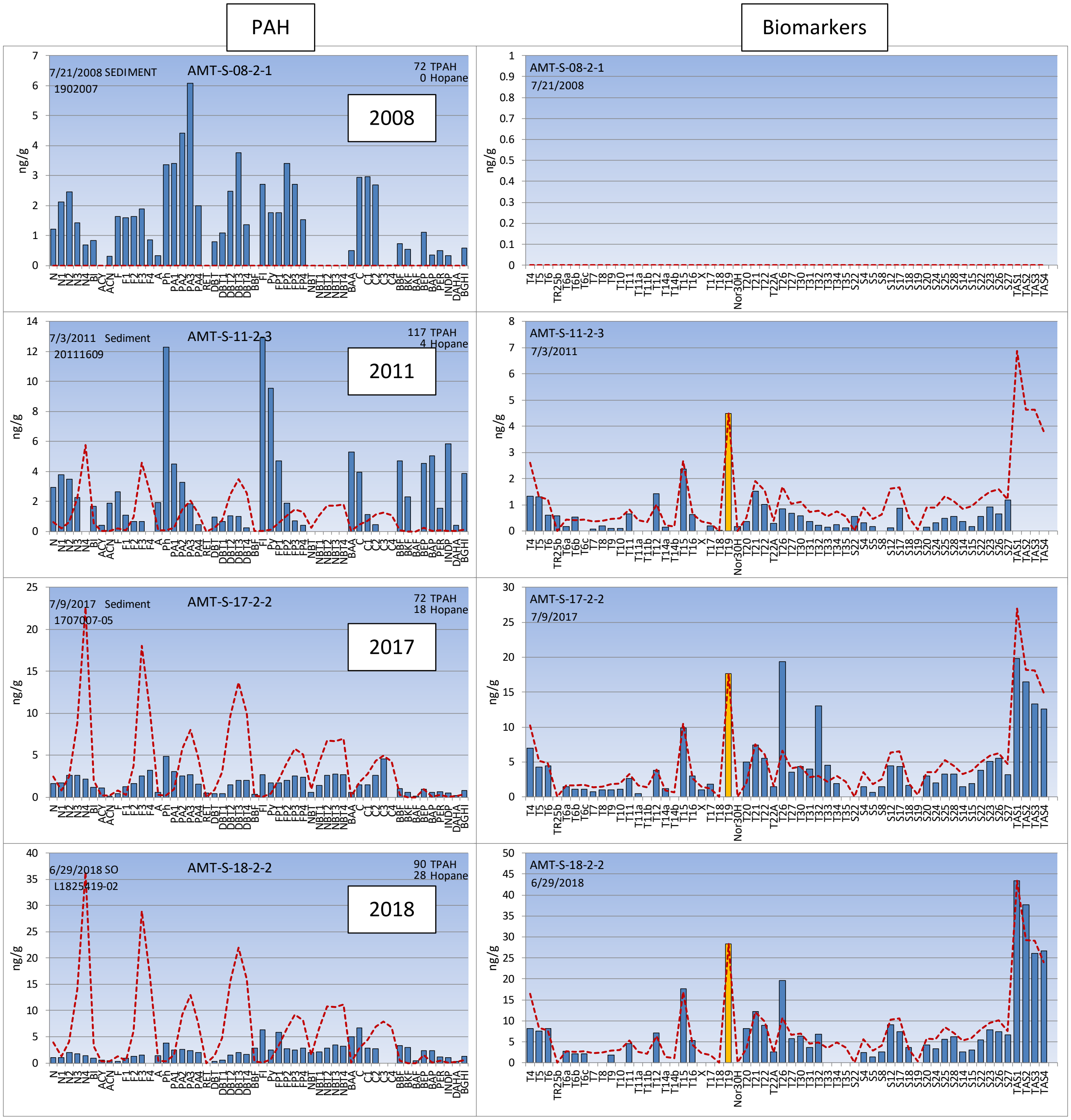

Figure 10. Time-series AMT sediment PAH profiles from 2008, 2011, 2017, and 2018 along with the biomarker profiles obtained after introducing those analyses to LTEMP in 2011. The dotted red line denotes the PAH and biomarker profiles from the July 2016 raw ballast water sample normalized to hopane (see Figure 3 top). No biomarker data are available from 2008, and ABL did not report triaromatic steroids (TAS compounds) in their pre-2016 sediment analyses. 2017 and 2018 samples were analyzed by Alpha/NewFields who do report the TAS.

GOLD CREEK SEDIMENTS

Sediments at the shallower (28-30m deep), GOC reference site have consistently exhibited lower TPAH concentrations than AMT throughout the duration of the program (Figure 6). In 2013, the GOC samples showed record-low concentrations (as did AMT) but unlike the sediments at the terminal which rebounded slightly in 2015, the GOC levels remained in single digits (2014 samples were not collected due to a program hiatus). The TPAH concentrations then increased from ~6 in 2015 to around 20 ng/g DW in 2016 and they have remained at this level through 2018. Although this represents a roughly 4-fold increase, the values are still quite low (also see ±SE data presented in Figure 6 demonstrating a tight precision about the measurements). Remarkable fidelity in profiles and concentrations was observed in the three 2018 GOC sediment grabs (Figure 11). The PAH profiles are derived from parent-dominated combustion products while the SHC patterns show a mix of trace-level marine planktonic alkanes (C_{15}, C_{17}, pristane) plus odd-carbon-numbered, terrestrial-plant-wax components (C_{25}, C_{27}, C_{29}, C_{31}) but no residual higher-molecular-weight C_{33}-C_{40} petrogenic waxes (Payne et al., 2015, 2017b).

The 2018 GOC PAH and SHC patterns were also essentially identical to those observed at this site since 2008 (Figure 12). Biomarker patterns observed in 2011, 2016 (not shown), 2017, and 2018 suggest that trace-level accumulations of biomarkers associated with the BWTF effluent are accumulating in GOC sediments (Figure 13); however, the overall concentrations were lower in 2018. The biomarker concentrations have consistently been very low, and there are numerous missing components, but the norhopane (T15) to hopane (T19) ratios in 2011 and 2017 are appropriate (Figure 13) and all of the samples have TAS relative to hopane that are close to those observed in the effluent (Figure 3). In contrast, GOC's SHC profiles (Figure 12) show no hint of ANS oil from the terminal. Over the last 10 years, the GOC sediment SHCs have been almost exclusively dominated by biogenic sources from marine phytoplankton and terrestrial plant waxes and there is no evidence of the higher-molecular-weight petrogenic waxes observed in the terminal sediments (Figure 9) between 2008 and 2011.

With the GOC patterns shifting from petrogenic to pyrogenic earlier than AMT's, the pyrogenic components have dominated since April 2000 (Payne et al., 2008a, b, 2010a, 2013, 2015, and Payne and Driskell 2017b) and with decreasing TPAH concentrations (Figure 6). The similarity in the time series plots of PAH and SHC profiles at GOC (Figure 12) further supports the relative stability in a common source over time. Over the 10-year period between 2008 and 2018, the PAH are primarily derived from parent-dominated combustion products with little change in the patterns. In addition to the pyrogenic components, GOC sediments also contain a moderate and relatively invariant suite of N_0-N_4 naphthalenes (Figure 12). These are believed to derive from glacial and riverine sediment input to the Port (Payne et al. 2010a, 2010b). Similar naphthalene contents were seen to varying degrees in all 10 major Cook Inlet rivers surveyed during the ICIEMAP program (Susan Saupe, personal communication, 2009) and in Cook Inlet sediments (Lees et al., 2000) where there is a tentative link to peat inputs.

In summary, the GOC sediment PAH profiles since 2000 have shown a pyrogenic pattern with little or no input from the terminal. Instead, they are dominated by ubiquitous low-level naphthalenes and combustion products. The 2018 sediment PAH patterns and concentrations are essentially identical to the 2016-2017 data. Nevertheless, the overall TPAH concentrations are still detectible in a just-above-MDL range. The SHC profiles in GOC sediments continue to be biogenic, reflecting only background inputs of terrestrial plant waxes. From the more extensive biomarker data reported in 2016, 2017, and 2018, it appears that, in addition to natural background biomarkers, low-level traces of some less degradable, ANS-derived biomarkers are accumulating in the GOC sediments, particularly in 2016 and 2017 with a slightly weaker signal in 2018. While the GOC sedimentary biomarker data are sparse (with many missing components), the observed constituents and diagnostic ratios are now unequivocally suggesting ANS-derived hydrocarbons, presumably from the BWTF. But despite these biomarkers, there is no evidence of BWTF-derived PAH or SHC accumulation at that site.

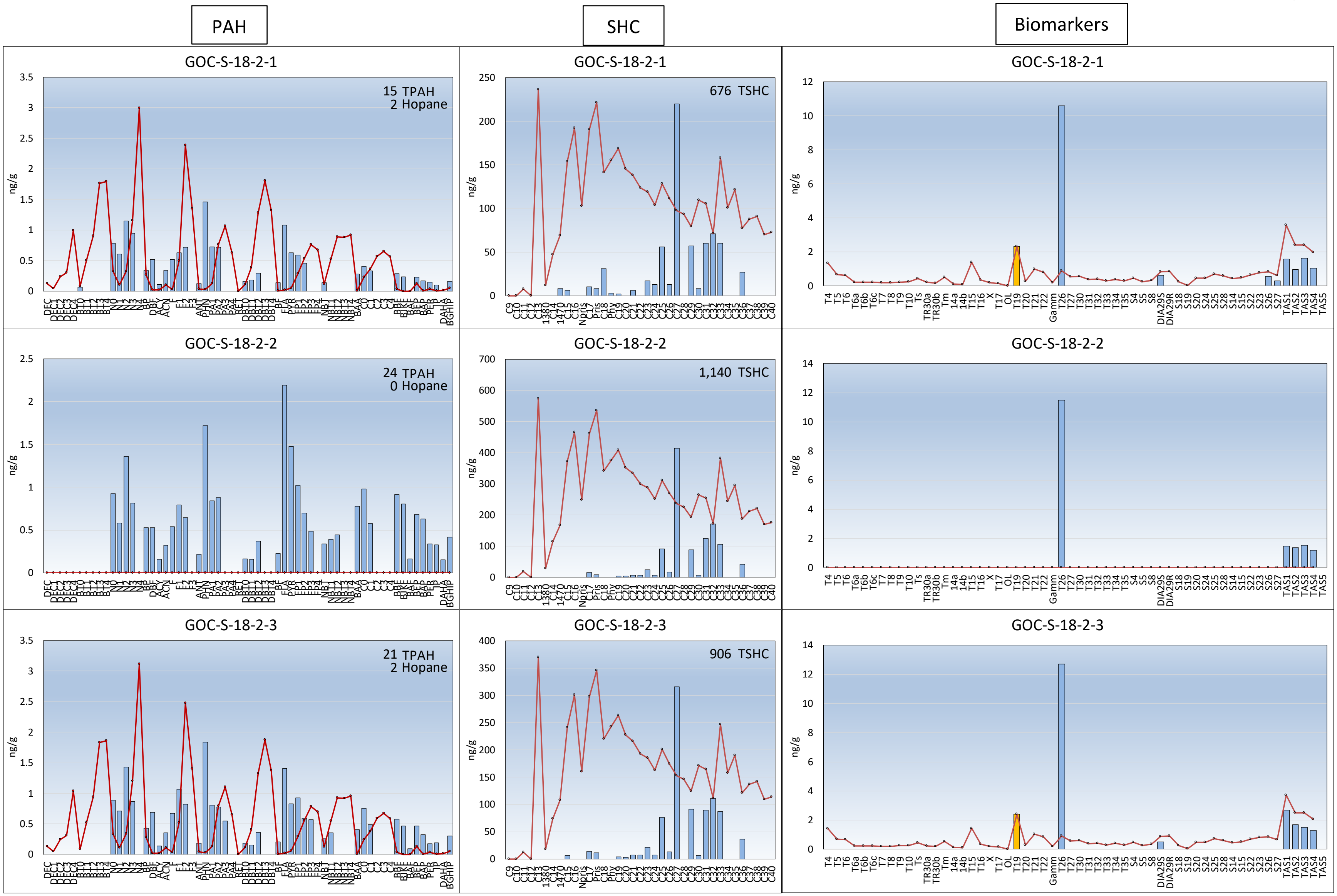

Figure 11. PAH, biomarker, and SHC concentrations and patterns of 2018 GOC sediment replicates. The dotted red line is July 2016 BWTF effluent (Figure 3) normalized against the sample's hopane; for SHC, normalized to C32 (Figure 4). The T26 biomarker spike is a laboratory artifact.

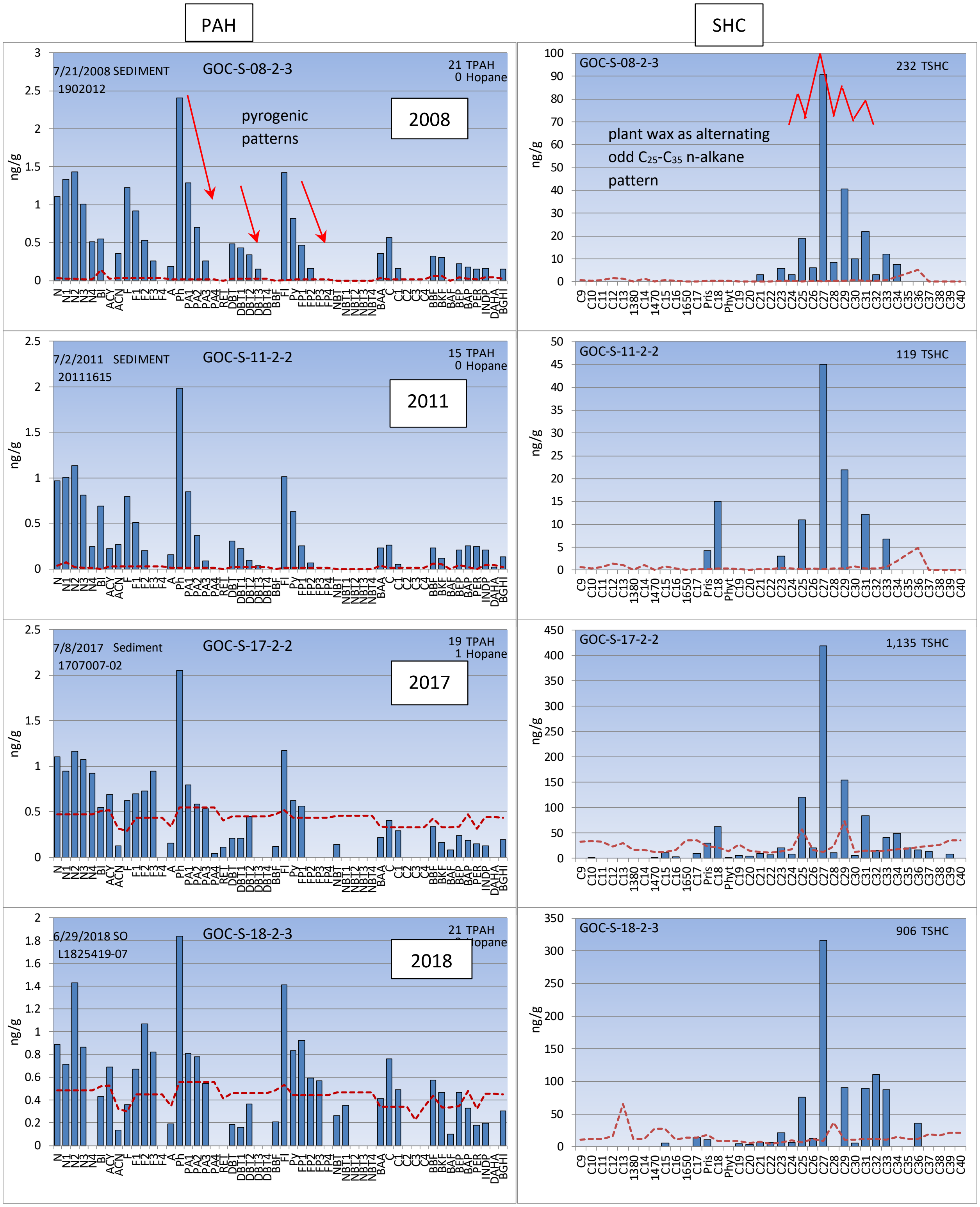

Figure 12. Representative PAH and SHC from Gold Creek sediments between July 2008 and June 2018 showing very similar, background naphthalene components and pyrogenic, parent-dominated, PAH. SHC patterns all reflect constant terrestrial and marine biogenic inputs. Red dashed line is sample-specific MDL.

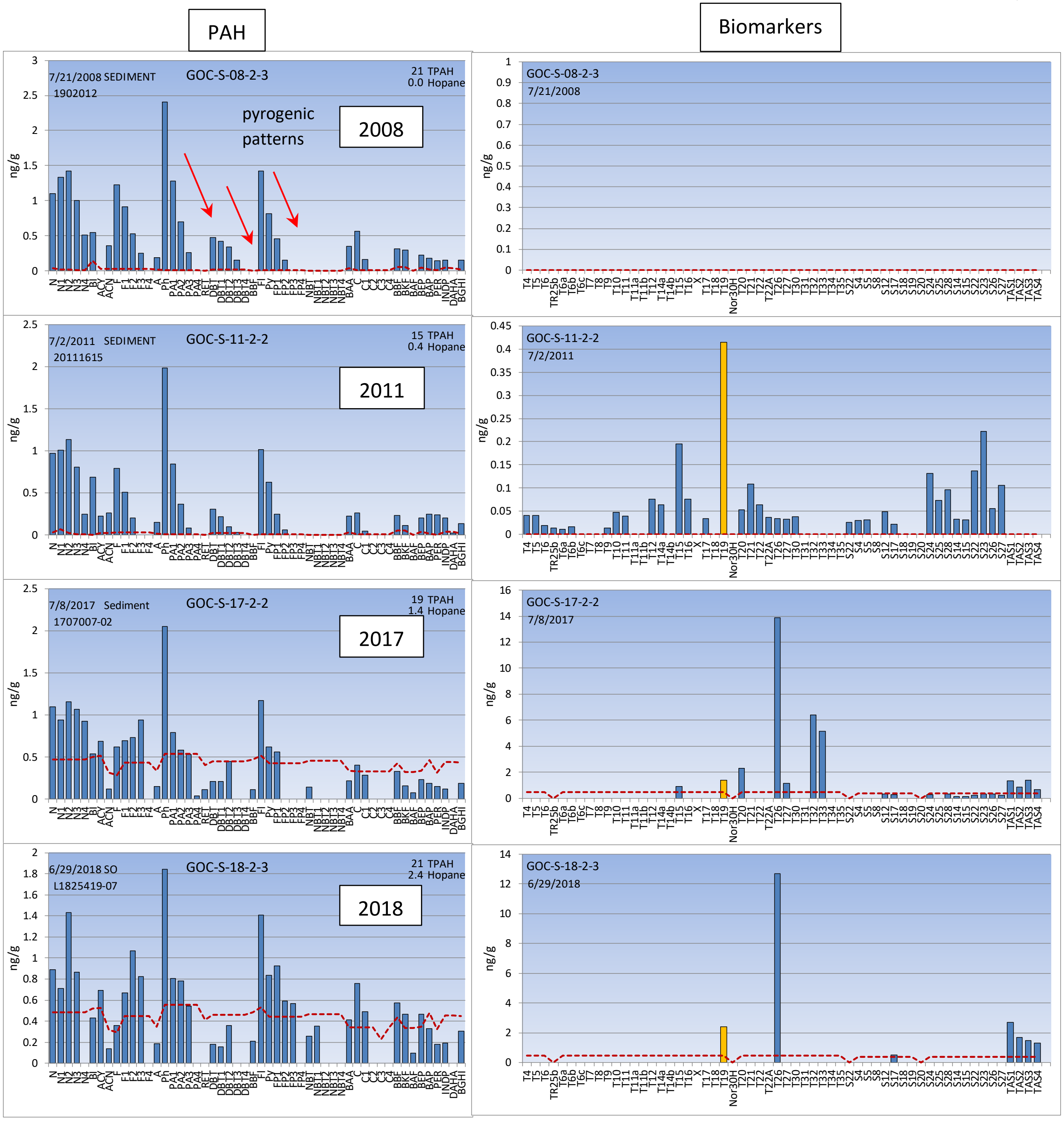

Figure 13. GOC sediment PAH and biomarker profiles from 2011, 2015, 2017 and 2018. The dotted red line denotes the sample-specific MDL. Analyses in 2011 and 2015 by ABL but they did not include the triaromatic steroids (TAS) in their suite of biomarker analytes. Analyses in 2017 and 2018 by Alpha/NewFields.

ALYESKA'S EMP SEDIMENT MONITORING

Previous LTEMP reports have demonstrated how the PAH, SHC, and biomarker chemical profiles at LTEMP sites preclude other broad-scale hydrocarbon sources from within and outside the Sound (Payne et al., 2015; Payne and Driskell 2017b). Alyeska's National Pollutant Discharge Elimination System (NPDES) required (now APDES), Environmental Monitoring Program (EMP) annually samples sediments in an expanded 14 station design within Port Valdez vs. LTEMP's two stations. Shaw and Blanchard, University of Alaska Fairbanks (UAF) contractors to Alyeska, concluded again from their 2017 EMP sediment biomarker data of hopane (T19), norhopane (T15) and oleanane (T18), that all stations in the port, including deep-water EMP stations along the midline of Port Valdez, contained petrogenic components derived from ANS crude oil (Shaw and Blanchard, 2018). Scatterplots of hopane and norhopane by year showed consistent ratios for all stations, which Shaw and Blanchard attribute to the presence of ANS oil throughout the Port. We agree.

Beginning in 2014, their assessment subtly suggested that while the consistent hopane ratios confirmed an ANS-derived, BWTF oil in shallow stations near the terminal, the reduced sediment hopane loads at deeper stations suggested a *refined* ANS source plus pyrogenics. The attribution to a refined ANS seems puzzling since the most abundant refined ANS source would likely be marine diesel or gasoline fuels for which the distillation points required in refining these fuels typically eliminate hopane and norhopane (Bence et al., 1996, Peters et al., 2004, Stout and Wang, 2016). An alternative explanation might be that the low-level biomarkers in the deeper sediments simply represent dilute, dispersed ANS crude inputs from terminal BWTF discharges rather than refined products. LTEMP's low-level biomarker data at GOC lacking much of the biomarker suite supports this concept.

Also note an opposite effect can occur, namely, increased biomarker levels. During deposition, biomarkers can only accumulate in their normal proportions relative to the PAH components (i.e., constrained water-insolubly within their oil droplet). But, by degrading markedly slower than PAH, biomarkers accumulate as residuals of the prior weathered ANS inputs and thus, appear in excess to expected proportions (Figure 7). Alyeska's EMP sites near the diffuser would be prone to acquire these "enhanced" biomarker profiles. As a forensic exercise, we note that scaling the BWTF source profile to fit the PAH in 2016 EMP, near-diffuser, sediment sample, 145A (adjusting the source to match the sample's most conservative PAH, chrysene) (Figure 14) required re-scaling the ANS overlay to roughly half of the hopane in ANS (hopane being the normal scalar of choice). In other words, there appears to be a two-fold excess portion of hopane biomarkers in this sediment sample relative to the PAH but actually, half of the accumulated PAH have been weathered away. This biomarker "enhancement" generally agrees with LTEMP's nearby AMT sediment sample which showed a weathered PAH profile that has accumulated approximately 2.7-fold excess hopane (i.e., two-thirds of the expected PAH have degraded)(Figure 7).

The PAH/hopane mass balance also has forensic utility. As a diagnostic ratio, scaling the effluent's particulate (oil droplet) profile by the relative proportion of hopane in a given sample versus the particulate reference's hopane provides an assessment of the expected hopane/PAH balance. The intersection of the scaled overlay to the most recalcitrant PAH in the EMP data, parent chrysene (C0), would indicate the hopane/chrysene mass balance is as should be expected for ANS oil (Figure 15) and that the sample has at least one of the critical characteristics of the ANS source oil. Half of the shallow near-field 2017 EMP stations (Figure 16), those closest to the outfall diffuser, showed good correspondence to the expected balance. This diagnostic single ratio is, of course, only one of multiple lines of evidence used to confirm a source identification. Unfortunately, due to the abbreviated analyte suite, other diagnostic patterns aren't available to make this assessment with confidence.

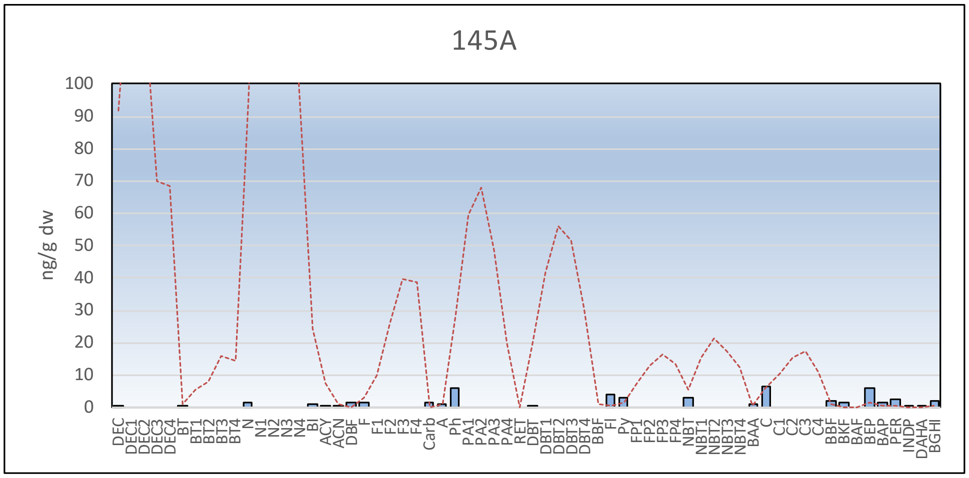

Figure 14. PAH profile of 2016 Alyeska EMP, near-diffuser, sediment sample 145A (showing Alyeska's abbreviated analyte reporting list). Red overlay represents a fresh ANS oil profile scaled to the recalcitrant chrysene (C). Alternatively, scaling to hopane inflates the overlay (not shown) and suggests that based on the amount of chrysene present, the sample should have only half of the reported hopane. These data imply that the two-fold surplus of biomarkers are residuals from degraded previous inputs of ANS.

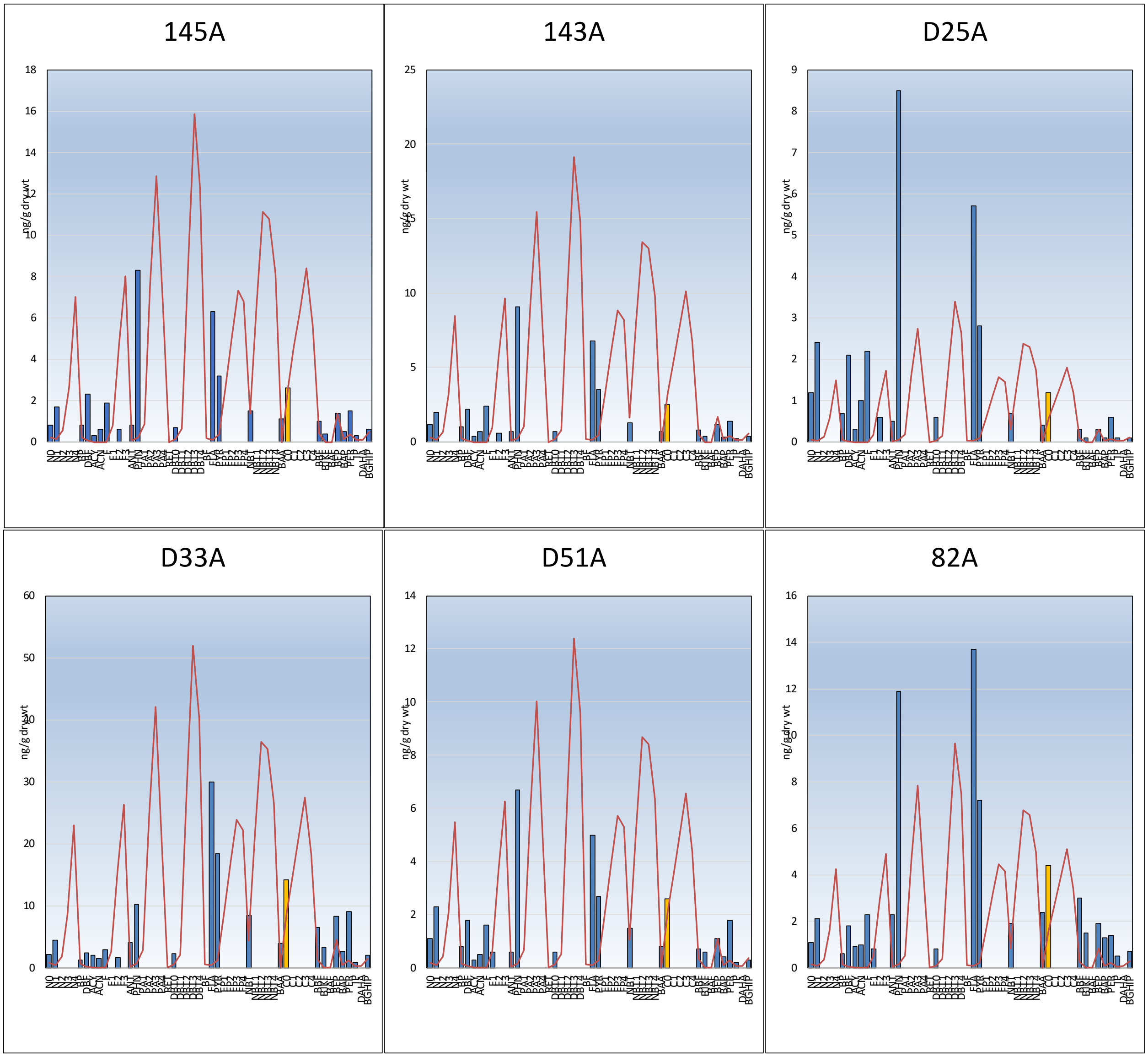

Figure 15. PAH profiles of 2017 Alyeska EMP, near-diffuser, sediment samples showing Alyeska's abbreviated analyte reporting list. Diagnostically, there is close fit to the samples' most recalcitrant PAH, chrysene (gold-filled bar), with the red overlay representing a BTT particulate oil profile (summer 2016) scaled to the recalcitrant hopane biomarker.

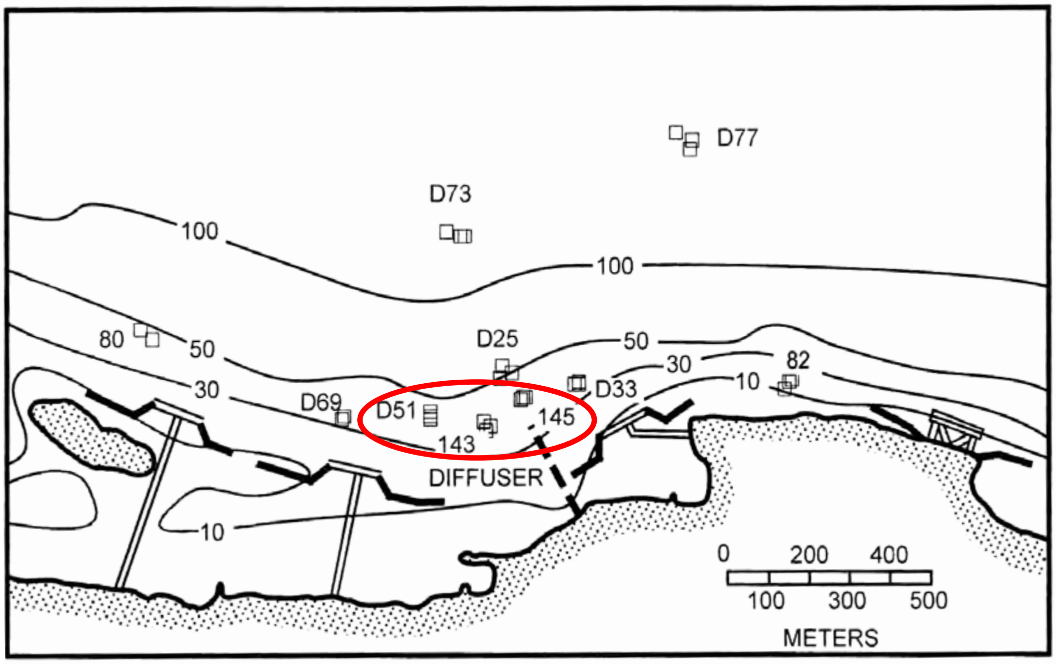

Figure 16. Alyeska EMP stations at the terminal. Red oval denotes stations with ANS-matching hopane/chrysene balance as seen in Figure 15. From Shaw and Blanchard, 2018.

In previous reports, Shaw and Blanchard rightly pointed out that one forensic telltale for non-ANS inputs is that oil from ANS formations lack oleanane, a biomarker derived from angiosperm plants absent during the geologic age of the formation (Moldowan et al., 1994). Thus, when oleanane was detected in most of their 2015-16 samples, it logically suggested that there must be a non-ANS source(s) in Port Valdez and that there must be some additional non-BWTF contributions to the sediment background. From our program, a handful of samples, including an ANS source sample analyzed at Alpha, showed minute levels of oleanane plus 28, 30-bisnorhopane, another biomarker not found in ANS oil. We subsequently re-identified these traces as lab artifacts; our samples have never contained oleanane or the bisnorhopane (Figure 17, Figure 18, and Figure 19). Shaw and Blanchard appropriately suggest, based on Kvenholden et al. 1995 (also, Savoie et al., 2006, Short et al., 2007), that the oleanane in their samples likely comes from California's Monterey formation oil that was imported in the pre-pipeline era and during the 1964 earthquake/tsunami was spilt from Valdez storage tanks. Indeed, traces of Monterey oil have been reported at numerous locations throughout PWS, mostly as high intertidal tarballs but also in the post-EVOS pit-digging studies of Auke Bay Lab (Short et al., 2006, Lindeberg et al. 2018). While it is certain that Port Valdez sediments do contain the 1964 spilt Monterey oil, it would seem unlikely that the oil remains would occur in near surface deposits considering the fjord's heavy depositional environment of glacial floc (~0.5 cm/year near the terminal). From another PWSRCAC study, deep sediment cores at the BWTF found the earthquake signature at 20cm depth (Savoie et al., 2006), a depth that would require either another major underwater slope failure or some very dynamic bioturbation to re-contaminate the entire Port. Furthermore, the event must have been episodic as no oleanane was detected in Shaw and Blanchard's 2018 samples. With only a three biomarker-analyte data set, the EMP's 2015-16 oleanane occurrence cannot be interpreted.

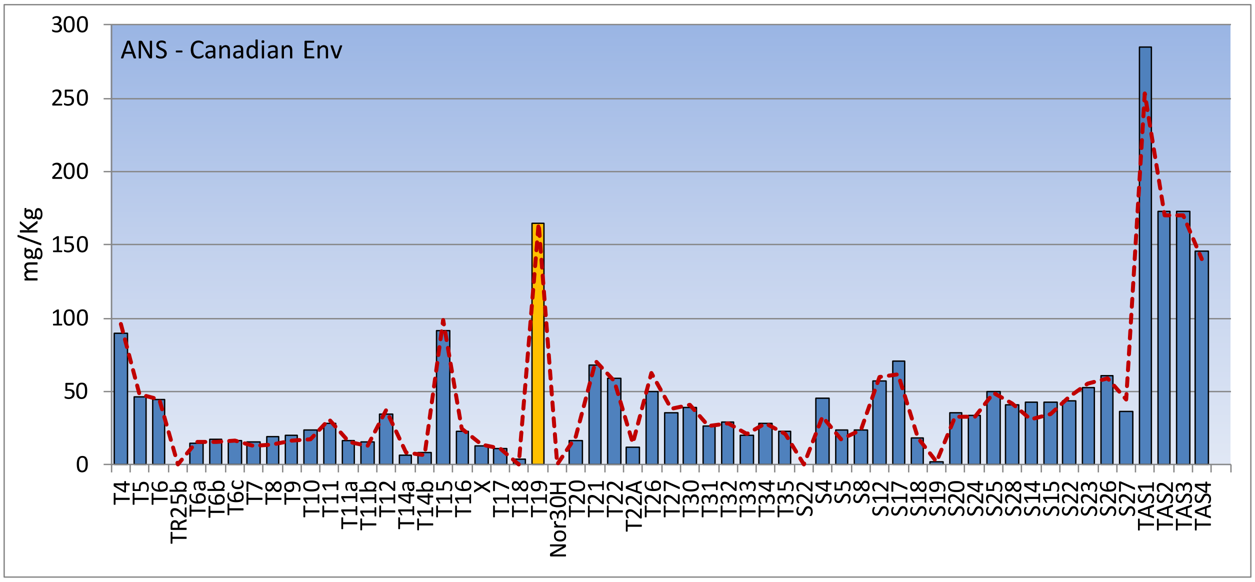

Figure 17. Triterpane biomarkers in ANS reference oil from split sample with Environment Canada as reanalyzed by Alpha Laboratory. Note traces of 28, 30-bisnorhopane (T14a) and oleanane (T18). Both are lab artifacts. Gold bar is C30-hopane (T19).

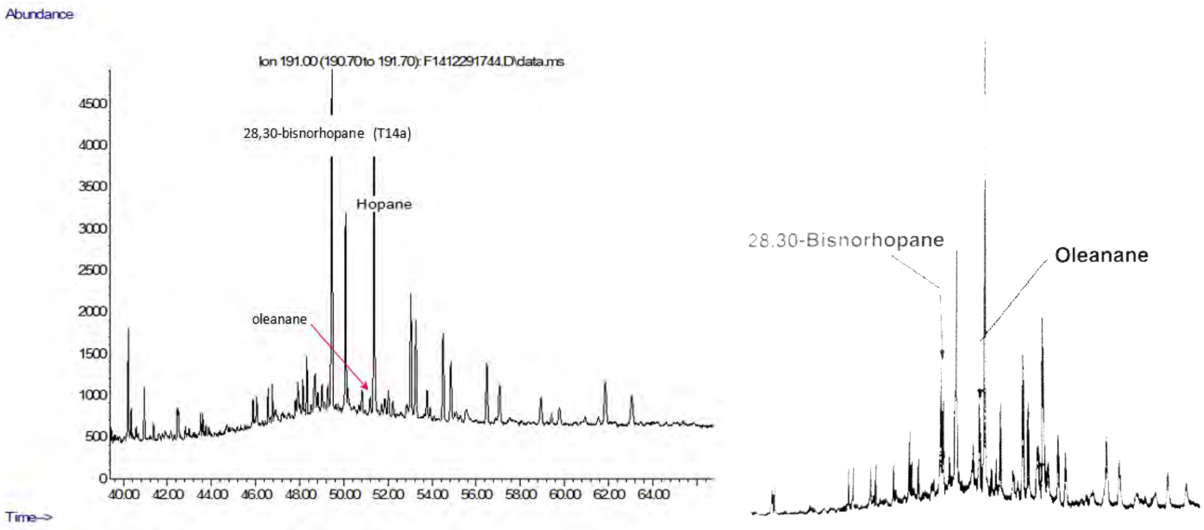

Figure 18. SIM chromatographic profiles of triterpane biomarkers (m/z 191) in (A) Monterey formation oil and (B) PWS beach tarball from Monterey oil showing relative abundance of hopane to 28, 30-bisnorhopane (T14a) and oleanane (T18), biomarkers not found in ANS oil. From (A) Alpha/NewFields Environmental and (B) Bence et al., 1996.

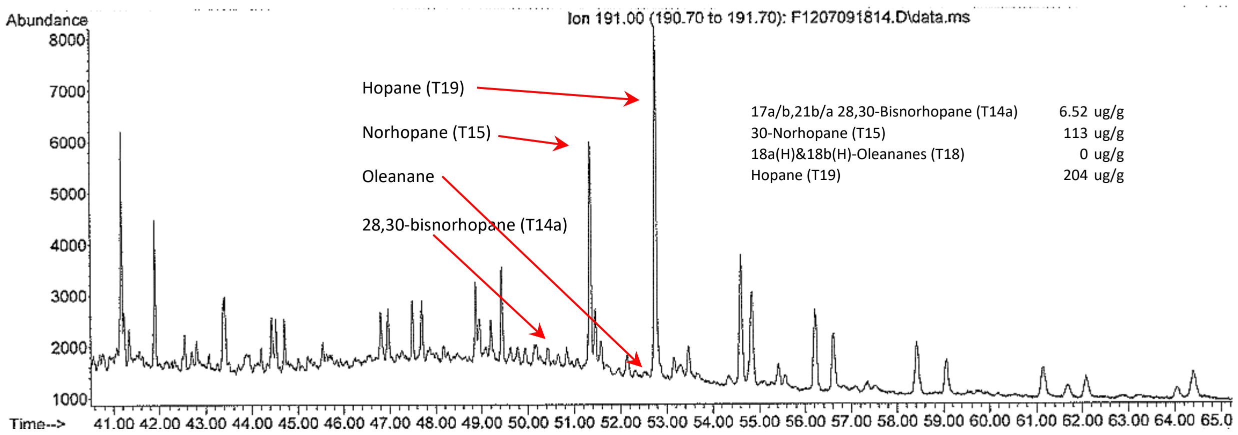

Figure 19. SIM chromatographic profiles of triterpanes (m/z 191) in ANS oil analyzed by Alpha Laboratory in 2016. Note trace presence of 28,30-bisnorhopane (T14a) and oleanane were both lab artifacts that also appeared as a minor signal in the AMT sediments.

The 2017 EMP interpretations and conclusions cannot be corroborated from the abbreviated PAH16 and biomarker data available in their report. Nevertheless, it can be said that despite highlighting our minor differences in interpreting Alyeska's EMP data, the EMP conclusions generally agree with LTEMP's recent findings of low-level petrogenic plus pyrogenic patterns

SEDIMENT GRAIN SIZE

The LTEMP sediment-sampling locations comprise a heterogeneous slope at AMT and sediment shelf at GOC inside a fjord dynamically swept by tidal currents (and prop wash at AMT). Plus, with LTEMP sampling guided by GPS, the sites have been accruing grab-sampler pock marks and drag scars at the same locations for 20 years. Reassuringly, when the sampling vessel gets off-site at GOC, we begin to see gravel tell-tales in the grab. The grain-size component trends are presented here with only modest confidence considering the non-rigorous collection methods (i.e., spooning up 250 mL of sediment remnants after collecting the less consolidated surface floc for hydrocarbon analyses). There was also a change in analytical labs in 2016.

Sediment grain-size samples are presented for all 2006-2018 collections in two formats: the standard cumulative (%) grain-size curves and a 3D trend plot. For this project, the grain-size data only serve to demonstrate the constancy and comparability of the sampling site environs.

Both sites are dominated by glacial flour inputs, showing approximately equal portions of clay and silt with minor sand components (Figure 20 and Table 7) and with both sites showing minor trends and outliers. In the 3D plots (Figure 21), note there are annual shifts at GOC (~30m depth) to higher sand content and back (albeit still a minor component, mostly ~10%) and with a return to earlier conditions in 2013. But in 2015, a shift to coarser particles occurred when silt increased and clay decreased dramatically. In 2016, 2017, and 2018, there was further return towards a clay- and slit-dominated substrate. At AMT (~70 m depth), there has been a cycle of increasing clay content through 2009 and then a decrease, returning to 2006 levels by 2015-16. In 2016, there was also a halving of sand, albeit still a minor component (~3%). In 2017, the sand portion decreased further as clay became dominant, but in 2018 all of the percentages more closely matched the 12-year averages with clay still being slightly dominant (Table 7).

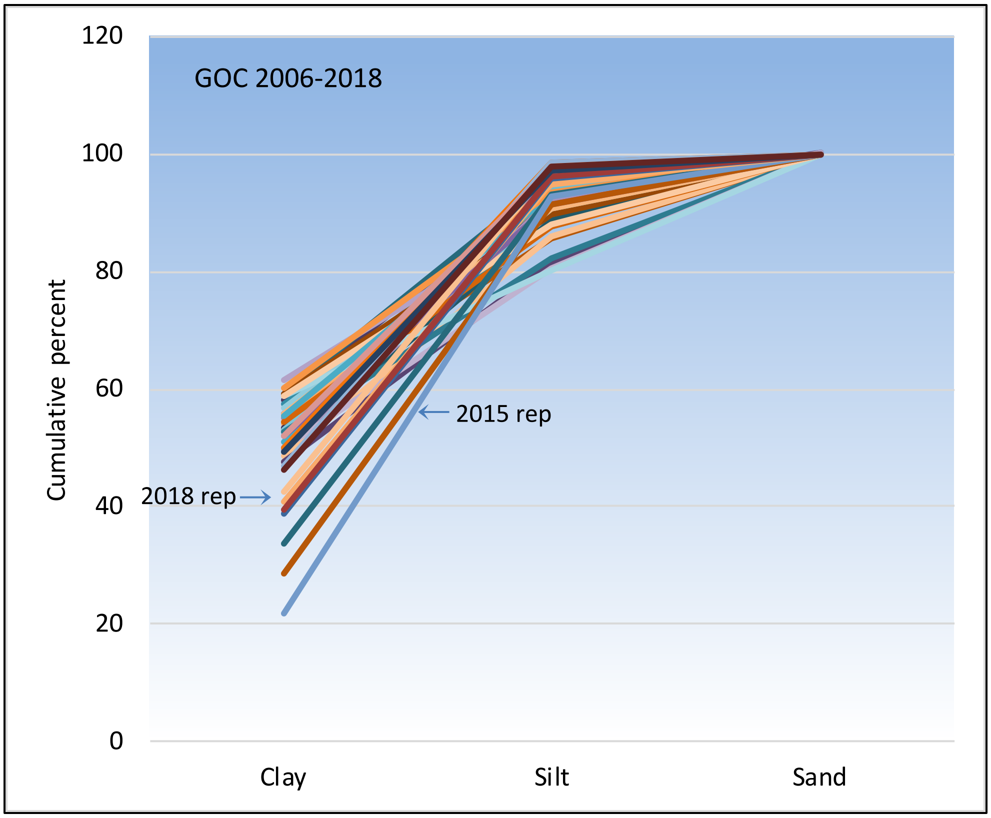

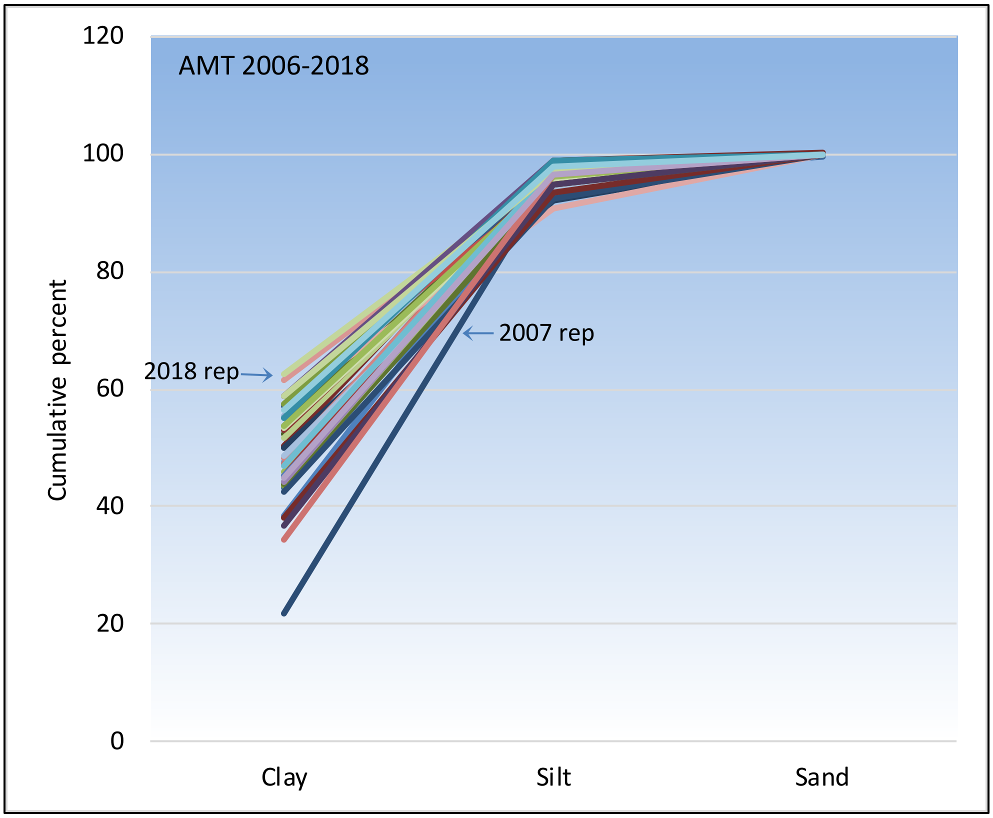

Figure 20. Individual replicate cumulative grain-size curves (%) for GOC and AMT, 2006-2018.

Table 7. Average grain size components for GOC and AMT, 2006-2016.

AMT				GOC			
Year	% Sand	% Silt	% Clay	Year	% Sand	% Silt	% Clay
2006	1	55	43	2006	6	44	51
2007*	2	54	44	2007*	7	37	56
2008	2	54	44	2008	9	36	55
2009*	4	40	56	2009*	10	35	55
2010	3	49	48	2010	9	38	53
2011	3	45	51	2011	16	32	52
2012	7	40	53	2012	17	27	56
2013	5	42	53	2013	7	37	56
2015	6	54	40	2015	8	64	28
2016	3	55	42	2016	4	56	40
2017	1	42	57	2017	2	49	50
2018	3	44	53	2018	2	52	46
avg	3	48	49	avg	8	42	50

*Combines two seasons of sampling

SEDIMENT TOC

Total organic carbon (TOC as the percentage of sediment dry weight) serves as a non-specific measurement of all organics in a sample. Typically ranging from 0.1 to 30% in marine sediments, it is used to express the nutritional quality of food available to benthic organisms. For pollution work, metals and anthropogenic organic compounds tend to sorb and concentrate in or on finer grained sediments and TOC, respectively, and thus TOC can be used to normalize contaminant concentrations in order to do site-to-site contaminant comparisons.

LTEMP TOC values showed seasonal cycles during the more frequent samplings early in the program but then showed a slow increase in concentration until plateauing sometime around 2003 (Figure 22 and Table 8). There was an uptick at GOC in 2012 and 2013 and mildly so at AMT in 2013. Since then, GOC TOC levels have dropped in 2015-2018 while AMT has ranged between 0.53 and 0.63% since 2012. Perhaps the only conclusion is to note that TOC tends to fall within the low 0.5 – 0.8% DW range and suggests similar organic-sparse sources at both locations within the fjord. This is not surprising considering the dominance of primarily inorganic glacial flour in the sediments. Also, note that the data are not continuous, that sampling prior to 2002 was performed by KLI, and that 2016 incorporates the third laboratory change for the project.

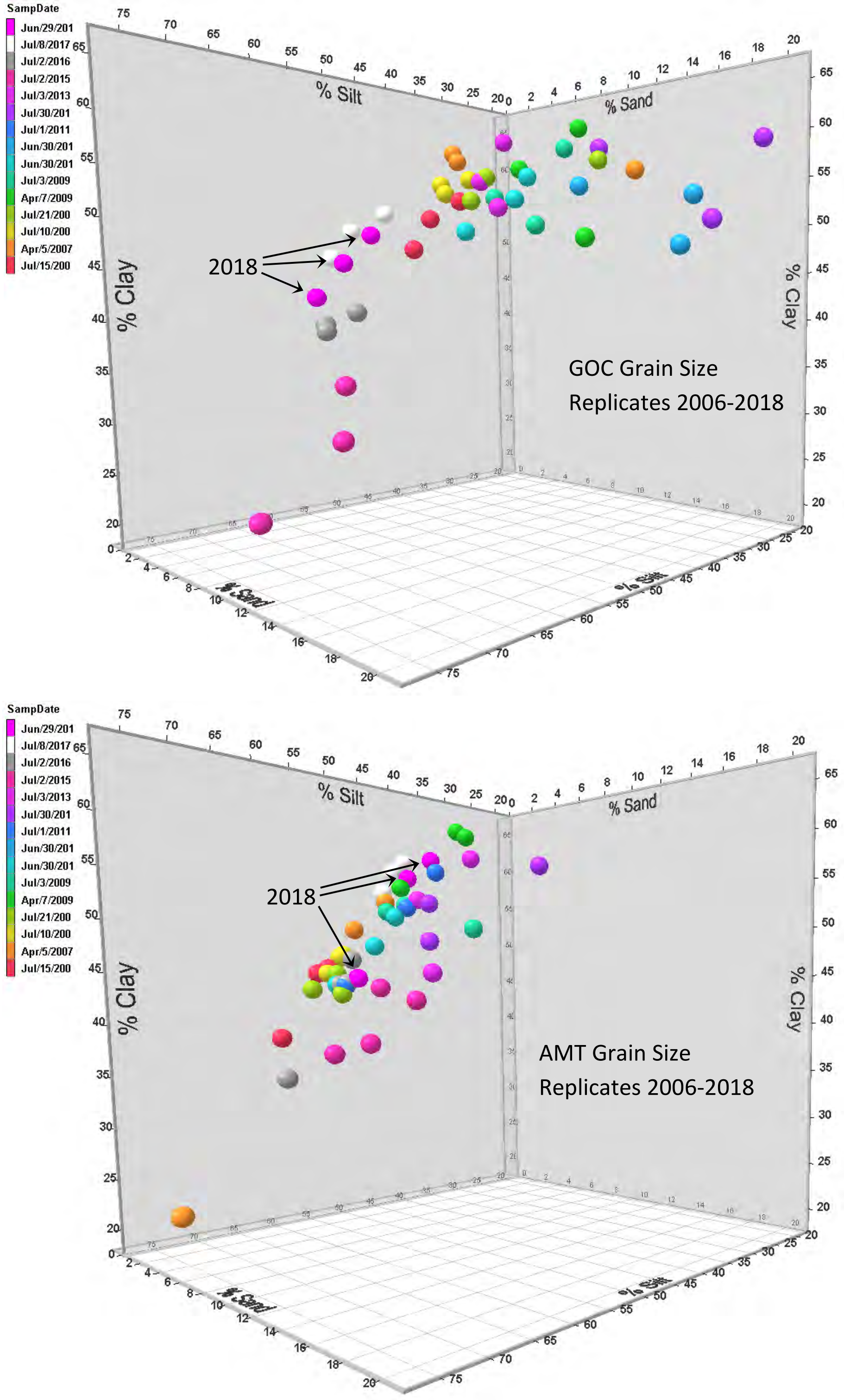

Figure 21. 3D plots of grain size components from GOC and AMT 2006-2018. Sampling years are color coded: blue to red, 2006-2017; pink, 2018. Note the clipped axes emphasize a decreasing shift in clay vs silt at GOC in 2015. Over the years, typically sand content has been most variable component at GOC, silt/clay at AMT.

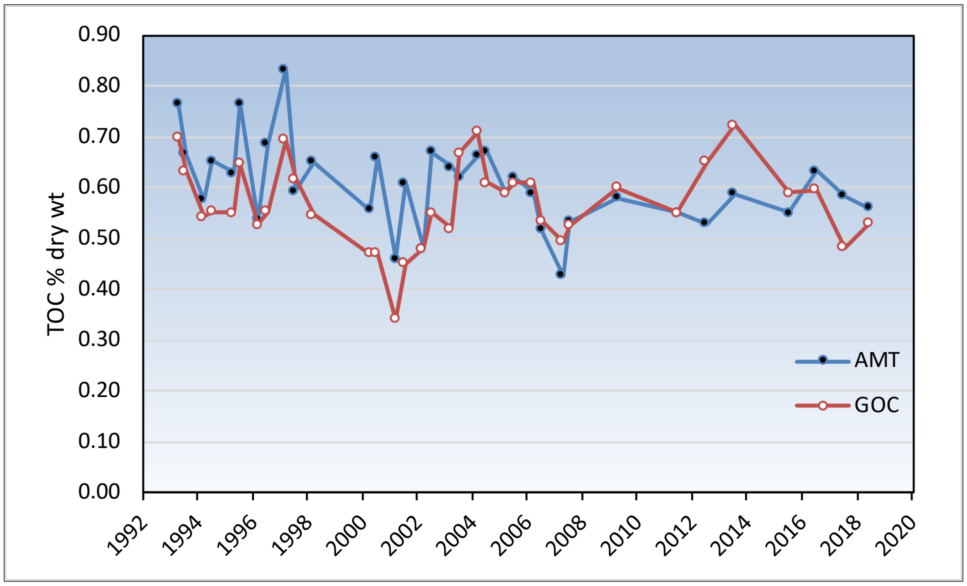

Figure 22. LTEMP Total Organic Carbon trends in AMT and GOC sediments (% DW), 1993-2018.

Table 8. LTEMP Total Organic Carbon in AMT and GOC sediments (% DW).

Sample Date	AMT	GOC	Sample Date	AMT	GOC	Sample Date	AMT	GOC
Apr-93	0.77	0.70	Jul-00	0.66	0.47	Jul-06	0.52	0.54
Jul-93	0.67	0.63	Mar-01	0.46	0.34	Apr-07	0.43	0.49
Mar-94	0.58	0.54	Jul-01	0.61	0.45	Jul-07	0.53	0.53
Jul-94	0.65	0.55	Mar-02	0.48	0.48	Apr-09	0.58	0.6
Apr-95	0.63	0.55	Jul-02	0.67	0.55	Jun-11	0.55	0.55
Jul-95	0.77	0.65	Mar-03	0.64	0.52	Jul-12	0.53	0.65
Mar-96	0.54	0.53	Jul-03	0.62	0.67	Jul-13	0.59	0.72
Jul-96	0.69	0.55	Mar-04	0.66	0.71	Jul-15	0.55	0.59
Mar-97	0.83	0.69	Jul-04	0.67	0.61	Jul-16	0.63	0.60
Jul-97	0.59	0.62	Mar-05	0.59	0.59	Jul-17	0.58	0.48
Mar-98	0.65	0.55	Jul-05	0.62	0.61	Jun-18	0.56	0.53
Apr-00	0.56	0.47	Mar-06	0.59	0.61			

LTEMP MUSSEL TISSUES

As in our previous LTEMP reports, individual sample profiles of all PAH, SHC, and S/T tissue data are presented by station in Appendix 2. Time-series data reported for AMT, JAP, and GOC stations show the profile trends dropping to lower and lower levels; however, because of the extremely low, below-MDL concentrations, and the presence of the same profiles in the associated laboratory method blanks, source identifications for the 2018 tissue samples are not possible. The following sections present representative samples and their respective contra-indicating blanks by region rather than by individual station replicates, as traditionally presented. Thus, this report will focus on examining, by geographic region, the similarities to the method blanks.

An expanded discussion of the 2017 Berth 5 Tanker Loading Arm spill of ANS crude oil is presented to demonstrate the utility of mussel sampling in delineating the extent of the contamination and suggest the time required for mussels to purge a contaminant signal.

PORT VALDEZ MUSSEL TISSUES

Although historically, TPAH concentrations in mussels sampled from both the AMT and the background-reference site at GOC were commonly reported in hundreds of ng/g DW, in 2002 the concentrations dropped to ~80 ng/g DW levels (Figure 23). One exception to this post-2002 range occurred with a diesel spill at GOC in the summer of 2004 when TPAH concentrations were approaching 1,000 ng/g DW. By the 2005 collections, the PAH were long purged and concentrations back in the pre-spill range. They continued to fall at both locations until summer 2013 when only very low, near-MDL, traces of petrogenic components were present. No samples were collected in 2014, but in 2015, the PAH tissue burdens at both locations increased slightly while the character of the PAH patterns further transitioned into primarily dissolved-phase, background patterns (see below). TPAH concentrations in 2016 remained essentially the same at GOC (~31 ng/g DW) but they dropped to single digits at AMT (Figure 23). In 2017, the TPAH concentrations remained in single digits at all three Port Valdez stations. Finally, in 2018, the TPAH again decreased to < 6 ng/g DW (Table 9). At these exceptionally low levels, the individual PAH components at all three Port Valdez sites were all below MDLs, and were essentially indistinguishable from laboratory method blanks except for traces of a few combustion products indicated in one or two samples.

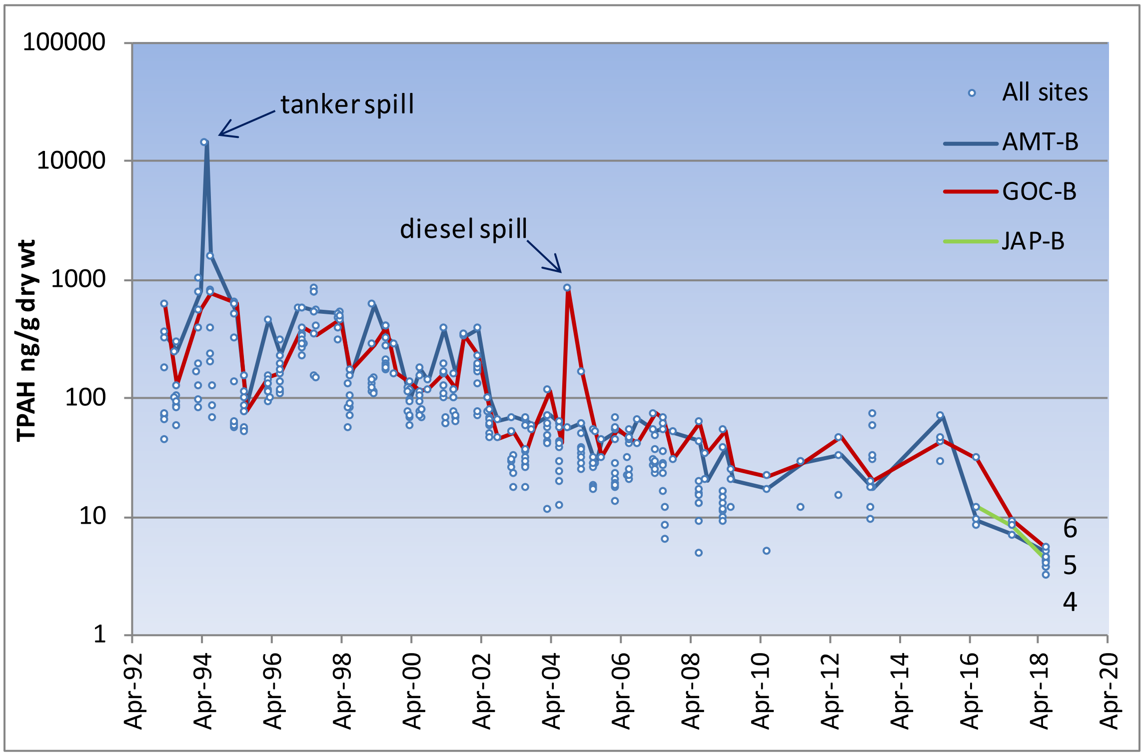

Figure 23. Time series of mean mussel log (TPAH43) comparing 2018 AMT and GOC with prior LTEMP collections at other regional sites shown as open circles. See standard errors of mean in Table 9.

Table 9. Time series of mean TPAH43 (ng/g DW, n=3) from AMT, GOC, and JAP mussels, 2008-2018. Sampling at JAP only started in July 2016.

	8-Jul	8-Sep	9-Apr	9-Jul	10-Jul	11-Jul	12-Jul	13-Jul	15-Jul	16-Jul	17-Jul	18-Jul
Mean TPAH												
AMT	43	20	38	20	17	29	33	17	70	9	7	5
GOC	62	34	54	25	22	29	46	20	43	31	9	6
JAP										14	9	4
± SE of means												
AMT	5.8	1.9	6.8	0.8	0.9	2.2	3.1	2.9	8.6	1.9	0.3	0.5
GOC	6.3	3.5	2.8	1.2	1.4	3.3	6.6	2.4	3.6	15.7	0.5	0.6
JAP										1.6	2.6	0.2

Reflecting the changing operations at the terminal, the trends of oil discharge into Port Valdez from terminal operations have been declining over the last two decades. This trend reflects a combination of reduced BWTF discharge volumes from historically decreased ANS oil production, the transition from single-hulled to double-hulled tankers with segregated ballast tanks, and improved BWTF efficiency in removing particulate/oil-phase PAH. As a result, over the last several years, contamination in mussels at the AMT sampling site has been generally shifting away from the terminal's petrogenic profiles to background dissolved-phase or pyrogenic (combustion-derived) PAH patterns. Sediments, as discussed above, still show BWTF oil accumulation near the terminal but much lower concentrations than in earlier years.

In June 2018, the tissue hydrocarbon concentrations at AMT, JAP, and GOC were all below MDLs, reaching all-time lows, and except for traces of a few combustion products, the PAH profiles were essentially indistinguishable from laboratory method blanks (Figure 24). At the GOC site, mussels have generally shown only low-level dissolved-phase and pyrogenic PAH profiles since 2006 but in 2016, traces of a diesel spill were observed (Payne and Driskell, 2017b). By the 2017 collections, there was no evidence of residual hydrocarbons from the 2016 diesel spill as the PAH pattern reverted to a trace-level dissolved-phase and pyrogenic profile (Figure 25, bottom panel). In 2018, the GOC PAH concentrations were all below the MDLs and, like the two stations adjacent to the terminal, the PAH profiles were almost identical to those observed in laboratory method blanks run in parallel with the samples (Figure 24).

Historical PAH data for the traditional AMT site (Figure 26) suggest the presence of dissolved-phase naphthalenes in 2015 and 2017 plus at- or below-MDL traces of combustion products in most of the samples. At these trace concentrations, results must be qualified as estimates but because of their patterns, they are not considered to be false positives. Although TPAH levels increased slightly in 2015 (Figure 23), the majority of the PAH were dissolved-phase naphthalenes (Figure 26), which also were observed to a lesser extent at GOC (see below). Recall that the source of dissolved-phase PAH cannot be definitively determined just from their profiles. These, however, did not match the pattern associated with BWTF effluent, so presumably they were derived from another unknown source.

In addition to the dissolved-phase components and parent-PAH dominated combustion products (e.g., phenanthrenes (P), fluoranthenes/pyrenes (FL/PY), and perylene (PER)) are occasionally observed.[3]

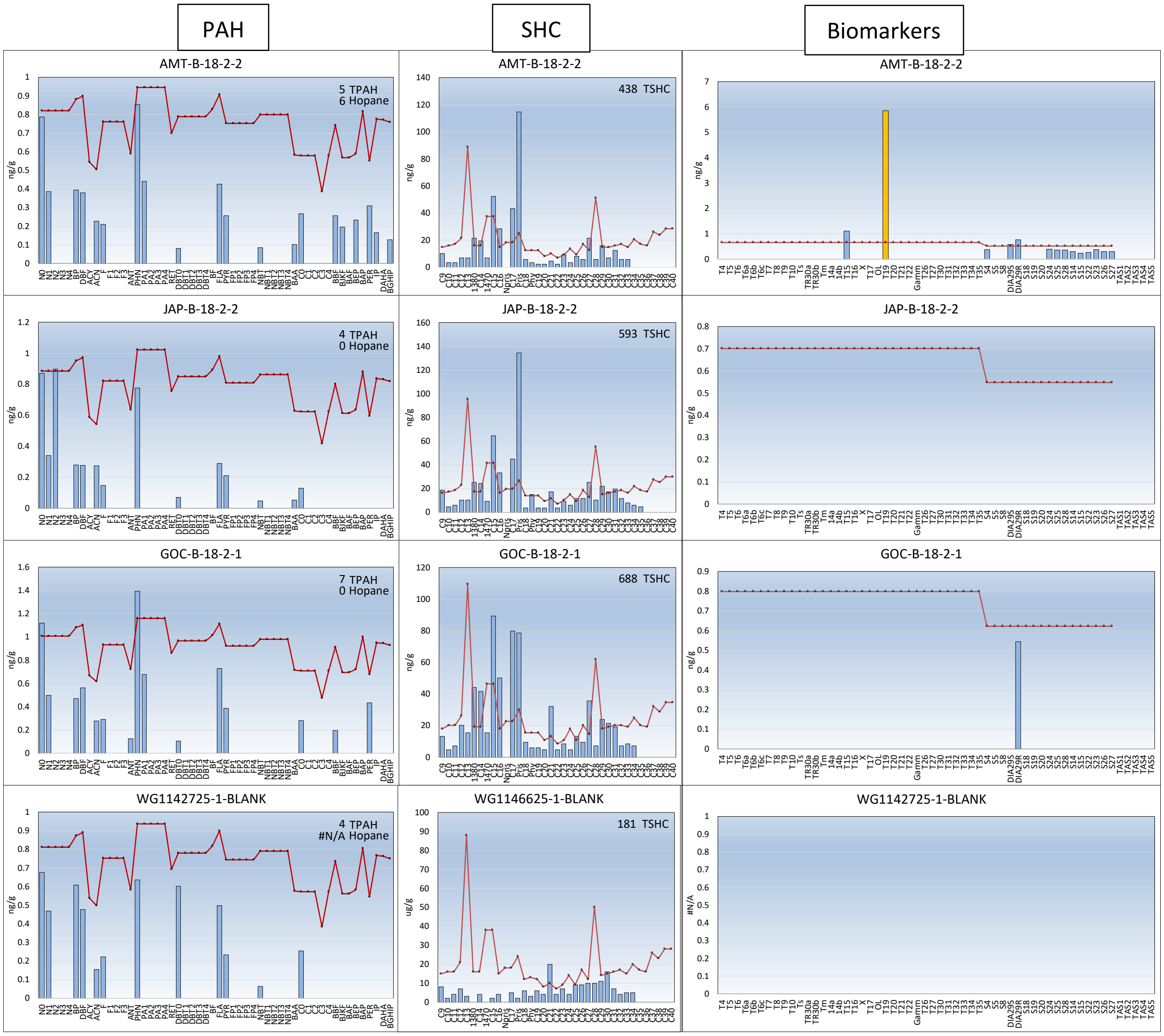

Figure 24. PAH, SHC, and biomarker profiles from representative 2018 mussel samples collected at AMT, JAP, and GOC along with the laboratory method blank extracted and run with the same batch of samples by Alpha/NewFields. The dotted red line above the PAH and Biomarker profiles is the sample-specific method detection limit. Note that most of the PAH in the field samples (with the exception of a few <MDL combustion products at AMT and GOC) are also in the method blank (bottom profile) at practically identical concentrations.

The SHC data for 2008 and 2015 AMT samples (Figure 26) show contributions from marine biogenic sources (Payne et al., 2015) and in the majority (27 of 31) of AMT tissues examined since 2008, the SHC have been dominated by

---

[3] Perylene, a 5-ringed PAH, occurs in crude oil but also is naturally generated from biologic processes or early stages of diagenesis in marine sediments (Bence et al., 2007) and thus, potentially being of non-petroleum origins, is not considered for forensics nor included in TPAH summations when evaluating non-oil matrices.

biogenic constituents (e.g., $n\text{-C}_{15}$, $n\text{-C}_{17}$, and pristane) with only very rare observations of petrogenic components (Payne et al., 2015). Quantified SHC data are not available for 2016 and 2017 mussels. The 2018 SHC profiles in the mussels at all three Port Valdez stations showed only biogenic marine plankton and terrestrial plant wax input with concentrations more that 10-times higher than, and profiles different from, those observed in the method blanks.

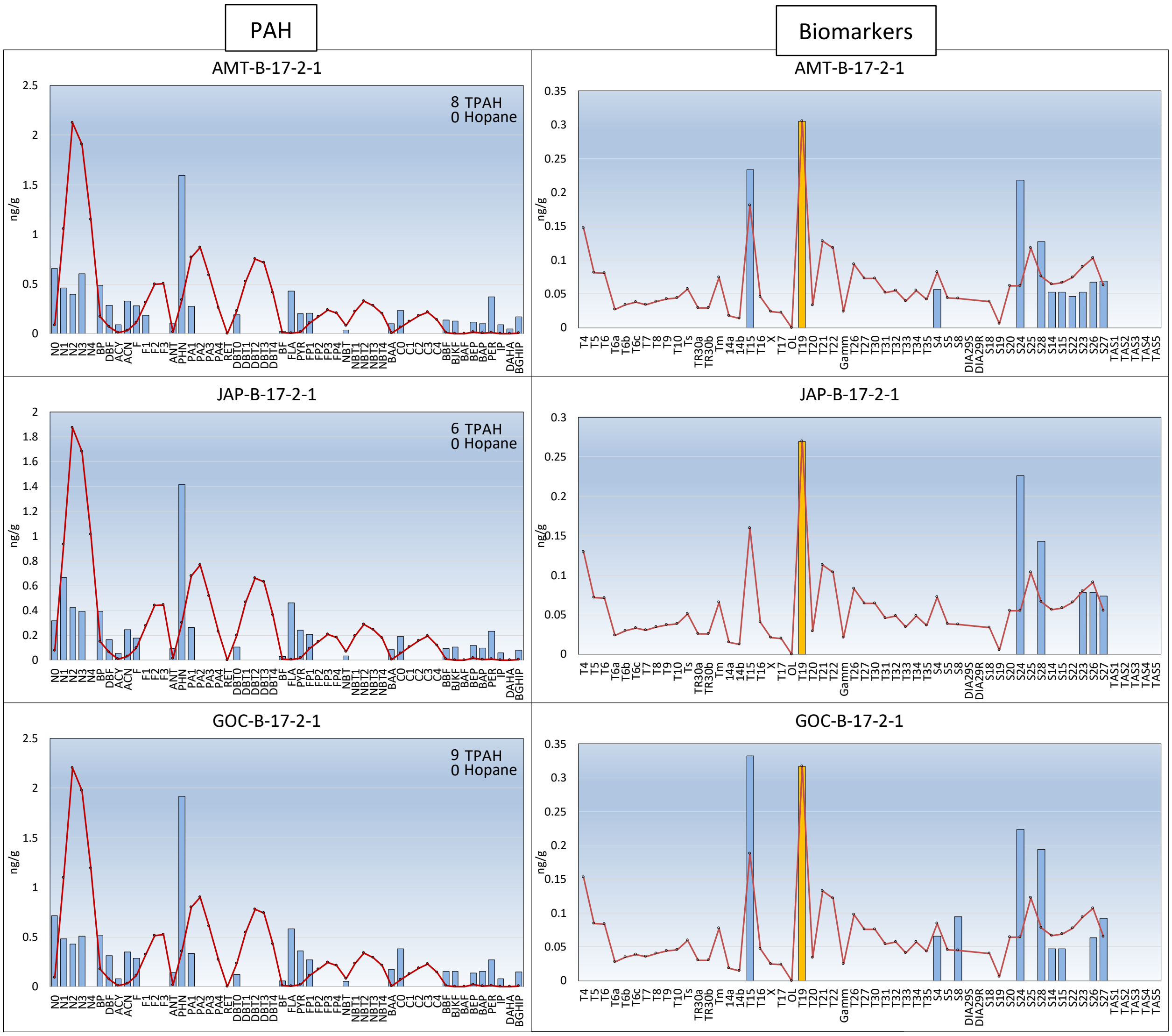

Figure 25. Representative PAH and biomarker profiles from July 2017 mussel collections at AMT, JAP, and GOC. The dotted red line shows the expected scaled profiles from the September 2017 tanker loading arm spill of fresh ANS oil normalized to hopane (discussed below). Note that the TAS do not appear in tissue samples because they are removed during L/C chromatography to separate lipids.

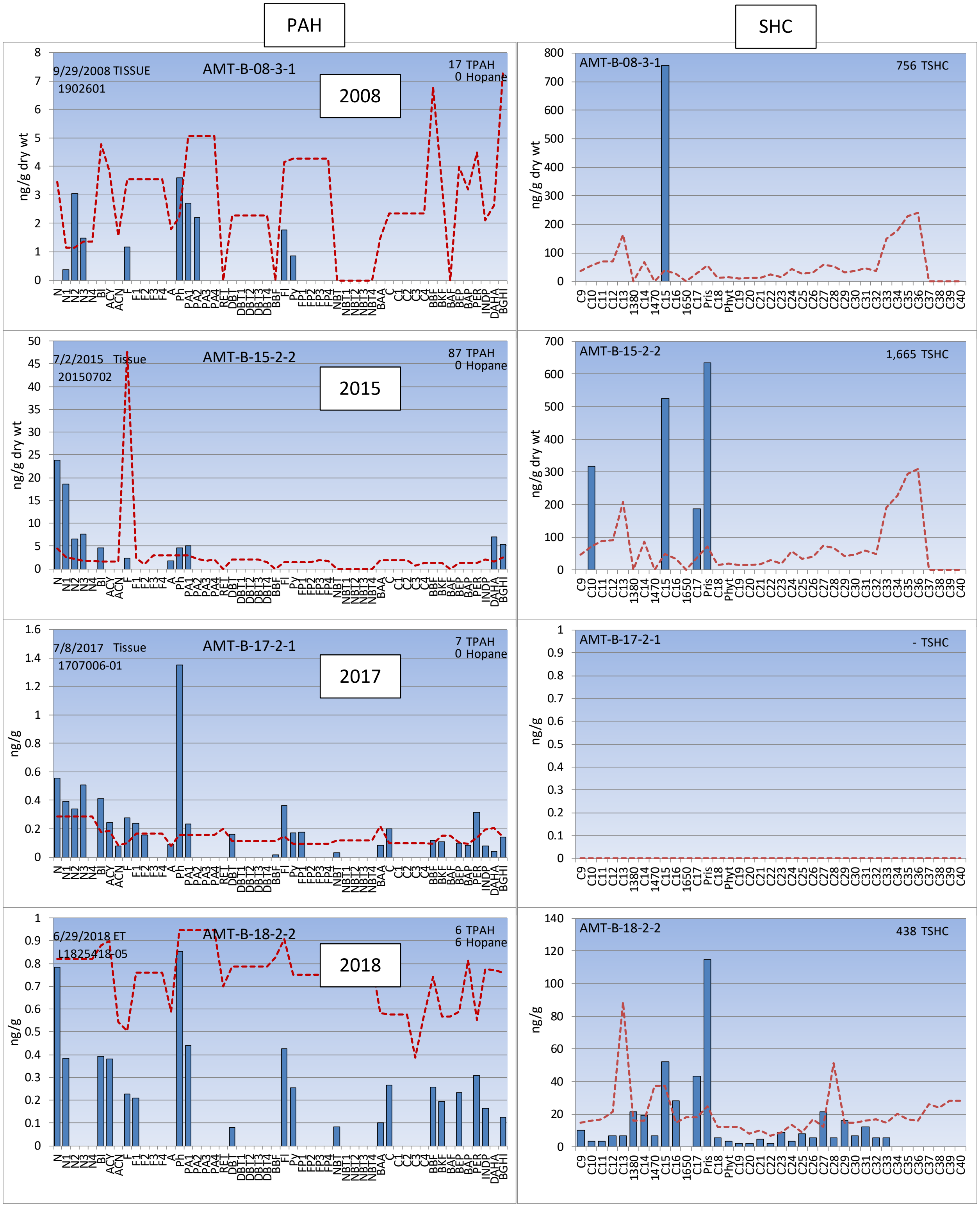

Figure 26. Time-series PAH and SHC profiles of mussels collected at AMT in 2008, 2015, 2017, and 2018 showing primarily below-MDL combustion products (P/A and FL plus PY) in 2008, dissolved-phase naphthalenes in 2015 and 2017 (along with trace-level combustion-product PAHs and perylene), and all <MDL components also associated with the lab blank (Figure 24) except for the combustion products in 2018. Planktonic biogenic SHC (n-C_{15}, n-C_{17}, and pristane) are also present in in other years. Quantified SHC data are not available for 2017 mussel samples. The dotted red line denotes the sample-specific MDL as neither hopane nor NBT2 were present for scaling.

As noted earlier, a notable exception to the declining trend of PAH levels at AMT occurred on 21 September 2017 (Figure 27) when an estimated 150 gallons of ANS crude oil were accidentally released during routine oil-loading-arm testing at Berth 5 of the Alyeska Marine Terminal (Payne and Driskell, 2018b). As part of the post-spill monitoring efforts, mussels were collected by PWSRCAC personnel one week after the spill and again 10 weeks later in December 2017. Following LTEMP protocols, mussels were obtained from the traditional LTEMP Port Valdez stations: AMT, JAP, and GOC. Pre-spill samples from the July 2017 LTEMP effort (Figure 25) showed traces of dissolved-phase hydrocarbons and combustion products (TPAH range 6-14 ng/g DW) whose signatures could not be attributed to the degraded oil discharges of the BWTF. In the week after the Berth 5 spill event, crude oil was present in the tissues from the adjacent AMT site (109-183 ng/g DW) and from JAP (21-30 ng/g DW), but the reference GOC site across the Port was unaffected (TPAH 4-6 ng/g DW) (Figure 28). By December, all three locations had returned to near-background concentrations (2-10 ng/g DW) and to patterns, nearly identical to pre-spill profiles.

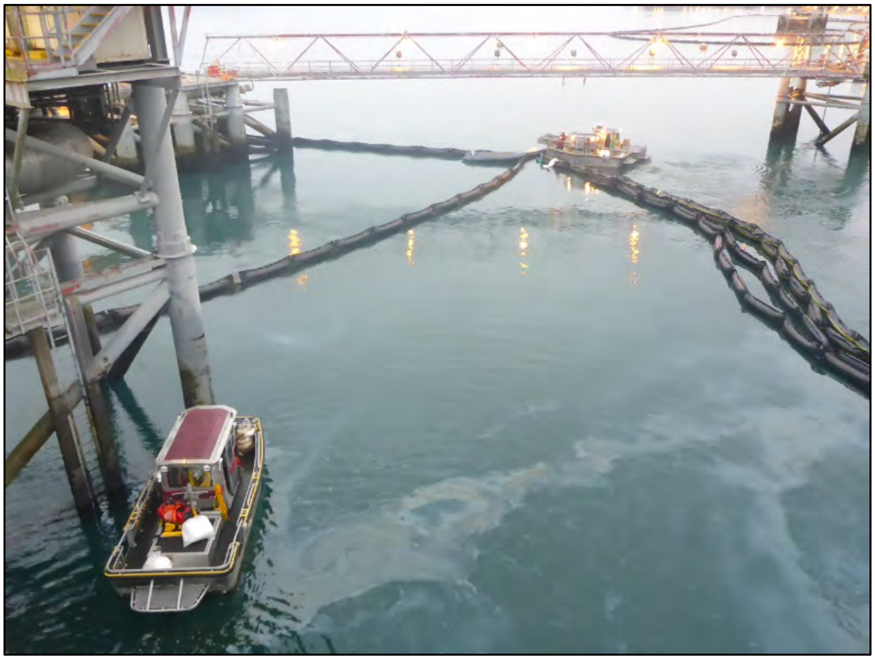

Figure 27. Sheen and containment boom beneath Berth 5 at the Alaska Marine Terminal on 22 September 2017 (PWSRCAC photo).

These data suggest that the mussels were able to completely depurate (purge) themselves of the oil within the 70-day interval although further detailing the actual depuration rate would have required a time series of samples. Other studies have suggested that mussels can purge themselves fairly rapidly following short episodic oil exposures with the decreases in the hydrocarbon concentrations following an exponential curve. Early work reported a depuration half-life of less than a week (Lee, 1977 and Mason, 1988). Later work following the 2002 *Prestige* oil spill suggested more complex processes with two phases of depuration (Neito et al., 2006) and completion within ~30 days. A diesel spill near an aquaculture facility in Washington state took significantly longer to return to background levels; 6-12 months, half-life of ~5 months (Mearns et al., 2014). Obviously, a number of factors may affect depuration rates: oil composition, exposure period, chronic levels, water temperature, mussel size, maturity, body lipid content, stress, etc. The Berth 5 spill data are too limited to establish depuration rates but suffice to say, 70 days after the event, the mussels were effectively clean.

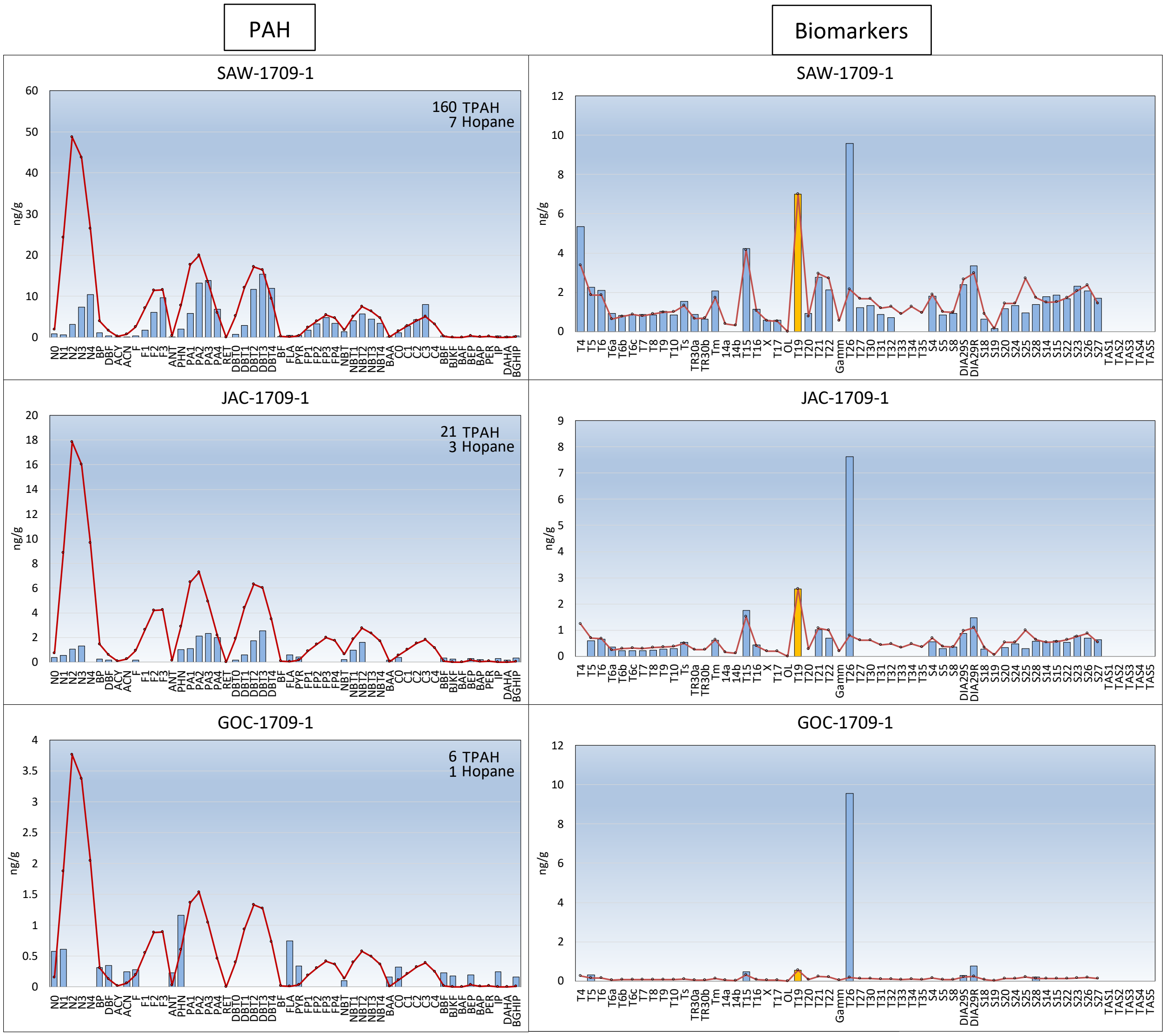

Figure 28. PAH and Biomarker patterns at SAW (AMT), JAC, and GOC collected on 29 September 2017, just over a week after the spill. The dotted red lines represent the anticipated profiles from the collected spill oil normalized to hopane and show the rapid loss of the lower-molecular-weight PAH due to evaporation and dissolution weathering. Biomarker T26 includes a lab artifact.

Because mussel samples were only collected from JAP starting in 2016, prolonged time-series data are not available. But comparisons of representative samples from 2016 and 2017 (Figure 29) show similar trace-level combustion-derived PAH and presumably biogenic steranes whereby the constituent patterns do not correspond with the BWTF effluent. Unfortunately, the source of the 2018 PAH cannot be attributed to the field because the same components were observed in the laboratory method blank at similar concentrations.

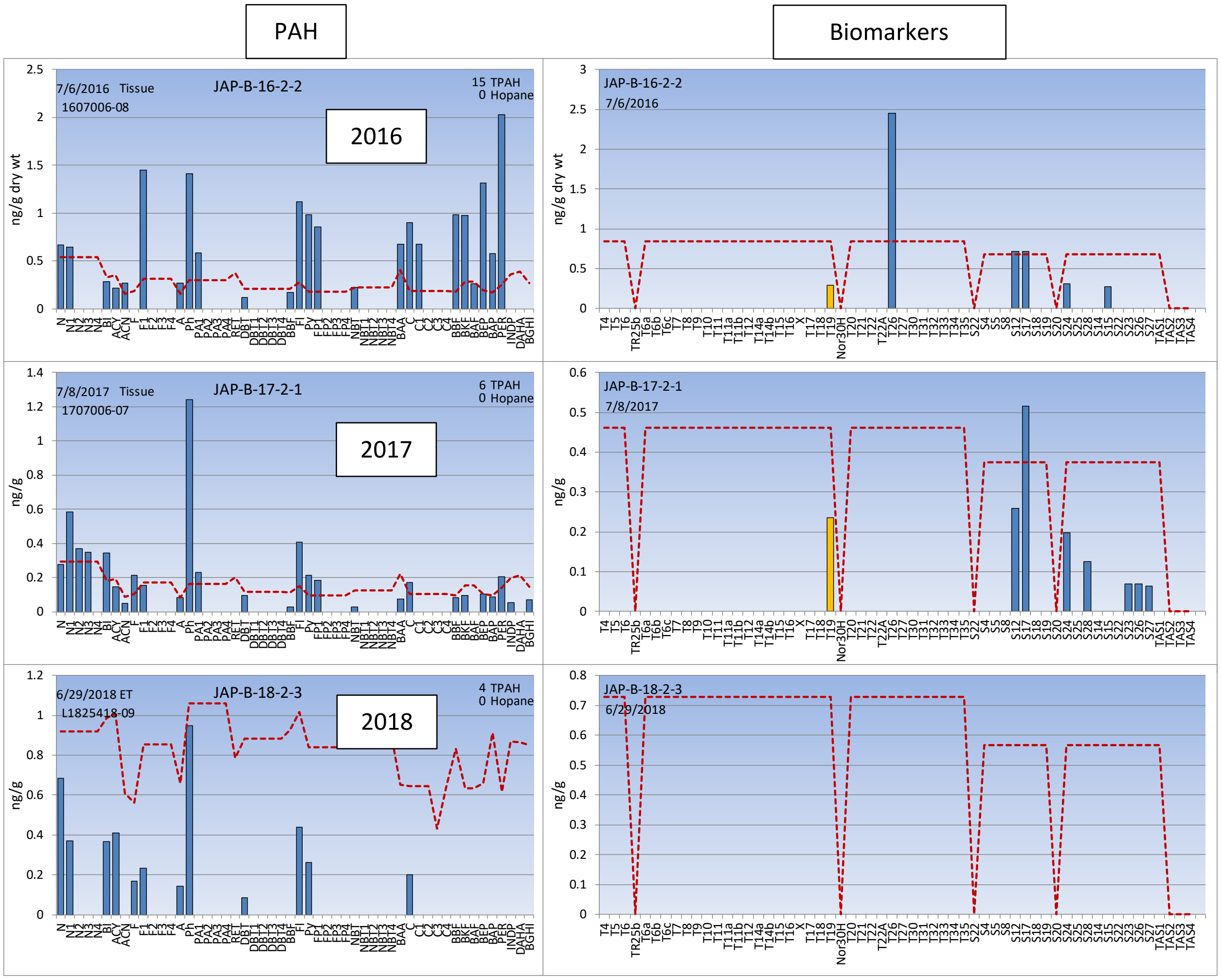

Figure 29. Time-series PAH and S/T profiles of mussels collected at JAP in 2016, 2017, and 2018 showing primarily trace-level dissolved-phase naphthalenes plus combustion product PAHs (Ph, FL, PY, C, BBF, BKE, BEP), and perylene (PER) in 2016 and 2017. Traces of hopane (T19) but not norhopane (T15) are observed along with other steranes, presumably of biogenic origin. T26 is a lab artifact. Quantified SHC data are not available for 2016 and 2017 mussel samples. The below MDL PAH in 2018 are suspected of being procedural artifacts associated with the laboratory procedural blanks (see Figure 24). The dotted red line denotes the sample-specific MDL as neither hopane nor NBT2 were present for scaling.

At GOC, average mussel TPAH levels during the early years of the program (1993-2003) were consistently lower than or very close to those at AMT (Figure 23 and Table 9). In GOC profiles from that era, mixed dissolved-phase, petrogenic, and pyrogenic signals were common and roughly trending with similar phase patterns or discharge events at AMT (Payne et al., 2008a,b; 2010a; 2015). After 2002, as TPAH levels in mussels at both stations trended lower, the signals at GOC have been close to or just slightly above those at AMT, largely due to pyrogenic and occasional petrogenic components. An exception to this mostly parallel trend occurred in 2004 when the PAH and SHC profiles at GOC showed evidence of a fresh diesel spill (Figure 23). The diesel signal had largely cleared by summer 2005, and then the TPAH levels again generally tracked with AMT through July 2015. In July 2016, the GOC TPAH concentrations dropped back to 27 ng/g DW while the corresponding levels at AMT dropped to all-time lows at 8 ng/g DW. In 2017, the TPAH at GOC and AMT were both in single digits at 8 and 6 ng/g DW, respectively.

The time-series PAH plots from Gold Creek (Figure 30) show dissolved-phase naphthalenes plus combustion products in 2008, and dissolved-phase naphthalenes along with at- or below-MDL traces of combustion products in the 2015 samples. By 2016, the PAH pattern shows a well-defined, above-MDL, alkylated fluorene (F) and phenanthrene/ anthracene (P/A) pattern (red tent) indicative of diesel contamination plus background combustion products and perylene (Figure 30 and Figure 31). There was no evidence of residual PAH from the 2016 GOC diesel spill in the 2017 samples (Figure 25). Perylene, can occur naturally, generated by biologic processes or early stages of diagenesis in marine sediments (Bence et al., 2007). Hence, it was no surprise that perylene traces seen in the AMT mussels in 2017 (Figure 25) were also observed at GOC in 2012, 2016, and 2017 (Figure 25 and Figure 30), thus supporting a ubiquitous biogenic-source concept.

SHC in 2008 and 2015 are mostly trace-level biogenic components (e.g., n-C_{15}, n-C_{17}, and pristane) derived from marine phytoplankton, algae, and copepods (Payne et al., 2015). No SHC data were obtained in 2016 or 2017 but as described in Payne and Driskell (2017b), SIM m/z 85 GC/MS profiles and T4 – T6 biomarkers (Figure 31) confirmed the presence of low-level diesel contamination.

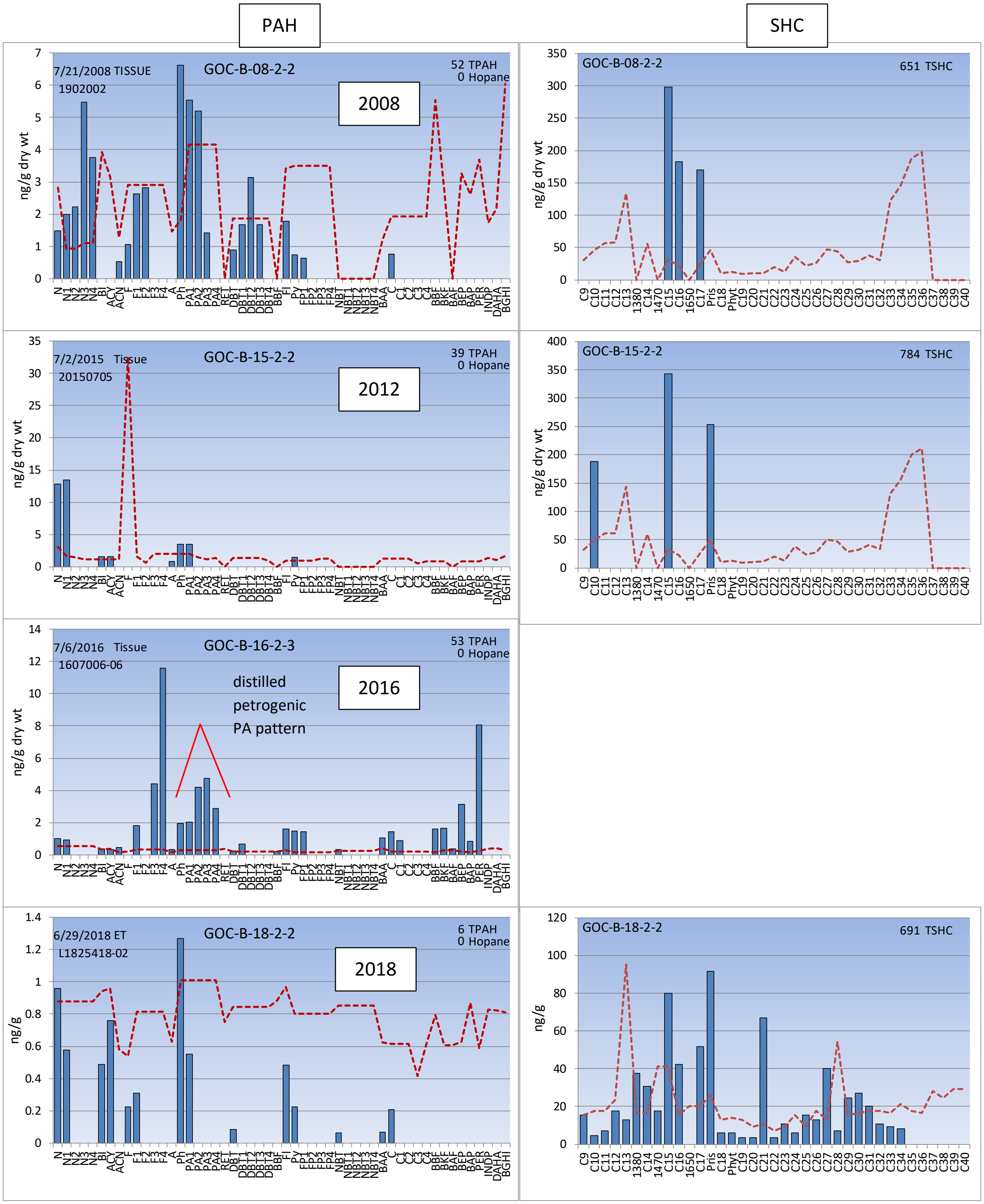

Figure 30. Time-series PAH and SHC profiles of mussels collected at GOC. Dotted red line denotes the sample-specific MDLs. PAH profiles suggest dissolved-phase naphthalenes plus combustion products in 2008, dissolved-phase naphthalenes in the 2015, and petrogenic fluorenes (F1, F3 and F4) and C1-C4 alkylated P/A from a diesel spill in 2016. There was no evidence of BWTF effluent or residual diesel at GOC in 2017 (Figure 25 bottom). SHC in all years are derived from marine phytoplankton, and copepods.

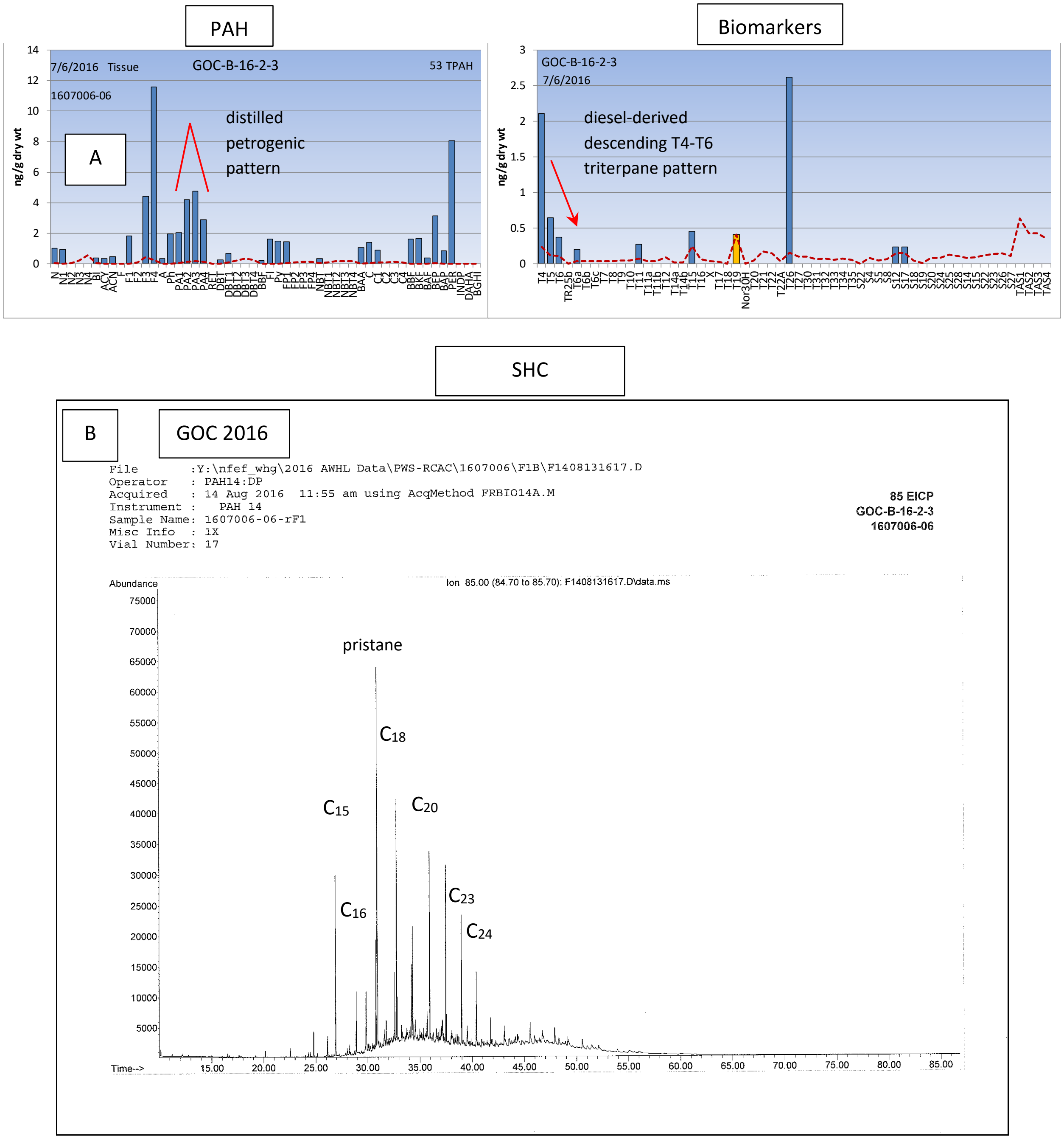

```
File       :Y:\nfef_whg\2016 AWHL Data\PWS-RCAC\1607006\F1B\F1408131617.D
Operator   : PAH14:DP
Acquired   : 14 Aug 2016   11:55 am using AcqMethod FRBIO14A.M
Instrument :    PAH 14
Sample Name: 1607006-06-rF1
Misc Info  : 1X
Vial Number: 17
```

Figure 31. PAH, biomarker, and SHC plots documenting the 2016 diesel spill at GOC: A) 2016 GOC mussel tissue PAH and biomarker patterns with red tent over the PA pattern and descending T4, T5 and T6 triterpanes (red arrow) over the biomarkers derived from a recent diesel input. The dotted red line in the upper plots is BWTF effluent normalized against the sample's hopane; B) Reconstructed ion chromatogram (*m/z* 85) of 2016 GOC tissue with biogenic C_{15} and pristane plus the characteristic C_{16}-C_{24} n-alkane pattern (odd-carbon number/even-carbon number ratio =1) from weathered diesel oil. No evidence of PAH, biomarker, or SHC accumulation from the BWTF effluent is observed but the data show unequivocal evidence of a recent diesel spill.

PRINCE WILLIAM SOUND AND THE GULF OF ALASKA MUSSEL TISSUES

Beginning with the 2009 LTEMP program, sampling frequencies in the greater PWS and GOA region (Figure 32) were reduced from twice annually to once every five years; last sampled in 2013, these stations were resampled in July 2018. Like the Port Valdez stations, the TPAH concentrations have continued to decline to all-time lows ranging from 4-6 ng/g DW (Figure 33). As previously mentioned, because of low TPAH concentrations and interference from laboratory method blanks, summary presentations of representative samples are presented by region; Eastern PWS, Central PWS, and the GOA. Each of these regional summary-plots also includes the laboratory method blank associated with that batch of samples so that the extent of the interference can be easily assessed. Individual PAH, biomarker, and SHC plots for all samples are also presented by region in Appendix 2.

The 2018 mussel-tissue samples from the Eastern PWS stations at KNH and SHB showed only below-MDL traces of PAH (TPAH range 4-5 ng/g DW), and all of the measured components were also present in the method blanks at similar concentrations (Figure 34). The SHC patterns showed primarily biogenic components from marine plankton and terrestrial plant waxes, and the concentrations were 10-times higher with different patterns than those observed in the accompanying method blanks.

The 2018 tissue samples from the Central PWS stations at DII, SLB, and ZAB were very similar to the Eastern PWS samples (compare Figure 34 and Figure 35), as they also showed only below-MDL traces of PAH (TPAH range 4-5 ng/g DW). All of the measured components were also present in the method blanks at similar concentrations. The SHC pattern at DII shows a modest increase in higher-molecular-weight (n-C_{29} to n-C_{33}) complexity that could be due to a very heavily weathered oil residue, but there is no evidence of petroleum in either the PAH or biomarker plots at that station. The other SHC patterns show planktonic alkanes (n-C_{15} and n-C_{17}) plus isoprenoids (Kovat Retention Index 1380 and pristane) and odd-carbon-number terrestrial plant waxes (n-C_{25}, n-C_{27}, n-C_{29}, and n-C_{31}) that were uniquely different from the laboratory method blank. All of the SHC components in the field samples are present at concentrations 10-times higher than those in their respective method blanks.

The 2018 mussel samples from the northwest GOA stations at AIB, WIB, and SHH again showed PAH below-MDL patterns and concentrations that matched those in the batch-specific method blank (Figure 36). In this regard, they were essentially identical to the other PWS and Port Valdez samples collected at the same time. The SHC pattern for AIB shows planktonic alkanes and odd-carbon-number terrestrial plant waxes similar to the patterns observed elsewhere in Prince William Sound. However, the WIB and SHH aliphatic patterns show the same lower-molecular-weight planktonic components, but the higher-molecular-weight waxes are even-carbon-number (n-C_{26}, n-C_{28}, and n-C_{30}) dominated. This unusual profile was also observed at Aialik Bay in April 2007 but the presumed biogenic source is unknown (NAS 1985). Even-carbon-numbered higher-molecular-weight waxes were also occasionally observed in a few near-shore marsh water/suspended sediment samples collected as part of the *Deepwater Horizon* NRDA program in 2010 (Driskell and Payne 2015).

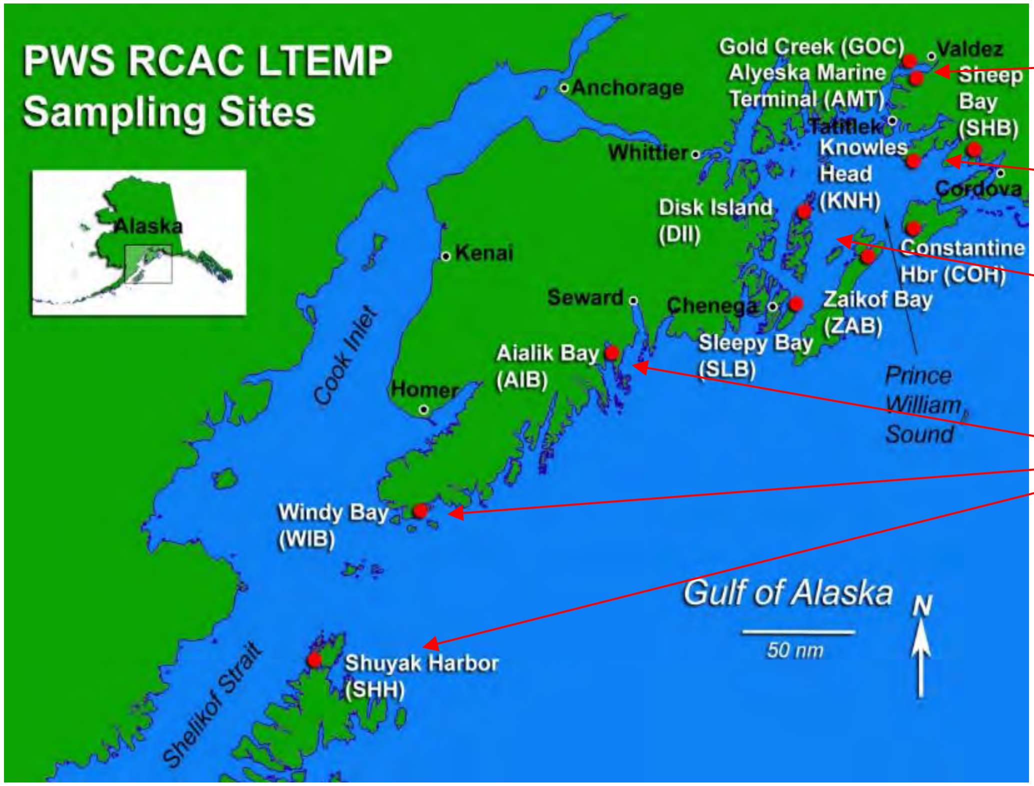

	Location	2008	2009	2013	2018
	Port Valdez				
	Alyeska Marine Terminal	43	38	17	5
GOC	Gold Creek	62	54	20	6
	Eastern PWS				
KNH	Knowles Head	13	17	12	4
SHB	Sheep Bay	15	16	9	5
	Central PWS				
SLB	Sleepy Bay	17	15	28	4
DII	Disk Island	20	13	30	4
ZAB	Zaikof Bay	5	11	33	5
	Western Gulf of AK				
AIB	Aialik Bay	13	10	18	5
WIB	Windy Bay	9	11	59	4
SHH	Shuyak Harbor	15	9	73	5

Figure 32. Map of regional sites now sampled every five years and summary of tissue TPAH43 values (ng/g) for the last four collections.

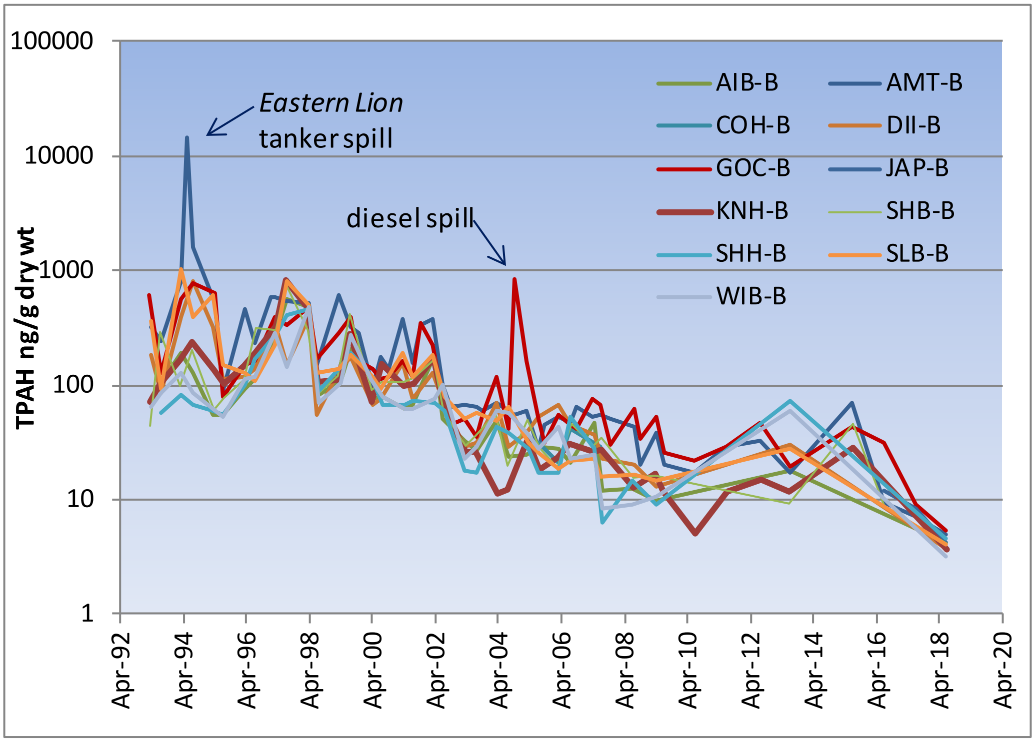

Figure 33. Semi-log plot of mean TPAH values for all LTEMP mussel collections 1993 through 2018. Note, PWS and GOA stations: AIB, GOH, SHH, WIB, DII, and SHB were only collected in 2009, 2013, and 2018. Summary statistics for 2018 (Table 10) show the mean TPAH concentrations ranging from only 3.5 to 5.5 ng/g dry weight with incredibly tight precision throughout the LTEMP study region.

Table 10. Summary TPAH43 statistics for 2018 Tissues (ng/g DW).

2018	avg	max	min	count	± SE
AIB-B	4.5	5.4	3.9	3	0.43
AMT-B	5.0	5.7	3.9	3	0.54
DII-B	4.0	4.1	3.9	3	0.04
GOC-B	5.5	6.5	4.4	3	0.63
JAP-B	3.9	4.3	3.5	3	0.24
KNH-B	4.2	4.7	3.8	3	0.26
SHB-B	4.6	4.8	4.4	3	0.12
SHH-B	4.9	7.4	3.1	3	1.25
SLB-B	4.4	4.6	4.1	3	0.13
WIB-B	3.5	3.7	3.3	3	0.12
ZAB-B	4.8	5.0	4.5	3	0.13

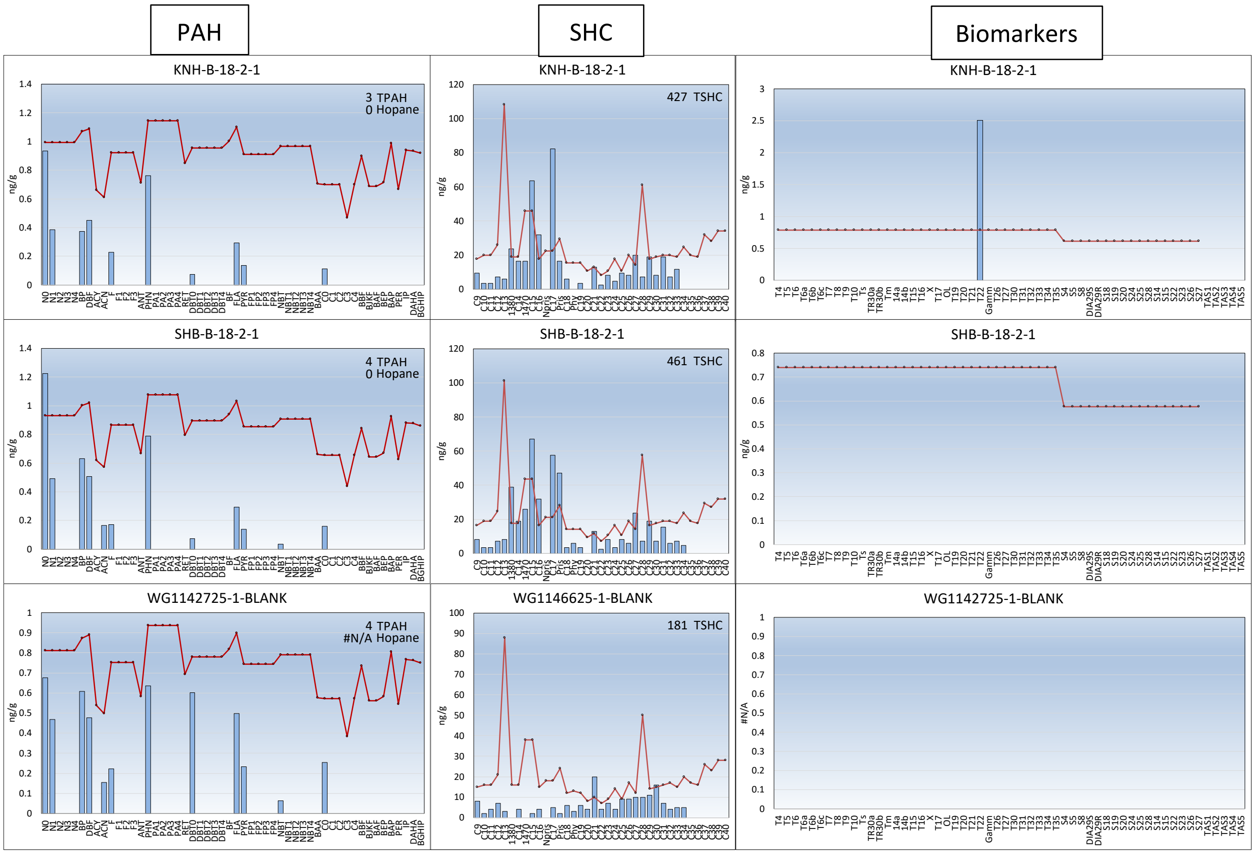

Figure 34. PAH, SHC, and biomarker plots of eastern PWS stations KNH and SHB along with the associated laboratory-batch method blank analyzed from the 2018 collections. All of the PAH are below the sample-specific MDLs shown by the dotted red lines in the plots, and the commonality between the samples and the blank in terms of both the constituent patterns and concentrations is readily apparent. The SHC patterns show planktonic alkanes (n-C_{15} and n-C_{17}) plus isoprenoids (1380 and pristane) and odd-carbon-number terrestrial plant waxes (n-C_{25}, n-C_{27}, n-C_{29}, and n-C_{31}) that were not present in the same distributions or concentrations as the laboratory method blank.

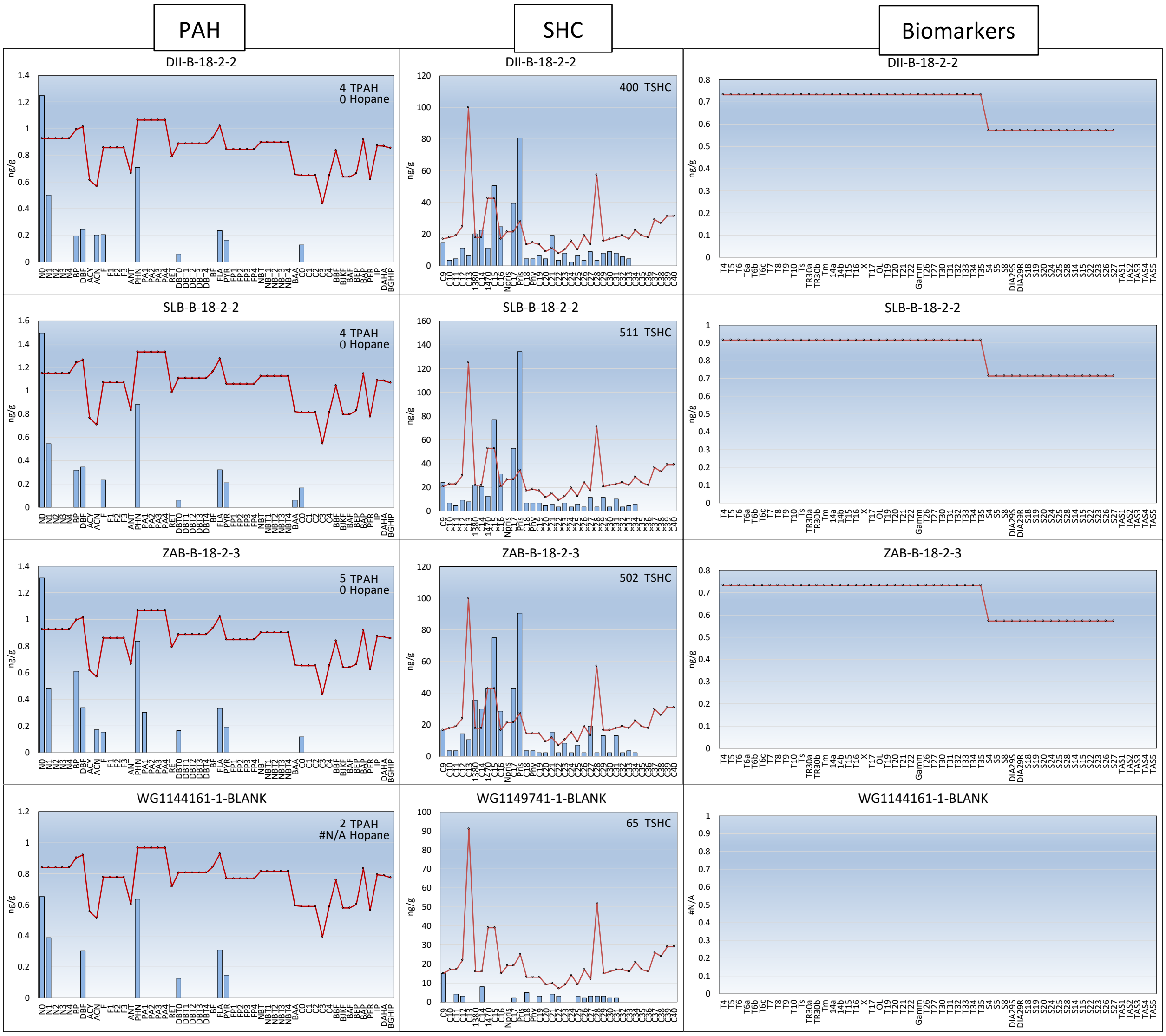

Figure 35. PAH, SHC, and biomarker plots of central PWS stations DII, SLB, and ZAB along with the associated laboratory-batch method blank analyzed from the 2018 collections. All of the PAH are below the sample-specific MDLs shown by the dotted red lines in the plots, and the commonality between the samples and the blank in terms of both the PAH constituent patterns and concentrations is readily apparent. The SHC patterns show planktonic alkanes (n-C_{15} and n-C_{17}) plus isoprenoids (1380 and pristane) and odd-carbon-number terrestrial plant waxes (n-C_{25}, n-C_{27}, n-C_{29}, and n-C_{31}) that were not present in the same distributions or concentrations as the laboratory method blank. The DII SHC pattern shows a little additional higher-molecular-weight complexity (n-C_{29} to n-C_{33}) that could be due to a very heavily weathered oil residue, but there is no evidence of petroleum in either the PAH or biomarker plots.

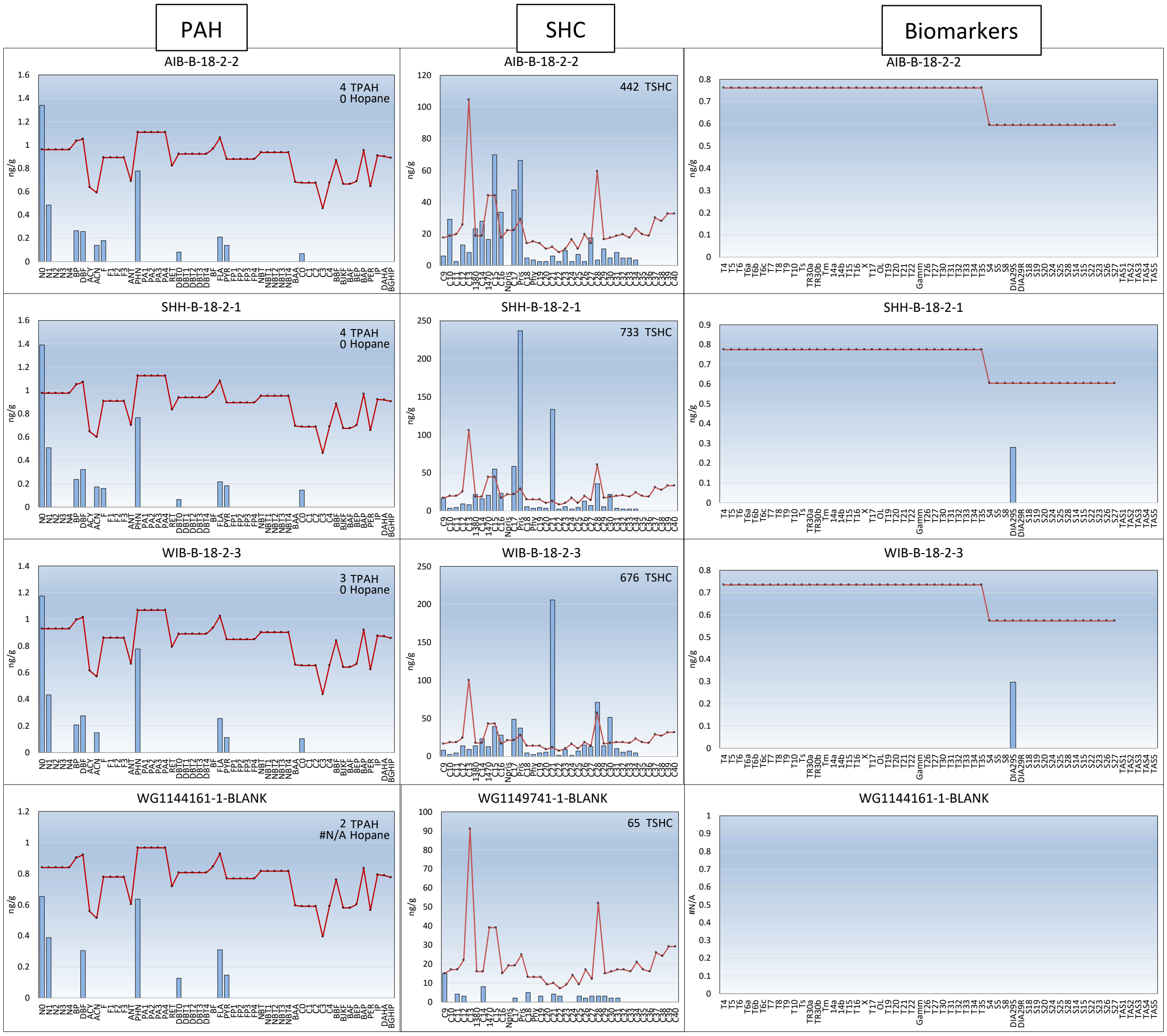

Figure 36. PAH, SHC, and biomarker plots of GOA stations AIB, WIB, and SHH along with the associated laboratory-batch method blank analyzed from the 2018 collections. All of the PAH are just at or below the sample-specific MDLs shown by the dotted red lines in the plots, and the commonality between the samples and the blank in terms of both the PAH constituent patterns and concentrations is readily apparent. The SHC pattern for AIB (top plot) shows planktonic alkanes (n-C_{15}, n-C_{17}, and n-C_{21}) plus isoprenoids (1380 and pristane) and odd-carbon-number terrestrial plant waxes (n-C_{25}, n-C_{27}, n-C_{29}, and n-C_{31}) that were not present in the same distributions or concentrations as the laboratory method blank. WIB and SHH's SHC patterns show the same lower-molecular-weight planktonic components, but the higher-molecular-weight waxes are even-carbon-number (n-C_{26}, n-C_{28}, and n-C_{30}) dominated. This was also observed at AIB in April 2007, but the presumed biogenic source is unknown (NAS 1985). Nevertheless, there is no evidence of petroleum in either the PAH or biomarker plots from these two stations.

OXYGENATED PRODUCTS IN TREATED BALLAST WATER DISCHARGES

As described in last year's report (Payne and Driskell 2018c), three effluent samples, raw, filtered (particulate oil droplets), and dissolved-phase, were collected from the BWTF discharge pipe in July 2016 and March 2017. In addition to the standard PAH, SHC, and biomarkers analyzed as part of LTEMP, we independently (without PWSRCAC support) had the July 2016 sample extracts screened for oxygenated products by a colleague, Dr. Christoph Aeppli of Bigelow Laboratory (Maine). Oxygenated hydrocarbons, whether created microbially, by solar radiation, or by chemical processes, are currently considered by hydrocarbon fate-and-weathering scientists to be the "Holy Grail" in understanding oil-degradation products. Conceptually, the effluent from a ballast water treatment facility designed to promote oil biodegradation would be an ideal substrate to use for method development and validation.

To date, Dr. Aeppli has used an Iatroscan (TLC-FID) method to separate components in the July 2016 extracts into saturated, aromatic, mono-oxygenates, and di-oxygenates. Extracts from fresh ANS crude oil and the three effluent samples from the July 2016 (Figure 37) showed the expected depletion of the saturate (SHC) and aromatic (PAH) in the fresh ANS oil with their subsequent conversion into oxygenated products with one- and two-oxygen additions. Because of the increased water solubility of oxygenated products, the highest relative concentrations of mono- and di-oxygenated constituents were observed in the filtered, dissolved-phase fraction sample. Over 93% of the measured components in that sample were oxygenates compared to only 36% in the starting oil. These results confirmed our expectations and help to document the biological treatment tank's efficacy in converting hydrocarbons into water-soluble, biodegradation-products. Subsequently, after discharge into the Port, oxygenated products are more easily diluted and further weathered.

Continuing with method development, additional analyses are being undertaken using HPLC/MS, GC x GC/MS, and by selected ion monitoring GC/MS after chemical derivatization into tri-methyl-silane (TMS) ethers and esters. To date, a series of alcohols, carboxylic acids, diols, and dioic acids have been detected although explicit compound identifications have not been completed. Nevertheless, these unfunded studies are expected to help expand this line of investigation and may eventually help to track oxygenated products as they further degrade following discharge from the BWTF or in future oil-spill releases.

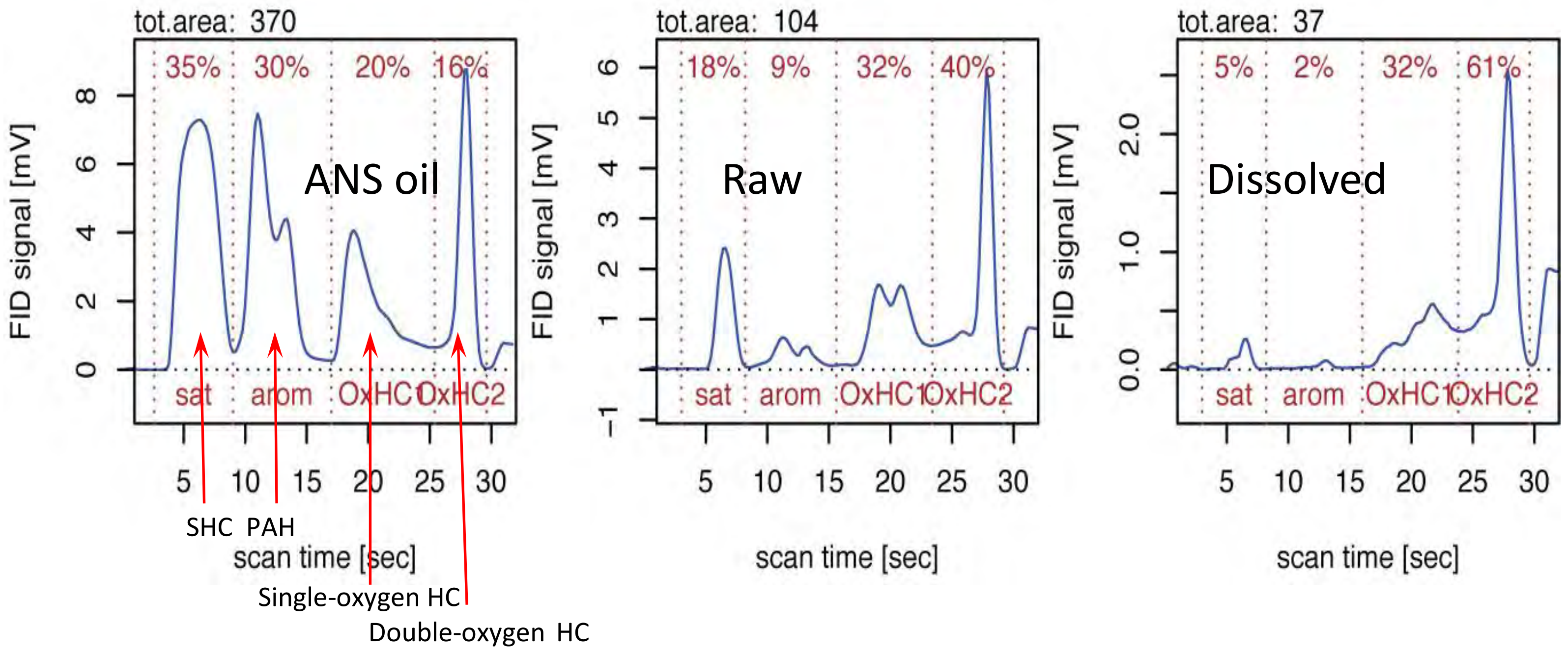

Figure 37. Iatroscan (TLC-FID) of ANS oil, BWTF raw effluent and BWTF dissolved components from July 2016 showing relative abundance of single- and double-oxygenated (weathered) hydrocarbons relative to SHC and PAH components. Courtesy of Christoph Aeppli.

PASSIVE SAMPLING DEVICES

Back in 2016 and 2017, PSDs were deployed at the three Port Valdez sites to sample concurrent with the LTEMP mussel collections (Minick and Allan, 2016; Allan, 2018). The goal was to compliment the LTEMP tissue data with integrative, longer-term sampling using these high-sensitivity devices. In 2018, the program was expanded to encompass KNH, a clean site originally located near a tanker anchorage, and DII, a site known to contain residual EVOS oil. Generally, the PSD, a low density polyethylene membrane in this case, is intended to only sample a fraction of the total hydrocarbon analytes present, namely, just freely dissolved compounds and labile complexes that diffuse into the membrane. For biota, these are the most bioavailable hydrocarbons. The LTEMP devices were expected to sample dissolved PAH and other oxygenated hydrocarbons. The PSD analytic laboratory, OSU's FSES Lab, reports 61 PAH isomers as their normal analyte list but for 2018, the analyte list was expanded to include 40 parent and alkylated PAH homologs used routinely for forensic interpretations. As a critical part of the method, various deuterated surrogate compounds that were pre-infused into the membrane are quantified to calculate dissolved-phase water concentrations. Their known rate of diffusion out of the membrane while the dissolved hydrocarbons are diffusing in enables the desired calculation of hydrocarbon concentrations in the water column. The LTEMP PSD were anchored and constantly submerged for approximately 30 days in shallow nearshore locations adjacent to the LTEMP mussel sites.

After processing and analysis at OSU, the 2016 data were somewhat ambiguous. The expected oxygenated forms seen in the BWTF effluent by initial Iatroscan analyses were not detected and the analyte list did not include the alkylated forensic PAH so, interpretive insights were limited. In the 2016 report, Allan (2018) suggests a pyrogenic naphthalene signature is the dominant feature but considering the sampling device, it's more likely a water-washed pattern of dissolved naphthalenes (Figure 38). However, there was another issue; the presence of two insoluble hopane biomarkers, 17α(H),21β(H)-30-norhopane and 17α(H),21β(H)-hopane, suggested the device and analyses were also seeing a trace level of particulate hydrocarbons. Unfortunately, biomarkers were not included in the 2017 or 2018 analyses, so results are still slightly equivocal as to the presence of particulate oils. From GOC, 2016 data showed slightly elevated parent phenanthrene (compared to AMT and JAP) but there was no discernible evidence of the 2016 diesel spill suggested in LTEMP data. In 2017 and 2018, the PSD patterns were all similar with a supra-dominant, water-washed naphthalene pattern and assorted traces of parent and alkylated PAH up to chrysene (Figure 38). Normally, such a naphthalene-dominated profile suggests a strong dissolved-phase signal. But within a dissolved pattern, the naphthalenes as a group are typically in a descending pattern of parent (N0) greater than N1, etc., based on decreasing solubility with increased alkylation. The ascending pattern seen in these samples is more typical of a water-washed particulate profile—but the analytes can't be particulate; the PAH must be in a dissolved phase in order to diffuse into the PSD device. The alternative explanation for this anomaly is that the original dissolved pattern (descending with alkylation) must have been previously weathered by some other mechanism prior to ending up in the water and subsequently the PSD.

So, what's with pre-weathering? Microbes preferentially work on the lesser alkylated PAH first. In the BTT, the effluent could have undergone extra microbial scavenging before discharge. The dissolved phase would then simply reflect diffusion of lighter-molecular-weight hydrocarbons from an already weathered particulate profile. We saw these profiles in near-surface water samples during the *Deepwater Horizon* spill where presumably a slick was subjected to evaporative or solar weathering while at same time was dissolving naphthalenes into the water column (Payne and Driskell, 2015a). But that scenario ignores two pieces of the 2018 PSD evidence. First, the excess

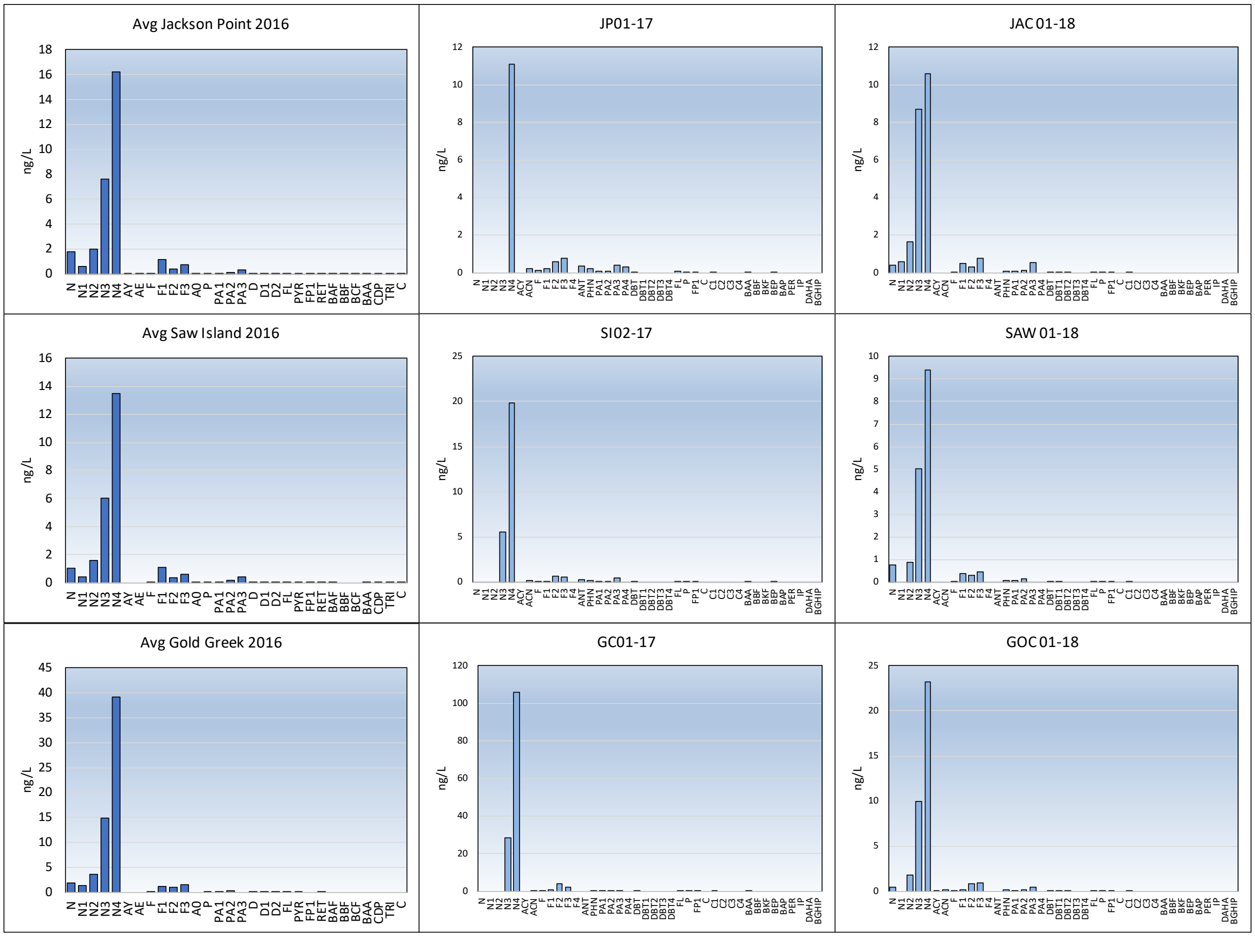

Figure 38. Example PAH profiles of PSD sampling from 2016 (avg), 2017, and 2018. Each show a dominant naphthalene group suggesting a mostly dissolved-phase but highly-weathered signal. Specifically, the more volatile naphthalene (N) and lower-alkylated homologues (N1 and N2) appear to have been lost to evaporation.

naphthalenes in all years are far too out of balance with the other PAH to have come from ANS oil (Figure 38). Secondly, the two PSD collections from outside Port Valdez, and thus quite distant from any BWTF influence, still show basically the same patterns (Figure 39). One of the stations, DII, is known to have fresh-looking, residual EVOS oil, the other, KNH, is essentially an extremely clean control site but both have essentially the same patterns as those in Port Valdez. And, it's important to remember that ALL the mussels in all the regions are reporting in clean. Furthermore, the dissolved profile we would expect to see from whole oil should resemble samples collected in a 2002 study (among others) from water leaching off/out of EVOS-oiled beaches 13 years after the spill (Figure 40); a dissolved profile distinctly different from the sparse PSD profiles (Payne et al. 2005d). Nor do the PSD profiles look like the dissolved effluent samples taken directly from the BWTF discharge pipe in 2016-17 (Figure 5c).

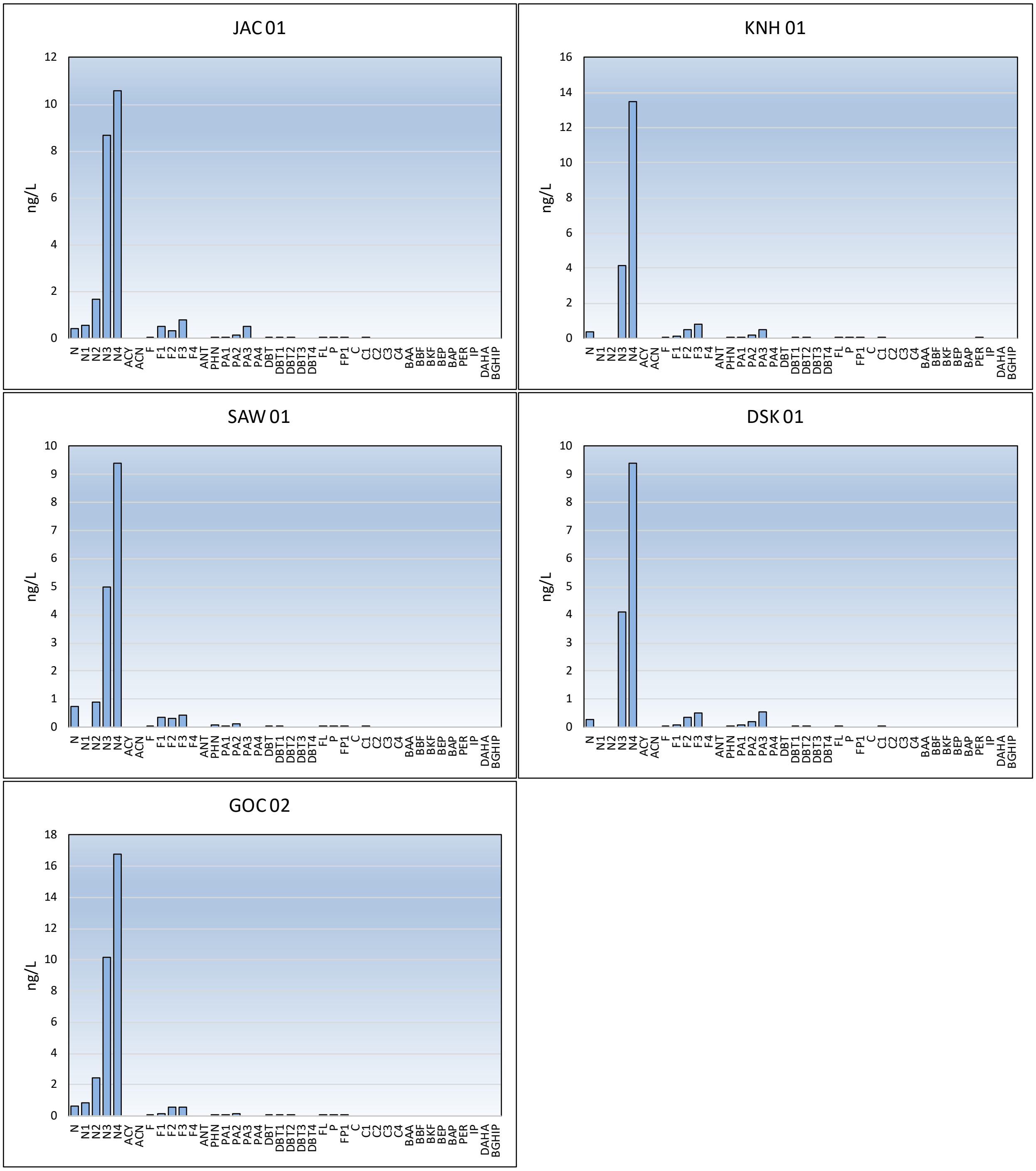

Figure 39. PAH profile examples from 2018 PSD deployment. Left panels from Port Valdez stations (see previous figure). Right panels from KNH and DII.

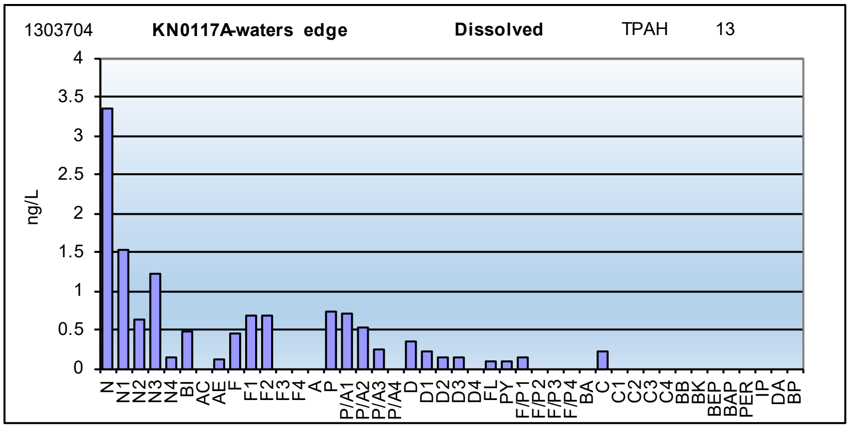

Figure 40. Dissolved PAH profiles from nearshore water sampled off EVOS interstitially oiled beach (Payne et al., 2005d).

In the 2013 LTEMP report, low-level, dissolved patterns in the regional mussel profiles invoked a hypothesis then, as now, that external natural background inputs of PAH derive from large-scale phenomena such as wildfires, glacial melts, riverine inputs, or terrestrial runoff (peat and coal are naphthalene rich). As an example of these large-scale processes, recall that following the EVOS event there was debate over the PAH found uniquely in the depths of PWS. Eventually, it was resolved to have originated from source rock formations in the Yakutat region (Deepthike et al. 2009). Later environmental mapping project (EMAP) survey work, a joint project of the EPA and Cook Inlet Regional Citizens Advisory Council, traced the non-bioavailable, PAH-laden particulates completely across the northern GOA and down the Alaska Peninsula (Saupe et al., 2005).

In summary, both the 2018 LTEMP mussels and PSDs were extremely clean with mussels showing only confounding components from the laboratory method blanks while the PSDs showed only a background pattern at all stations and with no recent petroleum hydrocarbon contamination. The dissolved source is irresolvable from the LTEMP and/or PSD data sets. But together, they say both Port Valdez and PWS contained few, if any, dissolved PAH contaminants in 2018. The expectation for the PSD method to detect some of the OPAH compounds seen in the BWTF effluent is still unrealized but for future work, the results from the oxygenated-compounds method development mentioned above may help select a different set of OPAH for the OSU lab to analyze.[4]

DISCUSSION AND SUMMARY TRENDS

A fundamental problem with the LTEMP program is the frequency of sampling. Essentially, the annual data within the Port is equivalent to just a snapshot of the constantly varying conditions both within the treatment system, the discharge, stratification of and transport in the receiving waters, subsequent oil weathering, and the seasonal condition of the mussel populations (feeding, purging, spawning, thermal and freshwater stresses, etc.). From Alyeska's DMRs to EPA, documenting the performance and any violations in the BWTF system, various parameters' time series demonstrate how little of the variability is observed with LTEMP collections (Figure 41).

---

[4] Dr. Sarah Allan, a member of the PWSRCAC's Scientific Advisory Committee and principal investigator for the PSD method, comments, "The primary motivation for putting PSDs out as part of LTEMP was to determine bioavailable water concentrations, with toxicologically relevant DLs, to assess possible IMPACTS to very sensitive species and life stages (e.g., Pacific herring). … The mussels and sediments are great for demonstrating trends over time and assessing sources. The PSDs provide complementary, biologically relevant data for assessing potential impacts. In this case, the data show dissolved PAHs below known toxicity thresholds for marine organisms."

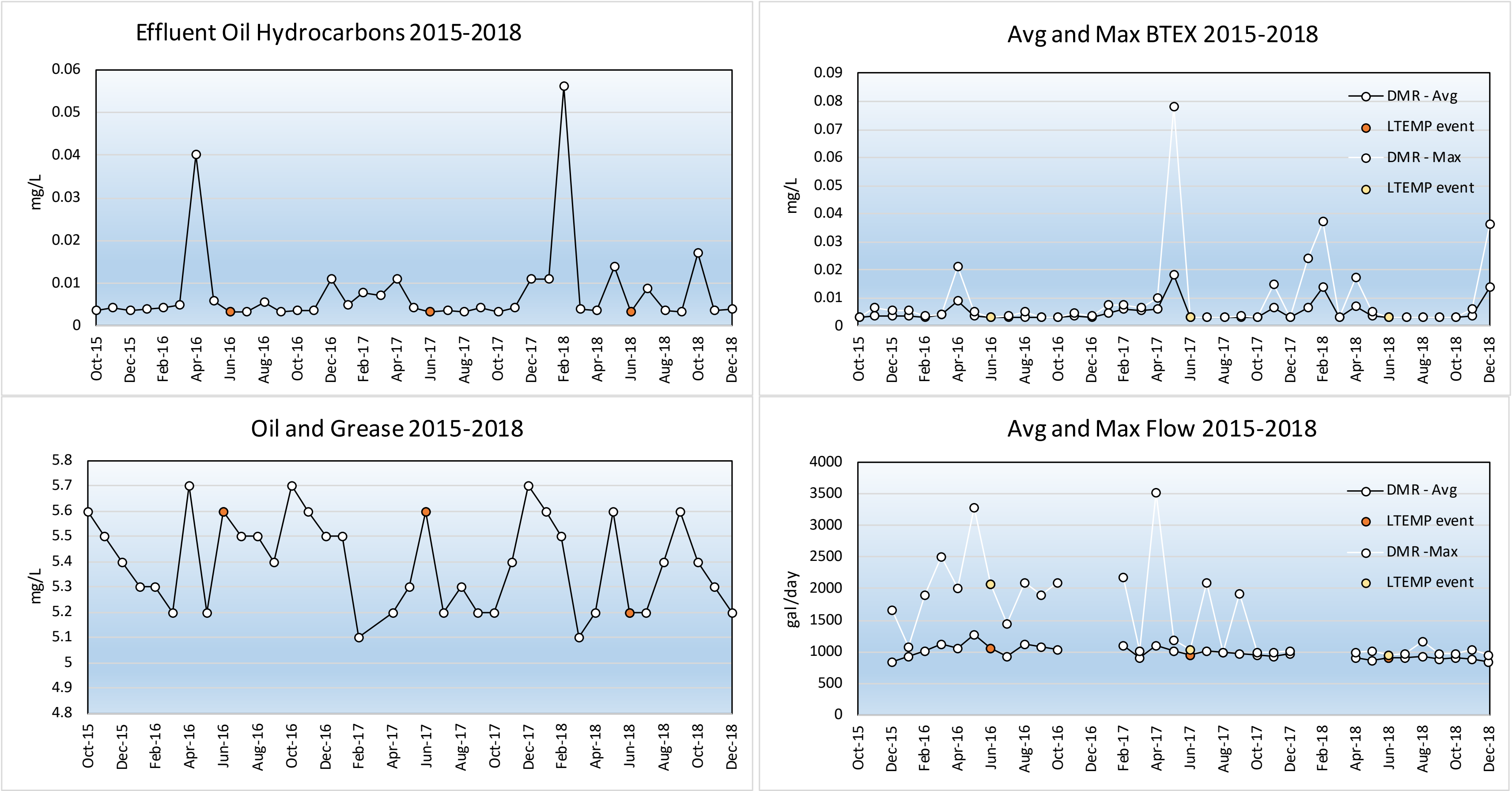

Figure 41. Time series of various DMR parameters as reported in Alyeska's monthly DMRs from October 2015 through December 2018. Orange and yellow dots represent the timing of LTEMP's July samplings demonstrating the variance not captured by "snapshot" mussel and sediment collection frequency.

It was fortunate that in 2016 and 2017, our forensics understanding was greatly improved by analyses (PAH, SHC, and biomarker) of phase-separated, seasonal effluent samples from the BTT at Alyeska's BWTF. These data provided a detailed fingerprint of the dominant hydrocarbon source to the Port and also allowed direct comparison of the effluent profiles to the time-series sediment and tissue data to parse the relative petrogenic (oil-based) vs. pyrogenic (combustion-derived) portions in the samples. Unfortunately, the two seasonally dissimilar profiles further emphasize the dynamically changing character of the effluent. Unlike an ANS-source oil, there is no standard effluent profile for forensic interpretations.

Two other studies should be mentioned in regard to assuming a sample should only pick up a dissolved signal. In 2015, ABL did a study for the PWSRCAC looking for oil in Port Valdez shrimp eggs (Carls et al. 2016). They posited that a clutch of eggs attached to the pleopods of gravid shrimp would be exposed to and absorb a dissolved PAH signal from residual hydrocarbons in the soft sediments. Although ABL did not analyze for (particulate-confirming) biomarkers, in at least one sample (Figure 42), the profile appears to be a water-washed particulate profile. Either particulate oil is capable of infusing through a shrimp's chitin egg shell and inner lipid membranes or there was a problem with the lab's sample cleanup methods. Another study, however, also showed a particulate signal, this time in eggs of red crabs sampled on the abyssal plain in the Gulf of Mexico during the *Deepwater Horizon* incident including a full suite of biomarkers (Douglas and Liu, 2015; G.S. Douglas, personal communication, 2015). Crustacean eggs appear to absorb more than just dissolved-phase contaminants. If this is the case, then the general supposition of dissolved-phase hydrocarbons' exclusive bioavailability versus particulate-phase non-bioavailability is perhaps over-simplified. This would certainly be the case when copepods that have ingested oil micro-droplets in Port Valdez (Carls et al., 2006) are later consumed by predators (e.g., salmon smolt) or when mussels filter micro-droplets from the water column.

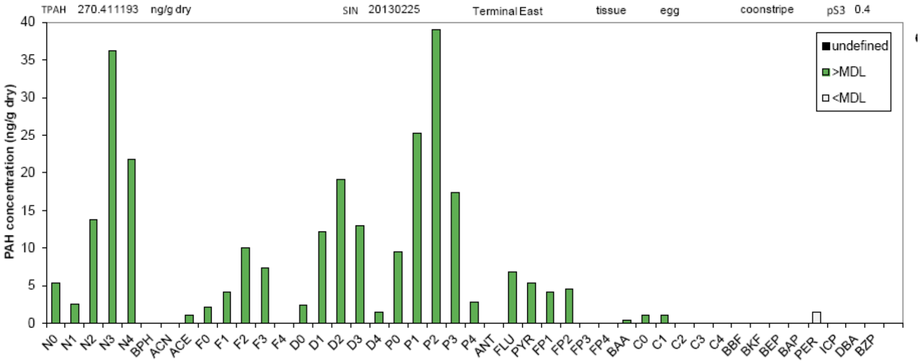

Figure 42. PAH plot of shrimp eggs taken east of Alyeska Marine Terminal, which in our assessment, shows a water-washed, weathered particulate-oil pattern absorbed through the chitin, lipid membrane and into the fat of the eggs. From Carls et al., 2016.

SUMMARY POINTS

Due to a combination of reduced BWTF discharge volumes from historically decreased North Slope oil production, the transition to double-hulled tankers with segregated ballast tanks, and improved BWTF efficiency in removing particulate/oil-phase hydrocarbons, permitted oil inputs into Port Valdez from the Alyeska Marine Terminal have been declining in recent years.

TPAH concentrations in mussels at AMT, JAP, and GOC are now reaching all-time, single-digit lows (4-6 ng/g DW, ppb).

- At AMT, mussel PAH contamination over the last 10-plus years has been shifting away from the earlier petrogenic profiles towards trace-level background, dissolved-phase or mixed pyrogenic and petrogenic patterns. In 2018 the concentrations were so low, that the PAH patterns could not be differentiated from below-MDL components in the laboratory method blanks.
- GOC mussels have generally shown only low-level pyrogenic PAH profiles since 2006 but in 2016, evidence of a diesel spill was observed. All evidence of the 2016 diesel spill had disappeared by 2017, and the 2018 PAH concentrations could not be differentiated from the laboratory procedural blanks.
- At the Eastern- and Central-PWS stations (KNH, SHB, DII, SLB, and ZAB) as well as the GOA stations (AIB, WIB, and SHH) the 2018 mussels all show below-MDL PAH components with the same concentrations and patterns as those observed in the laboratory blanks. As such, there is no evidence of any measurable petroleum hydrocarbon contamination at any of these sites. These areas were all approaching background levels in 2013, and it now appears that the concentrations have dropped to the point that we can no longer comment on regional patterns or sources for either petrogenic or pyrogenic hydrocarbons.
- The 2008-2018 SHC in mussels from all locations exhibited primarily background biogenic components with the exception of a petrogenic signal at AMT in 2013. Quantified mussel SHC data were not available for 2016 or 2017.
- Like their corresponding mussel samples, PSDs showed only a low level background pattern at all stations with no evidence of recent petroleum hydrocarbon contamination.

In sediments, Port Valdez TPAH levels have been decreasing and reached all-time lows in 2013 but unlike the trend observed with the mussel tissues, sediment TPAH concentrations at both stations have slightly increased over the last three years.

- At the terminal, the 2016 and 2017 AMT sediment PAH patterns are nearly identical but have shifted from a dominant pyrogenic pattern in earlier samples (2011–2015) to a mix in 2018 of combustion products and highly weathered petrogenic components derived from the BWTF effluent. Biomarker profiles from 2011 through 2018 strongly confirm the linkage to the BWTF effluent. SHC patterns show a mixture of marine and terrestrial biogenic components along with higher-molecular-weight petrogenic waxes at reduced levels compared to earlier years. Based on the signatures, these patterns suggest variable or increased background inputs of weathered ANS oil plus combustion products from local vessel traffic, runoff, or aerial deposition.
- At the GOC reference site, sediment PAH profiles since 2000 have shown a dominant pyrogenic pattern with little or no input from the terminal. Instead, they are dominated by low-level naphthalenes and combustion products. SHC profiles continue to be biogenic, reflecting only phytoplankton sources and terrestrial plant waxes. With the additional biomarker constituents now being reported, it appears that trace-level accumulations of biomarkers associated with the BWTF effluent are indeed accumulating in GOC sediments. They have been observed since biomarkers were first reported in 2011, however, the levels were lower in 2018 compared to 2016 and 2017. The concentrations are very low (at or just above the reporting limit), and there are numerous missing components but key diagnostic biomarkers are present and similar to the BWTF effluent in earlier samples. Because these petrogenic biomarker components are much more resistant to weathering compared to PAH and SHC, they can be observed and attributed to the terminal even when PAH and SHC are largely absent or dominated by combustion sources.

BEYOND LTEMP

How do these levels compare with other Alaska sites? Unfortunately, comparable studies are scarce, no longer current, and variable concerning which analytes are actually summed. Nevertheless, the earlier reported values still seem reasonable (Table 11). Follow-up sampling in 2004 for oil residues from the 1997 *M/V Kuroshima* grounding in Summer Bay, Unalaska, found TPAH levels between 25 and 85 ng/g DW, with an average of 57 ng/g DW (Helton et al., 2004). This is actually higher than LTEMP's July 2013 range of 9-33 ng/g DW inside the Sound but similar

Table 11. Most recent TPAH concentrations in regional mussel tissues (ppb, ng/g DW) relative to 2004-2010 NOAA Mussel Watch monitoring data and a recovered Alaska oil spill event.

LTEMP	2018	Port Valdez tissues	AMT, JAP & GOC	4-6
	2017	Port Valdez tissues	AMT, JAP & GOC	6-19
	2016	Port Valdez tissues	AMT, JAP & GOC	6-53
	2015	Port Valdez tissues	AMT & GOC	39-87
		PWS (KNH & SHB)	KNH & SHB	19-46
	2013	Port Valdez tissues	AMT & GOC	17-20
	2018	PWS	Five stations (see Figure 2)	4-5
		GOA	Three stations (see Figure 2)	4-5
	2013	PWS	Six stations (see Figure 2)	9-33
		GOA	Three stations (see Figure 2)	18-73
West Coast Mussel Watch		average (Kimbrough et al., 2008)		825
		So. Calif.	Santa Catalina Island	63
		Seattle	Elliot Bay, WA	6,962
Alaska Mussel Watch	2008	Cook Inlet	Bear Cove	119
		Cook Inlet	Homer Spit	208
		Port Valdez	Alyeska Marine Terminal	52
		Port Valdez	Gold Creek	31
	2009	Ketchikan	Mountain Point	231
		Nahku Bay	East Side	229
		Port Valdez	Mineral Creek Flats	332
		Resurrection Bay	Nash Road	602
		Resurrection Bay	Nash Road	765
		Resurrection Bay	Nash Road	929
		Resurrection Bay	Nash Road	713
		Unakwit Inlet	Siwash Bay	257
	2010	Resurrection Bay	Nash Road	1,570
		Nanwalek	Nanwalek	194
		Port Graham	Port Graham	376
		Port Graham	Murphy's Slough	428
		Seldovia Bay	Powder Island	652
M/V Kuroshima (1997)		Unalaska	2004 followup	25-85

to 19-46 ng/g DW from the two PWS sites in 2015 and also similar to the 2013 levels of 18-73 ng/g DW at GOA sites (overall average 50 ng/g DW). Compared to the 2018 data for all three LTEMP regions, the 2004 *Kuroshima* sites were significantly higher, but there are no more recent data against which to compare. The current LTEMP data suggest a natural dissolved-phase background TPAH somewhere below 5 ng/g DW.

Reaching farther, data from the 2004-2005 National Status and Trends, Mussel Watch Program (Figure 43) and 2008-2010 Alaska sites (Figure 44) (now summing only 38 parent and alkylated PAH homologues versus 43 LTEMP PAH analytes) show that average TPAH concentrations in mussels for other West Coast sites have been nearly 66 times higher (825 ng/g DW) than LTEMPs. The highest level reported on the West Coast was 6,962 ng/g DW in Seattle, Washington. The lowest, 63 ng/g DW, was from mussels collected on Santa Catalina Island, 26 miles offshore of Orange County in Southern California. In 2004-5, the average TPAH mussel concentration in mussels from the five Alaska Mussel Watch sites (Ketchikan, Nahku Bay, Port Valdez, Unakwik Inlet, and Cook Inlet) was 267 ng/g DW with levels ranging from 105-441 ng/g DW (Kimbrough et al., 2008). Considering these and even more recent 2008-2010 values from the Mussel Watch data portal (Table 11), the LTEMP results for Port Valdez, PWS, and GOA sites demonstrate that these remote locations are still exceptionally clean.

Finally, a 2005 EVOS Trustee Council Program, Long-Term Monitoring of Anthropogenic Hydrocarbons in the *Exxon Valdez* Oil Spill Region, examined 10 intertidal sites within the Naked-Knight-Southwest Island complex to measure the extent of buried oil still present 16 years after the spill. At previously heavily-oiled EVOS sites, 10 to 50 random pits (depending on the beach width) were excavated to a depth of ~0.5 m to look for residual oil. If oil was detected, available nearby mussels were also collected. The results have been published elsewhere (Short et al., 2007) but, as co-authors, PAH and SHC sample profiles were included in Appendix E of our 2005/2006 Report (Payne et al., 2008a). Briefly, TPAH levels in the oiled pits ranged from a low of 42 ng/g (on Knight Island) to a high of 567,000 ng/g (on Latouche Island) with the oil showing states of weathering varying from extensively degraded to very fresh. On the other hand, nearby mussel samples only showed low *dissolved-phase* TPAH (11-42 ng/g DW, derived primarily from naphthalenes and phenanthrenes/anthracenes) that were in the same concentration range but compositionally different from the signals observed at LTEMP PWS and GOA sites sampled in April 2009. From these studies, it was concluded that although in 2005, there were still persistent buried EVOS residues at a number of beaches, they were highly sequestered and did not appear to be bioavailable unless disturbed.

The extremely low 2018 TPAH values in mussels collected from these sites and the PSD data from the formerly oiled DII site seem to confirm these findings, although recent studies with oil-sniffing dogs suggest that bioavailability at concentrations below our analytical detection limits may still be a concern for sub-lethal effects with some species. In 2005, rates of disappearance had diminished to an estimated 4% per year. If left undisturbed, Short et al. (2007) predicted that sequestered hydrocarbons would be there for decades. Revisiting the sites in 2015, Auke Bay researchers found mostly unchanged conditions since 2001 (Lindeberg et al., 2018). Lindeberg again concluded that an estimated 0.6% EVOS oil would remain sequestered unless disturbed and will likely persist in the environment on a decadal scale. They also comment that viewing this survey in the context of previous surveys makes it clear that Exxon researcher claims made after the spill that beaches would clean themselves were overly optimistic. To address these residual deposits, the EVOS Trustee Council has sponsored various beach remediation studies and pilot projects (ADEC 2016).

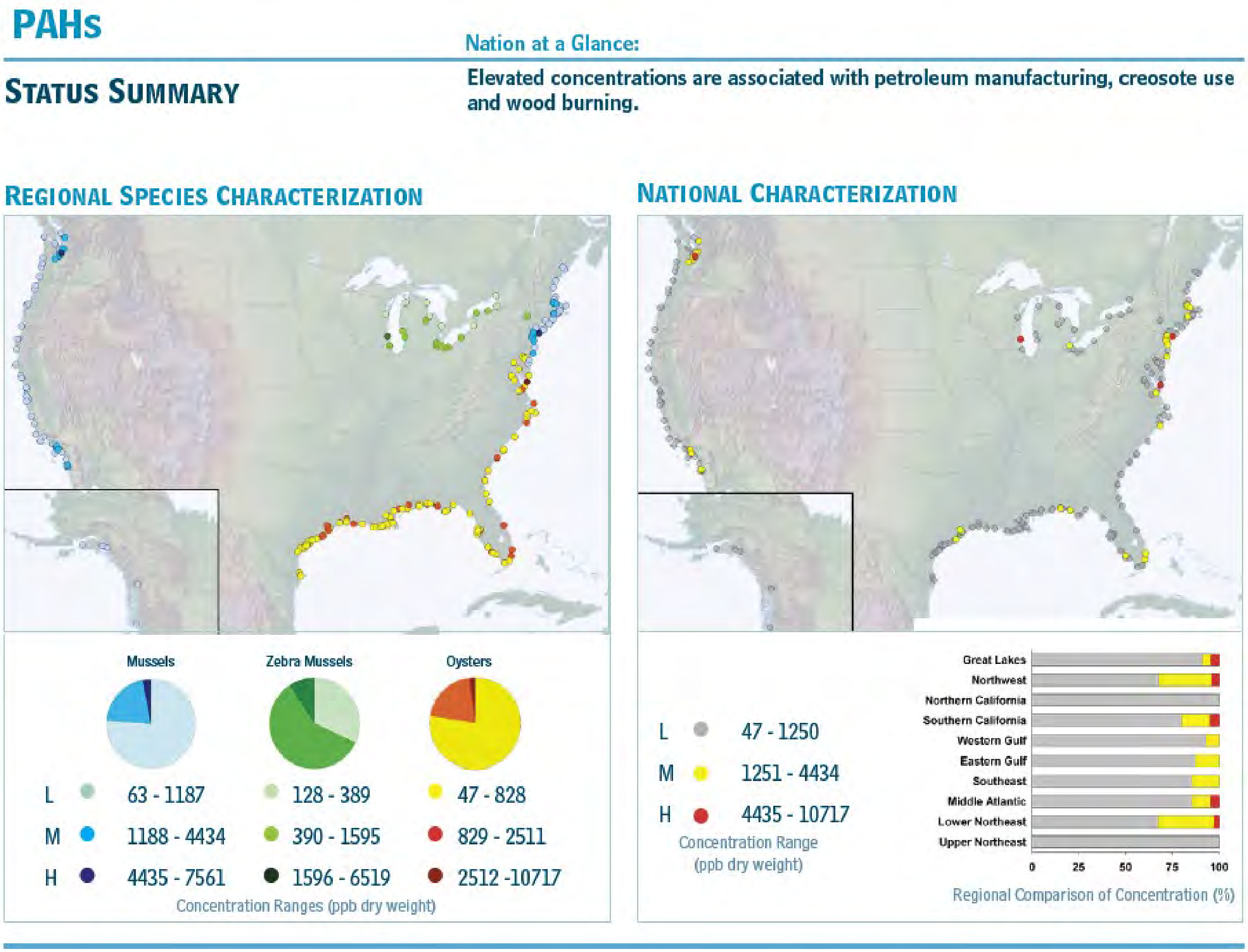

PAHs

STATUS SUMMARY

Nation at a Glance:

Elevated concentrations are associated with petroleum manufacturing, creosote use and wood burning.

REGIONAL SPECIES CHARACTERIZATION

	Mussels	Zebra Mussels	Oysters
L	63 - 1187	128 - 389	47 - 828
M	1188 - 4434	390 - 1595	829 - 2511
H	4435 - 7561	1596 - 6519	2512 -10717

Concentration Ranges (ppb dry weight)

NATIONAL CHARACTERIZATION

L	47 - 1250
M	1251 - 4434
H	4435 - 10717

Concentration Range (ppb dry weight)

Figure 43. Status and trends result from National Mussel Watch data (Kimbrough et al., 2008). All Alaska sites characterized as low concentrations.

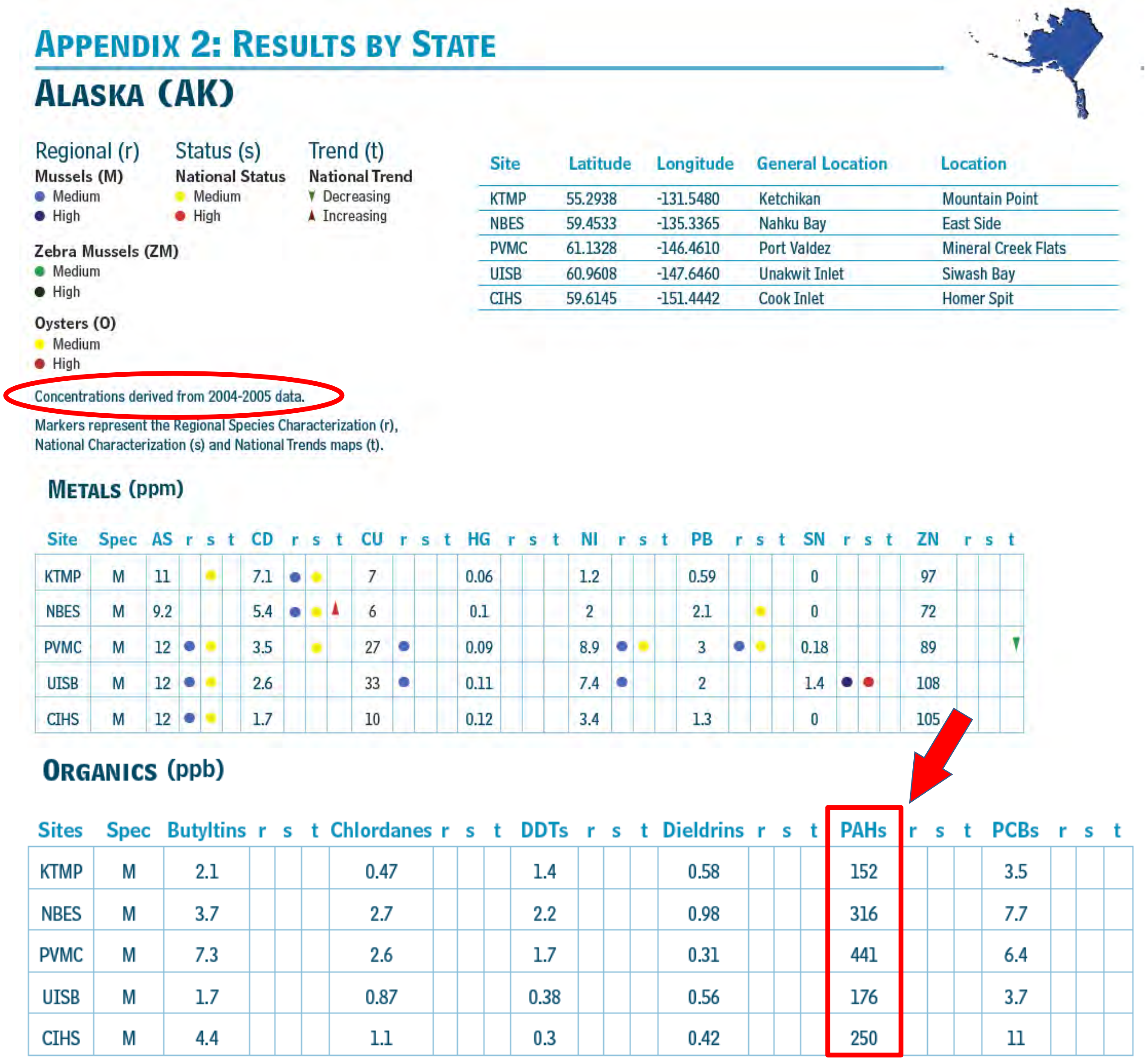

APPENDIX 2: RESULTS BY STATE

ALASKA (AK)

Regional (r)

Mussels (M)
- ● Medium
- ● High

Zebra Mussels (ZM)
- ● Medium
- ● High

Oysters (O)
- ● Medium
- ● High

Status (s)

National Status
- ● Medium
- ● High

Trend (t)

National Trend
- ▼ Decreasing
- ▲ Increasing

Concentrations derived from 2004-2005 data.

Markers represent the Regional Species Characterization (r), National Characterization (s) and National Trends maps (t).

Site	Latitude	Longitude	General Location	Location
KTMP	55.2938	-131.5480	Ketchikan	Mountain Point
NBES	59.4533	-135.3365	Nahku Bay	East Side
PVMC	61.1328	-146.4610	Port Valdez	Mineral Creek Flats
UISB	60.9608	-147.6460	Unakwit Inlet	Siwash Bay
CIHS	59.6145	-151.4442	Cook Inlet	Homer Spit

METALS (ppm)

Site	Spec	AS	r	s	t	CD	r	s	t	CU	r	s	t	HG	r	s	t	NI	r	s	t	PB	r	s	t	SN	r	s	t	ZN	r	s	t
KTMP	M	11		●		7.1	●	●		7				0.06				1.2				0.59				0				97			
NBES	M	9.2				5.4	●	●	▲	6				0.1				2				2.1		●		0				72			
PVMC	M	12	●	●		3.5		●		27	●			0.09				8.9	●	●		3	●	●		0.18				89			▼
UISB	M	12	●	●		2.6				33	●			0.11				7.4	●			2				1.4	●	●		108			
CIHS	M	12	●	●		1.7				10				0.12				3.4				1.3				0				105			

ORGANICS (ppb)

Sites	Spec	Butyltins	r	s	t	Chlordanes	r	s	t	DDTs	r	s	t	Dieldrins	r	s	t	PAHs	r	s	t	PCBs	r	s	t
KTMP	M	2.1				0.47				1.4				0.58				152				3.5			
NBES	M	3.7				2.7				2.2				0.98				316				7.7			
PVMC	M	7.3				2.6				1.7				0.31				441				6.4			
UISB	M	1.7				0.87				0.38				0.56				176				3.7			
CIHS	M	4.4				1.1				0.3				0.42				250				11			

Figure 44. Summary page of Alaska regional Mussel Watch results and trends based on 2004-05 report from Kimbrough et al., 2008.

CONCLUSIONS

In recent years, the petrogenic hydrocarbon (oil) inputs into Port Valdez from the Alyeska Marine Terminal and tanker operations have been declining as reflected in TPAH concentrations in both sediments and mussels. As concluded in our earlier reports, this trend reflects a combination of reduced BWTF discharge volumes from historically decreased North Slope oil production, the transition to double-hulled tankers with segregated ballast tanks, and improved BWTF efficiency in removing particulate/oil-phase PAH.

In 2016 and 2017, our forensics' approach to tracking ANS oil was greatly improved by the collection and detailed analyses of effluent samples from the BTT at Alyeska's BWTF. We recommend effluent sampling as a reoccurring component of the program.

Between 2016 and 2018, the AMT sediment PAH reverted back to a mix of low-level petrogenic components that showed significant additional hydrocarbon weathering compared to the recently sampled BWTF effluent. The biomarker profiles from 2011 through 2018 in AMT sediments, however, strongly confirm that the source is directly linked to the BWTF effluent. The sediment SHC patterns at the terminal show a mixture of marine and terrestrial biogenic components along with higher-molecular-weight petrogenic waxes at reduced levels compared to earlier years. Based on the signatures, these patterns suggest variable or increased inputs of weathered ANS oil plus combustion products from local vessel traffic, runoff, or aerial deposition.

At the GOC reference site, the sediment PAH profiles are dominated by low-level dissolved-phase naphthalenes and combustion products. The SHC profiles in GOC sediments continue to be biogenic, reflecting only background inputs of terrestrial plant waxes. With the more extensive Alpha/NewFields biomarker data set in 2016, 2017, and 2018, it appears that in addition to natural background biomarkers, near- or above-MDL-traces of some ANS-derived biomarkers are accumulating in the GOC sediments. While the GOC sedimentary biomarker data are sparse (with many missing components and generally lower concentrations in 2018 compared to earlier years), the observed constituents and hopane to norhopane ratios are now unequivocally ANS-derived, presumably from the BWTF. However, there is no evidence of BWTF-derived PAH or SHC accumulation at that site.

The 2016 addition of mussel collections at JAP just east of the traditional AMT station at Saw Island was meant to correlate tissue data with trial PSD being deployed subsurface at the same locations and to evaluate a potential PAH gradient to either side of the BWTF outfall. In 2018, both locations showed very similar tissue PAH and biomarker profiles but with no suggestion of BWTF-derived uptake. No gradient was found.

PSD data confirm the conclusions from LTEMP mussel tissue measurements that only extremely low concentrations of dissolved-phase PAH are present in the LTEMP region. Identical water-washed or heavily evaporated naphthalene patterns with traces of other weathered PAH were observed in all the PSDs, and there was no correlation with proximity to the BWTF discharge or previous EVOS oiling (e.g., at DII vs. KNH). The PSD data suggest a very low-level backgound pattern of water-soluble PAH with no useful information as to a logical source. These concentrations are well below any known toxicity thresholds for sensitive marine organisms and life stages (personal communication, Dr. Sarah Allan).

The GOC reference site mussels have generally shown only low-level pyrogenic PAH profiles since 2006 but in 2016, evidence of a diesel spill was observed. By 2017, all traces of the diesel spill had disappeared. The 2008-2015 SHC in mussels from both Port Valdez locations exhibited primarily background biogenic components with the exception of a petrogenic signal at AMT in 2013. Unfortunately, SHC data were not measured by GC-FID in 2016 but the laboratory did analyze for *m/z* 85 ions as part of the tissues' SIM GC/MS biomarker analyses and those data (while technically not quantifiable) along with the tissue biomarker profiles confirmed the presence of trace-level n-alkanes characteristic of diesel oil at GOC in 2016.

By comparison, analysis of the PSDs deployed at GOC during the preceding month and recovered during the mussel sampling in July 2016 showed slightly elevated parent phenanthrene (compared to AMT and JAP) but without the benefit of alkylated PAH analyses and biomarkers, there was no discernible evidence of the diesel spill.

Compared to the recent West Coast Mussel Watch data (2004-05) and the more recent 2008-10 Alaska Mussel Watch sites, the 2018 LTEMP results continue to demonstrate that the sampled region is exceptionally clean.

ACKNOWLEDGEMENTS

Once again, this project would not be achieving its goals without the efforts of many more individuals than currently appear in the author's list. We would especially like to thank our closet scientist, premiere naturalist, stalwart vessel operator and colleague, Dave Janka (and over-equally-so to Annette Janka); our all-wise collaborators at NewFields Environmental Forensics, Eric Litman and Scott Stout; our ever supportive facilitator and previous PWSRCAC project manager, Joe Banta; our enthusiastic colleague, wannabe-chemist, field sampler, and new PWSRCAC-project manager, Austin Love; our fellow chem nerd and PSD guru, Dr. Sarah Allan; our many prior and current PWSRCAC Scientific Advisory Committee advisors; and the ever-ready folks on PWSRCAC staff, particularly Nelli Vanderburg, who brought cookies to the field! And especially, to our wives, for enabling us to live the dream—science and Alaska!

REFERENCES

ADEC 2016. An Evaluation of Remedial Options for Lingering Oil from the Exxon Valdez Oil Spill. Prepared by the Alaska Department of Environmental Conservation Division of Spill Prevention and Response for the Exxon Valdez Oil Spill Trustee Council. 18 pgs.

Aeppli, C., Carmichael, C. A., Nelson, R. K., Lemkau, K. L.; Graham, W. M.; Redmond, M. C.; Valentine, D. L.; Reddy, C. M. 2012. Oil weathering after the Deepwater Horizon disaster led to the formation of oxygenated residues. *Environ. Sci. Technol*. 2012, 46 (16), 8799−8807.

Allan, S.E. 2018. Long-Term environmental Monitoring Program – Draft Supplemental report on monitoring for polycyclic aromatic hydrocarbons using passive samplers: 2016 sampling results and interpretation. 17 pp.

Bence, A.E., K.A. Kvenvolden, M.C. Kennicutt II. 1996. Organic geochemistry applied to environmental assessments of Prince William Sound, Alaska, after the Exxon Valdez oil spill—a review. *Organic Geochemistry*, Volume 24, Issue 1, January 1996, Pages 7-42, ISSN 0146-6380, http://dx.doi.org/10.1016/0146-6380(96)00010-1.

Bence, A.E., D.S. Page, and P.D. Boehm. 2007. Advances in forensic techniques for petroleum hydrocarbons: the *Exxon Valdez* Experience. Pp 449-487 *In* Wang, Z. and S.A. Stout (eds). Oil Spill Environmental Forensics: Fingerprinting and Source Identification. Academic Press, Burlington, MA, USA. 554 pp.

Carls, M.G., J.W. Short, and J.R. Payne. 2006. Accumulation of polycyclic aromatic hydrocarbons by *Neocalanus* copepods in Port Valdez, Alaska. *Marine Pollution Bulletin* 52: 1480-1489.

Carls MG, Holland L, Pihl E, Zaleski MA, Moran J, Rice SD. 2016. Polynuclear Aromatic Hydrocarbons in Port Valdez Shrimp and Sediment. Arch Environ Contam Toxicol. 71(1):48-59.

Deepthike, H.U., R. Tecon, G. Van Kooten, J.R. Van der Meer, H. Harms, M. Wells, J. Short. 2009. Unlike PAHs from Exxon Valdez crude oil, PAHs from Gulf of Alaska coals are not readily bioavailable. *Environ Sci Technol*. 2009 Aug 1;43(15):5864-70.

Douglas, G.S. and Liu, B. 2015. Chemical Evidence for Exposure of Red Crabs and Other Deep Benthic Organisms to Macondo Oil. (CHEM_TR.24). Seattle, WA. DWH Natural Resource Exposure NRDA Technical Working Group Report.

Driskell, W.B. and J.R. Payne. 2015. Forensic assessment of 2010 DWH nearshore water samples. PECI Technical Report to the *Deepwater Horizon* Oil Spill Trustees in support of the PDARP. August 20, 2015. 31 pp.

Driskell, W.B. and J.R. Payne. 2018a. Macondo oil in northern Gulf of Mexico waters – Part 2: Dispersant-accelerated PAH Dissolution in the *Deepwater Horizon* plume. *Marine Pollution Bulletin* 129(1): 412-419.

Driskell, W. B., and J.R. Payne. 2018b. Development and application of phase-specific methods in oiled-water forensic studies. Chapter 14 in (S. Stout and Z. Wang, eds). Oil Spill Environmental Forensics Case Studies. Butterworth-Heinemann/Elsevier Publishers, Oxford, United Kingdom and Cambridge, Massachusetts. 2018: 289-323.

EPA. 2012. U.S. EPA Fact Sheet for reissue of a National Pollutant Discharge Elimination System (NPDES) permit to Alyeska Pipeline Service Co. for the Valdez Marine Terminal (AK-002324-8). February 8, 2012. 57 pp.

Fingas, M.F. and J. Banta. 2016. Polar Compounds in Oils and their Aquatic Toxicity, *Proceedings of the Thirty-ninth AMOP Technical Seminar,* Environment and Climate Change Canada, Ottawa, ON, pp. 197-259, 2016.

Helton, D., A. Moles, J. Short, J. Rice. 2004. Results of the *M/V Kuroshima* Oil Spill Shellfish Tissue Analysis 1999, 2000 and 2004. Report to the *M/V Kuroshima* Trustee Council. Prepared by NOAA Office of Response and Restoration, Seattle, Washington and NOAA Auke Bay Laboratory, Juneau, Alaska. December 2004, 7 pp.

Huckins, J. N.; Petty, J. D.; Booij, K. 2006. Monitors of Organic Chemicals in the Environment: Semipermeable Membrane Devices; Springer: New York, 2006. 229 pp.

Kimbrough, K. L., W. E. Johnson, G. G. Lauenstein, J. D. Christensen and D. A. Apeti. 2008. An Assessment of Two Decades of Contaminant Monitoring in the Nation's Coastal Zone. Silver Spring, MD. NOAA Technical Memorandum NOS NCCOS 74. 105 pp.

Kvenvolden K. A., F. D. Hostettler, P. R. Carlson, J. B. Rapp, C. Threlkeld, and A. Warden. 1995. Ubiquitous tar balls with a California source signature on the shorelines of Prince William Sound, Alaska. *Environ. Sci. Technol*. 29(10), 2684–2694.

Lee, R.F. 1977. Accumulation and turnover of petroleum hydrocarbons in marine organisms. *In*: Fates and effects of petroleum hydrocarbons in the marine environment. Wolfe, DA (ed). New York: Pergammon Press.

Lees D.C., W.B. Driskell, J.R. Payne, M.O. Hayes 2000. Intertidal Reconnaissance Survey in Middle and Upper Cook Inlet. Report prepared for Cook Inlet Regional Citizens Advisory Council.

Lindeberg, M.R., J. Maselko, R.A. Heintz, C.J. Fugate, L. Holland. 2018. Conditions of persistent oil on beaches in Prince William Sound 26 years after the *Exxon Valdez* spill. *Deep-Sea Research Part II*, 1(47) 9-19. http://dx.doi.org/10.1016/j.dsr2.2017.07.011

Liu, Y., E. B. Kujawinski. 2015. Chemical composition and potential environmental impacts of water-soluble polar crude oil components inferred from ESI FT-ICR MS. *PLoS ONE*, 10(9), e0136376. doi.org/10.1371/journal.pone.0136376

Mason, R.P. 1988. Accumulation and depuration of petroleum hydrocarbons by black mussels. 1. Laboratory exposure trials, *South African Journal of Marine Science*, 6:1, 143-153, DOI: 10.2989/025776188784480582

McKenna, A.M., R.K. Nelson, C.M. Reddy, J.J. Savory, N.K. Kaiser, J.E. Fitzsimmons, A.G. Marshall, and R.P. Rodgers 2013. Expansion of the analytical window for oil spill characterization by ultrahigh resolution mass spectrometry: beyond gas chromatography. *Environ. Sci. Technol*. 2013 47 (13), 7530-7539. DOI: 10.1021/es305284t

Mearns, A.J., G. Shigenaka, B. Meyer, and A. Drury 2014. Contamination and recovery of commercially-reared mussels exposed to diesel fuel from a sunken fishing vessel. International Oil Spill Conference Proceedings: May 2014, Vol. 2014, No. 1, pp. 1686-1705. doi.org/10.7901/2169-3358-2014.1.1686

Minick, J. and S. Allan. 2016. Long-Term Environmental Monitoring Program – Supplemental Report on monitoring for polycyclic aromatic hydrocarbons using passive samplers: 2016 Sampling Results and Interpretation. PowerPoint presented to SAC.

Moldowan, J. M., J. Dahl, B. J. Huizinga, F. J. Fago, L. J. Hickey, T. M. Peakman, and D. W. Taylor. 1994. The molecular fossil record of oleanane and its relation to angiosperms. *Science*, 265, 768-771.

National Academy of Sciences (NAS). 1975. Petroleum in the Marine Environment. National Academy of Sciences, Washington, D.C., 107 pp.

National Academy of Sciences (NAS). 1985. Oil in the Sea: Inputs, Fates, and Effects. National Academy Press, Washington, D.C., 601 pp.

National Academy of Sciences (NAS). 2003. Oil in the Sea III: Inputs, Fates, and Effects. National Academies Press, Washington, D.C., 265 pp.

Neito, O., J. Aboigor, R. Buján, M. N'Diaye, J. Graña, L. Saco-Álvarez, Á. Franco, J.A. Soriano, R. Beiras. 2006. Temporal variation in the levels of polycyclic aromatic hydrocarbons (PAHs) off the Galician Coast after the *Prestige* oil spill. *Marine Ecology Progress Series* 328:41-49, DOI10.3354/meps328041

O'Connell, S. G.; Haigh, T.; Wilson, G.; Anderson, K. A. 2013. An analytical investigation of 24 oxygenated-PAHs (OPAHs) using liquid and gas chromatography–mass spectrometry. *Anal. Bioanal. Chem.* 2013, 1–12.

Payne, J.R. and W.B. Driskell. 2015a. 2010 DWH offshore water column samples—Forensic assessments and oil exposures. PECI Technical Report to the *Deepwater Horizon* Oil Spill Trustees in support of the PDARP (www.doi.gov/deepwaterhorizon/admin record, DWH-AR0039118, 37 pp.).

Payne, J.R. and W.B. Driskell. 2015b. Forensic fingerprinting methods and classification of DWH offshore water samples. PECI Technical Report to the *Deepwater Horizon* Oil Spill Trustees in support of the PDARP. (www.doi.gov/deepwaterhorizon/admin record, DWH-AR0039170, 31 pp.).

Payne, J.R. and W.B. Driskell. 2016. Water column sampling for forensics. In: Standard Handbook Oil Spill Environmental Forensics – Fingerprinting and Source Identification (2nd Edition), S. Stout and Z. Wang (eds.) Elsevier/Academic Press, 2016: 983-1014.

Payne, J.R. and Driskell, W.B. 2017a. Water-column measurements and observations from the *Deepwater Horizon* oil spill Natural Resource Damage Assessment. *Proceedings of the 2017 Oil Spill Conference*. American Petroleum Institute, Washington, DC. Paper No. 2017-167.

Payne, J.R. and W.B. Driskell. 2017b. Long-Term Environmental Monitoring Program – Final Report: 2016 Sampling Results and Interpretations. Final Report Prepared for Prince William Sound Regional Citizens' Advisory Council Contract No. 951.17.01. Prepared by Payne Environmental Consultants, Inc., Encinitas, CA. August 2017. 69 pp.

Payne, J.R. and W.B. Driskell. 2018a. Macondo oil in northern Gulf of Mexico waters – Part 1: Assessments and forensic methods for *Deepwater Horizon* offshore water samples. *Marine Pollution Bulletin* 129(1): 399-411.

Payne, J.R. and W.B. Driskell. 2018b. September 2017 Berth 5 Oil Spill – Sampling results and interpretations. Final Report Prepared for Prince William Sound Regional Citizens' Advisory Council Contract No. 951.18.08. Prepared by Payne Environmental Consultants, Inc., Encinitas, CA. April 2018. 14 pp plus appendices.

Payne, J.R. and W.B. Driskell. 2018c. Long-Term Environmental Monitoring Program – Final Report: 2017 Sampling Results and Interpretations. Final Report Prepared for Prince William Sound Regional Citizens' Advisory Council Contract No. 951.18.02. Prepared by Payne Environmental Consultants, Inc., Encinitas, CA. September 2018. 60 pp.

Payne, J.R., W.B. Driskell, and D.C. Lees. 1998. Long Term Environmental Monitoring Program data analysis of hydrocarbons in intertidal mussels and marine sediments, 1993-1996. Final Report prepared for the Prince William Sound Regional Citizens Advisory Council, Anchorage, Alaska 99501. (PWSRCAC Contract No. 611.98.1). March 16, 1998. 97 pp plus appendices.

Payne, J.R., T.J. Reilly, and D.P. French. 1999. Fabrication of a portable large-volume water sampling system to support oil spill NRDA efforts. *Proceedings of the 1999 Oil Spill Conference*, American Petroleum Institute, Washington, D.C., 1179-1184.

Payne, J.R., W.B. Driskell, M.G. Barron, D.C. Lees. 2001. Assessing transport and exposure pathways and potential petroleum toxicity to marine resources in Port Valdez, Alaska. Final Report Prepared for Prince William Sound Regional Citizens' Advisory Council Contract No. 956.02.1. Prepared by Payne Environmental Consultants, Inc., Encinitas, CA. December 21, 2001. 64 pp plus appendices.

Payne, J.R., W.B. Driskell, M.G. Barron, D.C. Lees, L. Ka'aihue, and J.W. Short. 2003a. Assessing transport and exposure pathways and potential petroleum toxicity to marine resources in Port Valdez, Alaska. Poster No. PT214 presented at the SETAC 24th Annual Meeting in North America. November 9-13, 2003, Austin, Texas.

Payne, J.R., W.B. Driskell, and J.W. Short. 2003b. 2002-2003 LTEMP Monitoring Report. Final Report prepared for the Prince William Sound Regional Citizens' Advisory Council, Anchorage, Alaska 99051. PWSRCAC Contract No. 951.03.1. Prepared by Payne Environmental Consultants, Inc., Encinitas, CA. Nov. 6, 2003. 107 pp.

Payne, J.R., W.B. Driskell, M.G. Barron, J. A. Kalmar, and D.C. Lees. 2003c. Public comment regarding the Draft NPDES Permit for BWTF at Alyeska Marine Terminal. Final Report prepared for the Prince William Sound Regional Citizens' Advisory Council, Anchorage, Alaska 99051. PWSRCAC Contract No. 551.02.01. Prepared by Payne Environmental Consultants, Inc., Encinitas, CA. June 2, 2003, 21 p.

Payne, J.R., W.B. Driskell, and J.W. Short. 2005a. 2003-2004 LTEMP Monitoring Report. Final Report prepared for the Prince William Sound Regional Citizens' Advisory Council, Anchorage, Alaska 99051. PWSRCAC Contract No. 951.04.1. Prepared by Payne Environmental Consultants, Inc., Encinitas, CA. April 18, 2005. 123 pp.

Payne, J.R., W.B. Driskell, J.F. Braddock, J. Bailey. 2005b. Hydrocarbon biodegradation in the Ballast Water Treatment Facility, Alyeska Marine Terminal. Final Report prepared for the Prince William Sound Regional Citizens' Advisory Council, Anchorage, Alaska 99051. PWSRCAC Contract Numbers 558.04.01 and 560.2004.01. Prepared by Payne Environmental Consultants, Inc., Encinitas, CA. May 2, 2005. 48 pp.

Payne, J.R., W.B. Driskell, J.F. Braddock, J. Bailey, J.W. Short, L. Ka'aihue, T.H. Kuckertz. 2005c. From tankers to tissues – tracking the degradation and fate of oil discharges in Port Valdez, Alaska. *Proceedings of Arctic Marine Oil Spill Conference* 2005, Calgary, Alberta, Canada. pp 959-991.

Payne, J.R. and W.B. Driskell, M.R. Lindeberg, W. Fournier, M.L. Larsen, J.W. Short, S.D. Rice, and D. Janka. 2005d. Dissolved- and particulate-phase hydrocarbons in interstitial water from Prince William Sound beaches containing buried oil thirteen years after the *Exxon Valdez* oil spill. *Proceedings of the 2005 International Oil Spill Conference*, American Petroleum Institute, Washington, D.C., pp 83-88.

Payne, J.R., W.B. Driskell, J.W. Short, and M.L. Larsen. 2006. 2004-2005 LTEMP Monitoring Report. Final Report prepared for the Prince William Sound Regional Citizens' Advisory Council, Anchorage, Alaska 99051. PWSRCAC Contract No. 951.05.1. (Restoration Project No. 040724). Prepared by Payne Environmental Consultants, Inc., Encinitas, CA. November 2006. 149 pp.

Payne, J.R., W.B. Driskell, J.W. Short, M.L. Larsen. 2008a. Final 2005-2006 LTEMP Oil Monitoring Report, *Exxon Valdez* Oil Spill Restoration Project Final Report (Restoration Project 050763), Prince William Sound Regional Citizen's Advisory Council, Anchorage, Alaska. 137 pp.

Payne, J.R., W.B. Driskell, J.W. Short and M.L. Larsen. 2008b. Long-term monitoring for oil in the *Exxon Valdez* spill region. *Marine Pollution Bulletin* 56: 2067-2081.

Payne, J.R., W.B. Driskell, J.W. Short, and M. Larsen. 2010a. Long-Term Environmental Monitoring Program: Final 2006-2008 LTEMP Monitoring Report. Prince William Sound Regional Citizen's Advisory Council, Anchorage, Alaska. 198 pp

Payne, J.R., W.B. Driskell, and D. Janka 2010b. A possible source for dissolved-phase PAH signals observed in *Mytilus* samples throughout Prince William Sound, Alaska. *Proceedings of Arctic Marine Oil Spill Conference* 2010. Halifax, Nova Scotia, CA.

Payne, J.R., W.B. Driskell, J. A. Kalmar. 2012. Review of EPA Draft Permit, Fact Sheet, and other documents for Proposed Reissuance of Valdez Marine Terminal NPDES Wastewater Discharge Permit (AK-002324-8). Final Report prepared for the Prince William Sound Regional Citizens' Advisory Council, Anchorage, Alaska 99051. PWSRCAC Contract No. 551.09.01. Prepared by Payne Environmental Consultants, Inc., Encinitas, CA. March 6, 2012. 29 pp.

Payne, J.R., W.B. Driskell, M.G. Carls, M. Larsen, and L.G. Holland. 2013. Long-Term Environmental Monitoring Program: Results and Interpretations from sampling, 2008-2012. Prince William Sound Regional Citizen's Advisory Council, Anchorage, Alaska. 89 pp.

Payne, J.R., W.B. Driskell, M.G. Carls, M.L. Larsen, and L.G. Holland. 2015. Long-Term Environmental Monitoring Program: Results and Interpretations from sampling, 2008-2013. Prince William Sound Regional Citizen's Advisory Council, Anchorage, Alaska. 125 pp.

Payne, J.R., W.B. Driskell, M.G. Carls, and L.G. Holland. 2016. Long-Term Environmental Monitoring Program – Final Report: 2015 Sampling Results and Interpretations. Prince William Sound Regional Citizen's Advisory Council, Anchorage, Alaska. 47 pp.

Peters, K., C. Walters, and J. Moldowan. 2004. The Biomarker Guide: Volume 1 Biomarkers in the Environment and Human History. 2nd edition. Cambridge: Cambridge University Press. doi:10.1017/CBO978051152486

Prince William Sound Regional Citizens' Advisory Council (PWSRCAC). 2019. Public comment on Alaska Pollutant Discharge Elimination System Individual Permit No. AK0023248 for Alyeska Pipeline Service Company's Valdez Marine Terminal. April 26, 2019. 38 pp.

Saupe, S.M., J. Gendron, and D. Dasher. 2005. The Condition of Southcentral Alaska Coastal Bays and Estuaries. A Statistical Summary for the National Coastal Assessment Program. Alaska Department of Environmental Conservation. 136 pp.

Savoie, M. A., Savoie, J. M., Trefry, J. H., Semmler, C. M., Woodall, D. W., Trocine, R. P., Brooks, J.M and McDonald, T. 2006. Port Valdez sediment coring program—Final 2004 Monitoring Report. Anchorage AK: Prince William Sound Regional Citizen's Advisory Council. www.pwsrcac.org.

Shaw, D. G. and A.L Blanchard. 2016. Environmental Studies in Port Valdez, Alaska: 2015. Final Report to Alyeska Pipeline Service Co., Institute of Marine Science, University of Alaska Fairbanks, 130 pp.

Shaw, D. G. and A.L Blanchard. 2017. Environmental Studies in Port Valdez, Alaska: 2016 Including Supplemental Overview. Final Report to Alyeska Pipeline Service Co., Institute of Marine Science, University of Alaska Fairbanks, 213 pp.

Shaw, D. G. and A.L Blanchard. 2018. Environmental Studies in Port Valdez, Alaska: 2017. Final Report to Alyeska Pipeline Service Co., Institute of Marine Science, University of Alaska Fairbanks, 127 pp.

Short, J.W., G.V. Irvine, D.H. Mann, J.M. Maselko, J.J. Pella, M.R. Lindeberg, J.R. Payne, W.B. Driskell, and S.D. Rice. 2007. Slightly weathered *Exxon Valdez* oil persists in Gulf of Alaska beach sediments after 16 years. *Environmental Science & Technology*. 41(4): 1245-1250.

Sower, G. J.; Anderson, K. A. 2008. Spatial and temporal variation of freely dissolved polycyclic aromatic hydrocarbons in an urban river undergoing superfund remediation. *Environmental Science & Technology*. 2008, 42 (24), 9065–9071.

Stout, S.A. and J.R. Payne. 2016a. Chemical composition of floating and sunken *in-situ* burn residues from the *Deepwater Horizon* oil spill. *Marine Pollution Bulletin* 108: 186-202.

Stout, S.A. and J.R. Payne. 2016b. Macondo oil in deep-sea sediments: Part 1 – sub-sea weathering of oil deposited on the seafloor. *Marine Pollution Bulletin*, 111, 365-380.

Stout, S.A. and J.R. Payne. 2017. Footprint, weathering, and persistence of synthetic-base drilling mud olefins in deep-sea sediments following the *Deepwater Horizon* disaster. *Marine Pollution Bulletin* 118: 328-340.

Stout, S.A., J.R. Payne, S.D. Emsbo-Mattingly, and G. Baker. 2016a. Weathering of field-collected floating and stranded Macondo oils during and shortly after the *Deepwater Horizon* oil spill. *Marine Pollution Bulletin* 105: 7-22.

Stout, S.A., J.R. Payne, R.W. Ricker, G. Baker, C. Lewis. 2016b. Macondo oil in deep-sea sediments: Part 2 – Distribution and distinction from background and natural oil seeps. *Marine Pollution Bulletin* 111: 381-401.

Stout, S.A. and Z. Wang, 2007. Chemical fingerprinting of spilled or discharged petroleum – methods and factors affecting petroleum fingerprints in the environment. Chapter 1, Oil Spill Environmental Forensics – Fingerprinting and Source Identification. 1st Edition. Wang, Z. and S.A. Stout (eds), Academic Press (an imprint of Elsevier), Burlington, MA. 554 pp. ISBN 10: 0-12-369523-6.

Stout, S.A. and Z. Wang, 2016. Chemical Fingerprinting Methods and Factors Affecting Petroleum Fingerprints in the Environment. Chapter 3, Standard Handbook Oil Spill Environmental Forensics: Fingerprinting and Source Identification. 2nd Edition. Stout, S.A. and Z. Wang (eds), Academic Press, Burlington, MA. 1107 pp. DOI: 10.1016/B978-0-12-809659-8.00003-6

Appendix 1 POLYCYCLIC AROMATIC HYDROCARBON (PAH), SATURATED HYDROCARBON (SHC), AND BIOMARKER ANALYTES

ANALYTES	**Abbreviation**
PAH	
Naphthalene	N
C1-Naphthalene	N1
C2-Naphthalene	N2
C3-Naphthalene	N3
C4-Naphthalene	N4
Biphenyl	BI
Acenaphthylene	ACY
Acenaphthene	ACN
Fluorene	F
C1-Fluorene	F1
C2-Fluorene	F2
C3-Fluorene	F3
C4-Fluorene	F4
Anthracene	A
Phenanthrene	Ph
C1-Phenanthrene/Anthracene	PA1
C2-Phenanthrene/Anthracene	PA2
C3-Phenanthrene/Anthracene	PA3
C4-Phenanthrene/Anthracene	PA4
Retene	RET
Dibenzothiophene	DBT
C1-Dibenzothiophene	DBT1
C2-Dibenzothiophene	DBT2
C3-Dibenzothiophene	DBT3
C4-Dibenzothiophene	DBT4
Benzo(b)fluorene	BF
Fluoranthene	FL
Pyrene	PY
C1-Fluoranthene/Pyrene	FP1
C2-Fluoranthene/Pyrene	FP2
C3-Fluoranthene/Pyrene	FP3
C4-Fluoranthene/Pyrene	FP4
Napthobenzothiophene	NBT
C1-Napthobenzothiophene	NBT1
C2-Napthobenzothiophene	NBT2
C3-Napthobenzothiophene	NBT3
C4-Napthobenzothiophene	NBT4
Benzo(a)Anthracene	BAA
Chrysene	C
C1-Chrysene	C1
C2-Chrysene	C2

C3-Chrysene	C3
C4-Chrysene	C4
Benzo(b)fluoranthene	BBF
Benzo(k)fluoranthene	BKF
Benzo(a)fluoranthene	BAF
Benzo(e)pyrene	BEP
Benzo(a)pyrene	BAP
Perylene	PER
Indeno(1,2,3-cd)pyrene	IND
Dibenzo(a,h)anthracene	DAHA
Benzo(g,h,i)perylene	BGH
Total PAH	TPAH

Saturated hydrocarbons (SHC or n-alkanes)

Analyte	Abbrev
Nonane (C9)	C9
Decane (C10)	C10
Undecane (C11)	C11
Dodecane (C12)	C12
Tridecane (C13)	C13
2,6,10 Trimethyldodecane (1380)	1380
Tetradecane (C14)	C14
2,6,10-Trimethyltridecane (1470)	1470
Pentadecane (C15)	C15
Hexadecane (C16)	C16
Norpristane (1650)	Pristane
Heptadecane (C17)	C17
Pristane	Phytane
Octadecane (C18)	C18
Phytane	Phy
Nonadecane (C19)	C19
Eicosane (C20)	C20
Heneicosane (C21)	C21
Docosane (C22)	C22
Tricosane (C23)	C23
Tetracosane (C24)	C24
Pentacosane (C25)	C25
Hexacosane (C26)	C26
Heptacosane (C27)	C27
Octacosane (C28)	C28
Nonacosane (C29)	C29
Triacontane (C30)	C30
Hentriacontane (C31)	C31
Dotriacontane (C32)	C32
Tritriacontane (C33)	C33
Tetratriacontane (C34)	C34
Pentatriacontane (C35)	C35
Hexatriacontane (C36)	C36
Heptatriacontane (C37)	C37
Octatriacontane (C38)	C38
Nonatriacontane (C39)	C39
Tetracontane (C40)	C40
Total SHC	**TSHC**

Petroleum Biomarkers

Class	Biomarker	Abbrev
Terpanes	C23 tricyclic terpane	T4
	C24 tricyclic terpane	T5
	C25 tricyclic terpane (a)	T6
	C25 tricyclic terpane (b)	T6
	C24 tetracyclic terpane	T6a
	C26 tricyclic terpane (a)	T6c
	C26 tricyclic terpane (b)	T6b
	C28 tricyclic terpane (a)	T8
	C28 tricyclic terpane (b)	T7
	C29 tricyclic terpane (a)	T10
	C29 tricyclic terpane (b)	T9
Hopanes	18α(H),21β(H)-22,29,30-trisnorhopane	Ts
	17α(H),21β(H)-22,29,30-trisnorhopane	Tm
	17α(H),18α(H),21β(H)-28,30-bisnorhopane	14a
	17α(H),21β(H)-25-norhopane	14b
	17α(H),21β(H)-30-norhopane	T15
	18α(H),21β(H)-30-norneohopane	T16
	17β(H),21α(H)-30-norhopane (normoretane)	T17
	18α(H) and 18β(H)-oleanane	T18
	17α(H),21β(H)-hopane	T19
	17α(H)-30-nor-29-homohopane	
	17β(H),21α(H)-hopane (moretane)	T20
	22S-17α(H),21β(H)-30-homohopane	T21
	22R-17α(H),21β(H)-30-homohopane	T22
	Gammacerane	T22a
	22S-17α(H),21β(H)-30,31-bishomohopane	T26
	22R-17α(H),21β(H)-30,31-bishomohopane	T27
	22S-17α(H),21β(H)-30,31,32-trishomohopane	T30
	22R-17α(H),21β(H)-30,31,32-trishomohopane	T31
	22S-17α(H),21β(H)-30,31,32,33-tetrakishomohopane	T32
	22R-17α(H),21β(H)-30,31,32,33-tetrakishomohopane	T33
	22S-17α(H),21β(H)-30,31,32,33,34-pentakishomohopane	T34
	22R-17α(H),21β(H)-30,31,32,33,34-pentakishomohopane	T35
Steranes	13b(H),17a(H)-20S-Diacholestane (S4)	S4
	13b(H),17a(H)-20R-Diacholestane (S5)	S5
	13b,17a-20S-Methyldiacholestane (S8)	S8
	17a(H)20SC27/C29dia	DIA29S
	17a(H)20RC27/C29dia	DIA29R
	Unknown Sterane (S18)	S18

	13a,17b-20S-Ethyldiacholestane (S19)	S19
	14a,17a-20S-Methylcholestane (S20)	S20
	14a,17a-20R-Methylcholestane (S24)	S24
	14a(H),17a(H)-20S-Ethylcholestane (S25)	S25
	14a(H),17a(H)-20R-Ethylcholestane (S28)	S28
	14b(H),17b(H)-20R-Cholestane (S14)	S14
	14b(H),17b(H)-20S-Cholestane (S15)	S15
	14b,17b-20R-Methylcholestane (S22)	S22
	14b,17b-20S-Methylcholestane (S23)	S23
	14b(H),17b(H)-20R-Ethylcholestane (S26)	S26
	14b(H),17b(H)-20S-Ethylcholestane (S27)	S27
Triaromatic Steroids	C26,20R- + C27,20S- triaromatic steroid	TAS1
	C28,20S-triaromatic steroid	TAS2
	C27,20R-triaromatic steroid	TAS3
	C28,20R-triaromatic steroid	TAS4
	C29,20S-triaromatic steroid	TAS5
	C29,20R-triaromatic steroid	TAS6

APPENDIX 2. Analytic Results for 2018 Field Samples and Blanks

2018 AMT Sediments (PAH, SHC, and Biomarkers)

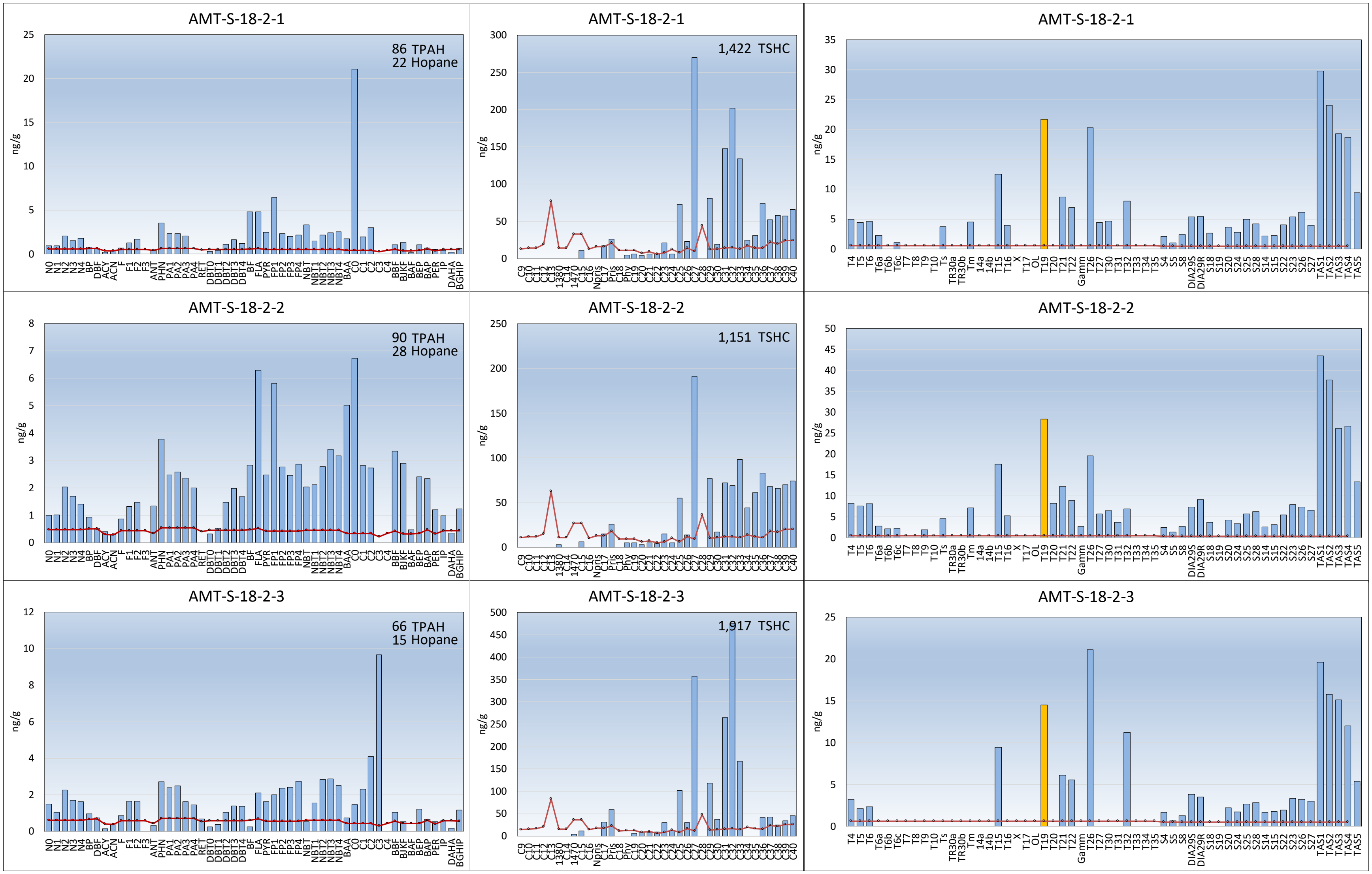

The dotted red line represents the sample-specific MDL for PAH, SHC, and biomarkers.

2018 GOC Sediments (PAH, SHC, and Biomarkers)

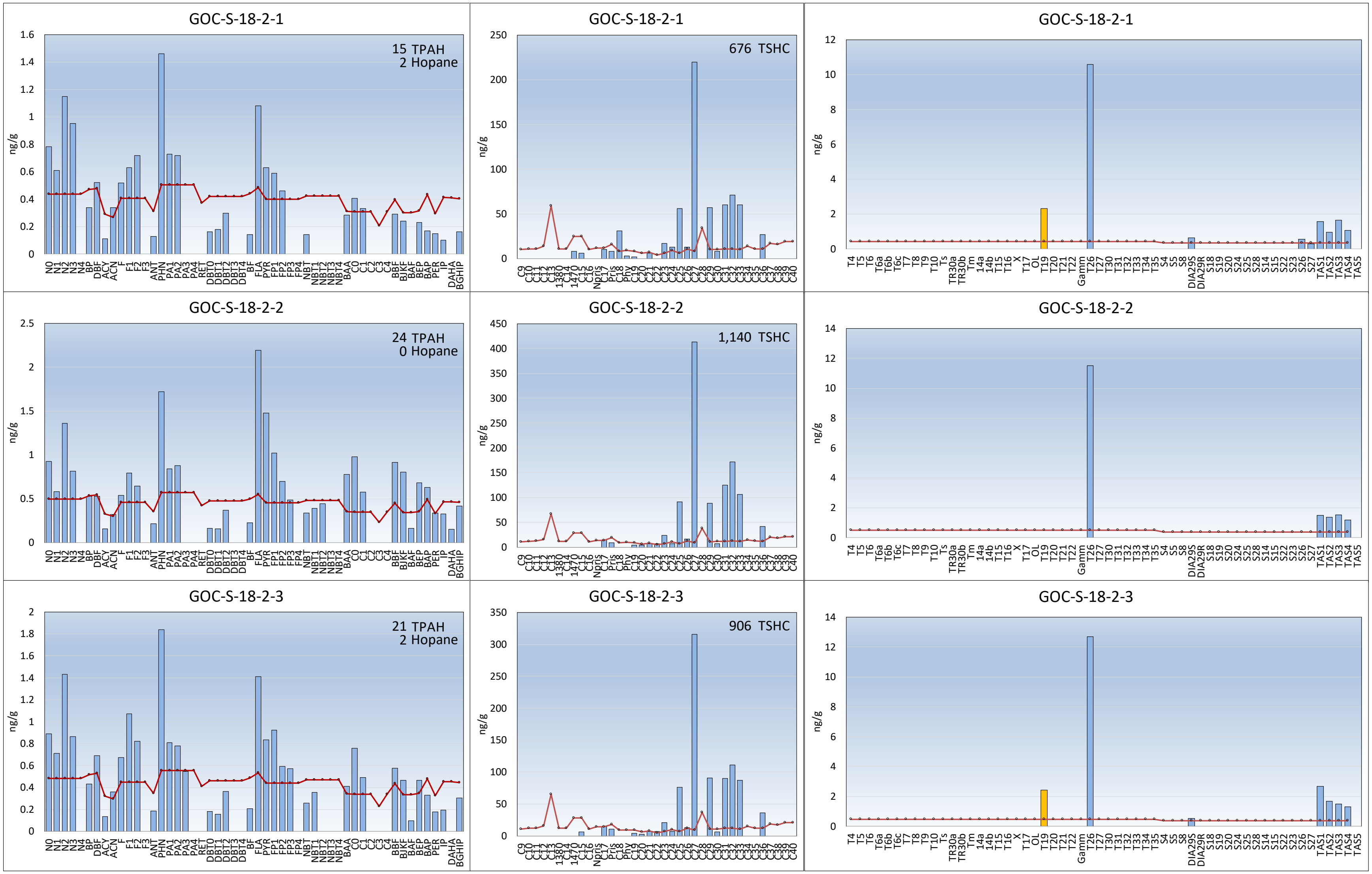

The dotted red line represents the sample-specific MDL for PAH, SHC, and biomarkers.

2018 AMT Tissues (PAH, SHC, and Biomarkers)

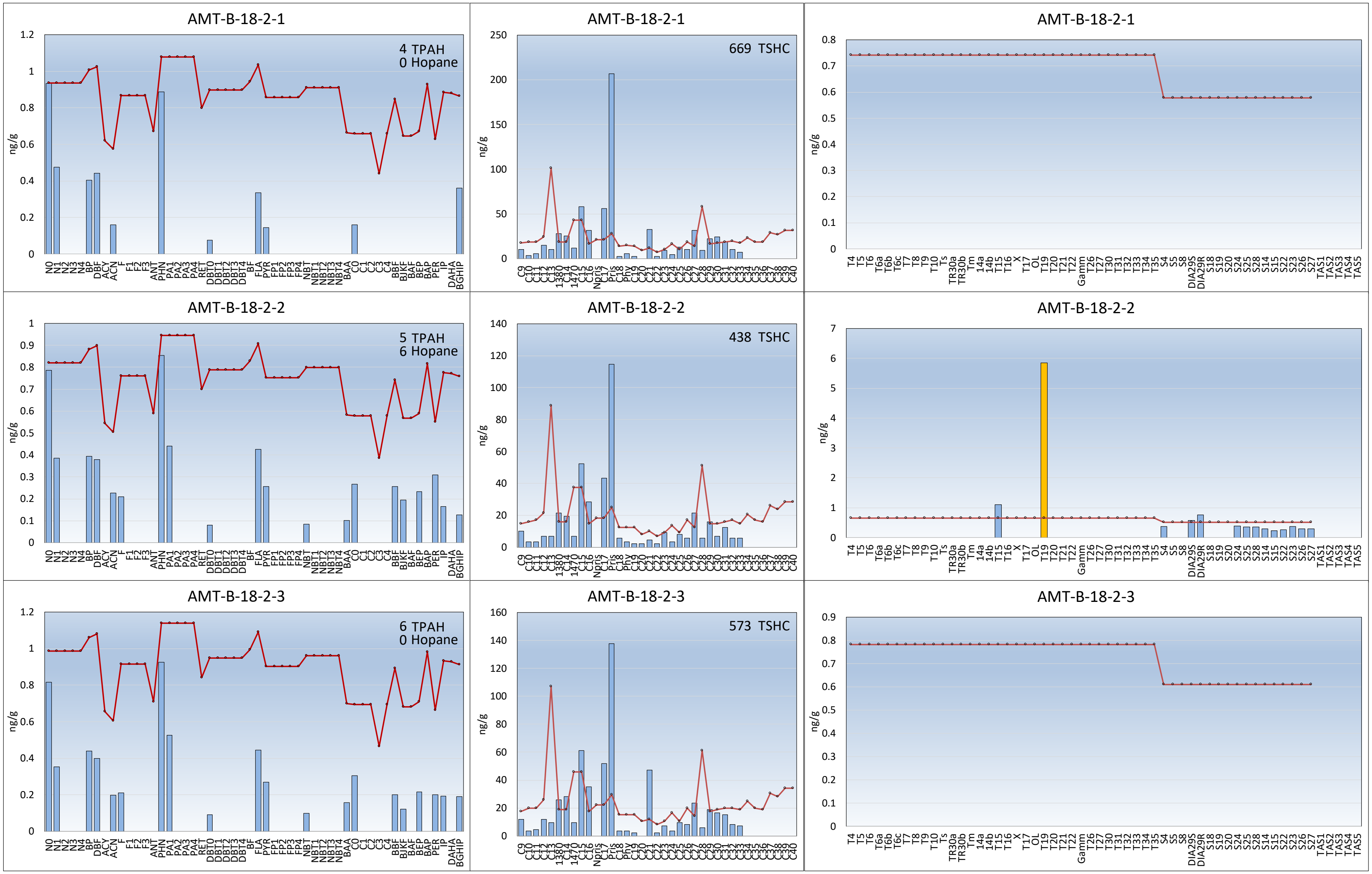

The dotted red line represents the sample-specific MDL for PAH, SHC, and biomarkers.

2018 JAP Tissues (PAH, SHC, and Biomarkers)

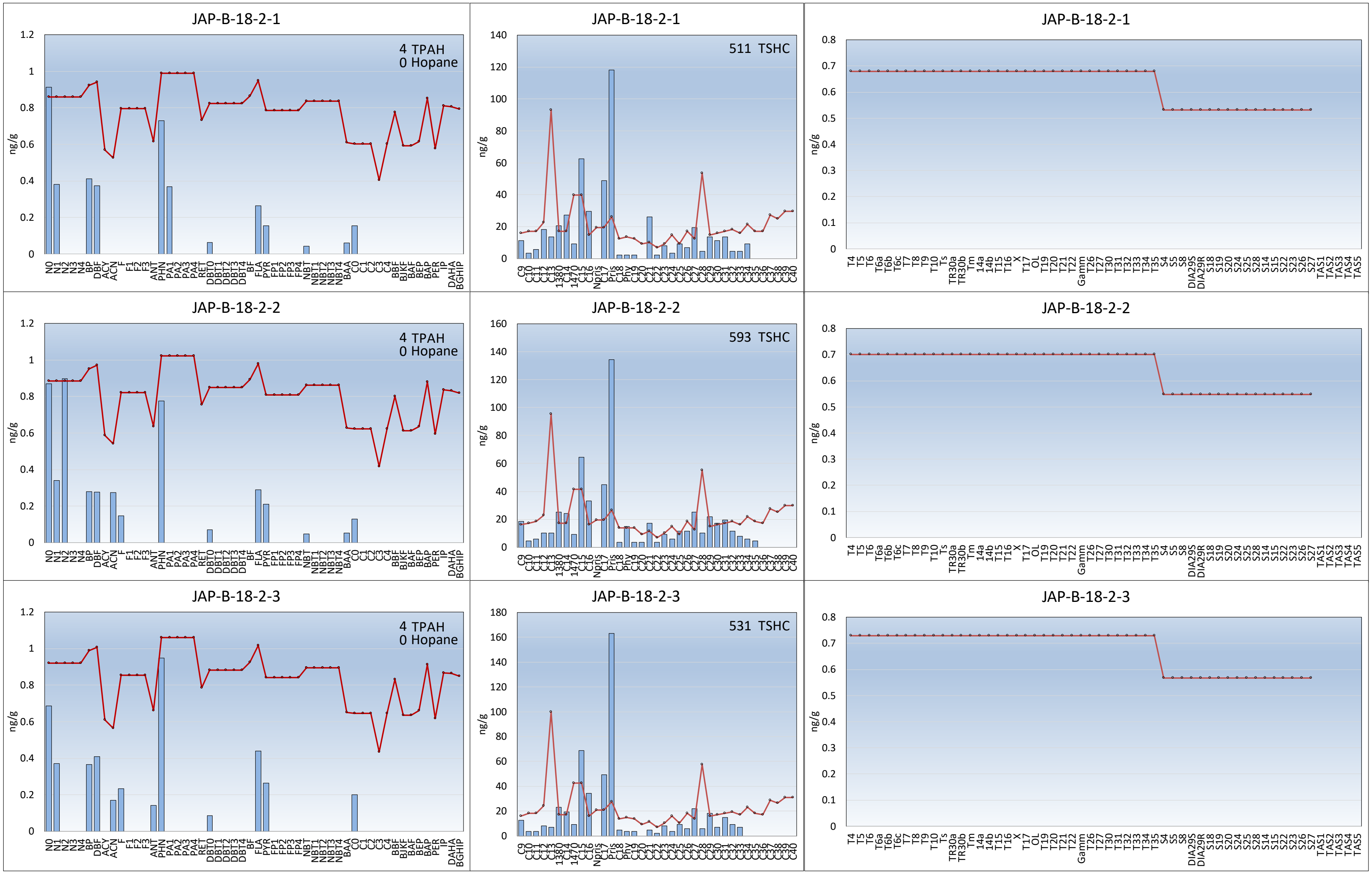

The dotted red line represents the sample-specific MDL for PAH, SHC, and biomarkers.

2018 GOC Tissues (PAH, SHC, and Biomarkers)

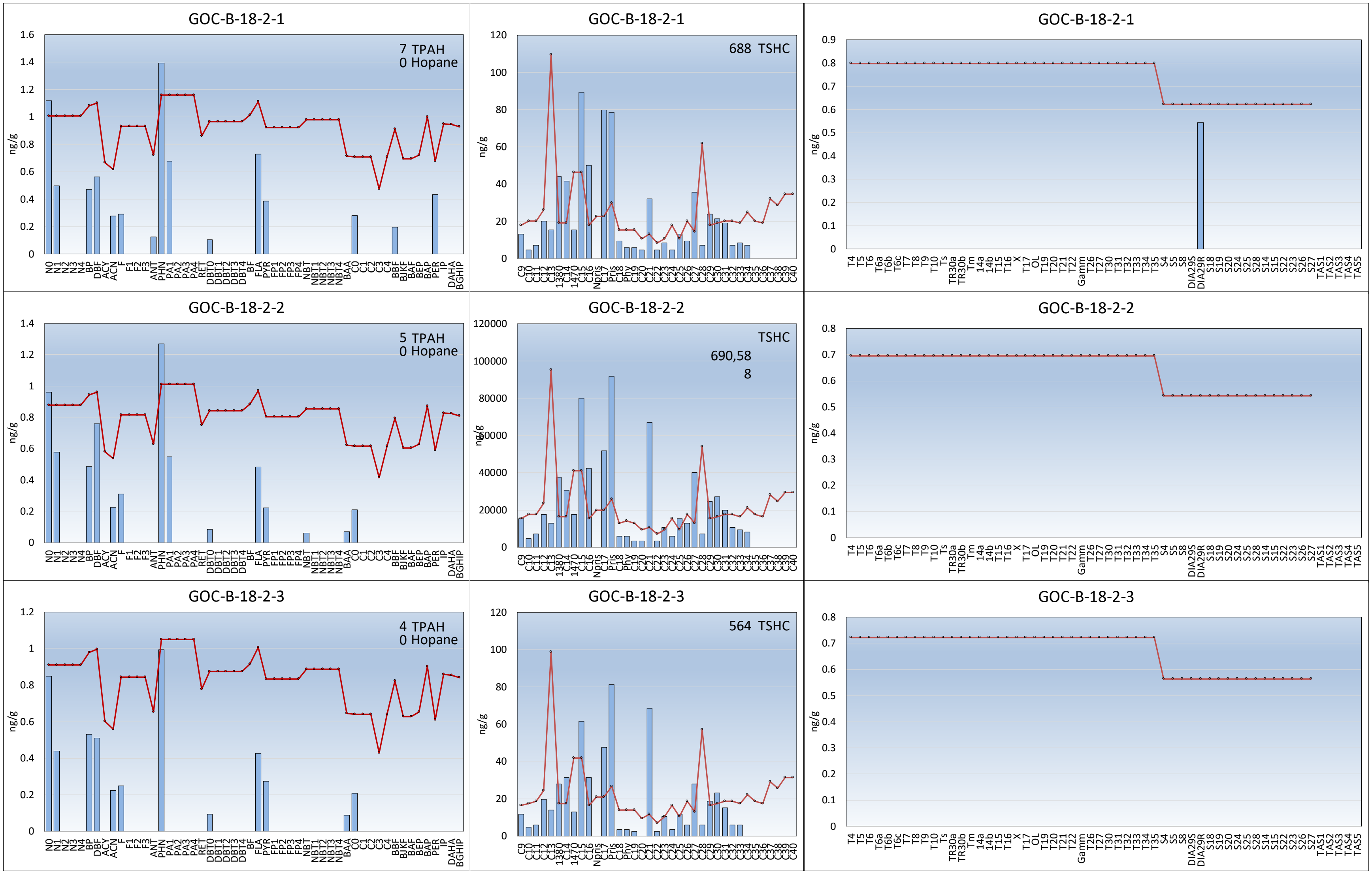
GOC-B-18-2-1

GOC-B-18-2-1

GOC-B-18-2-1

GOC-B-18-2-2

GOC-B-18-2-2

GOC-B-18-2-2

GOC-B-18-2-3

GOC-B-18-2-3

GOC-B-18-2-3

The dotted red line represents the sample-specific MDL for PAH, SHC, and biomarkers.

2018 KNH Tissues (PAH, SHC, and Biomarkers)

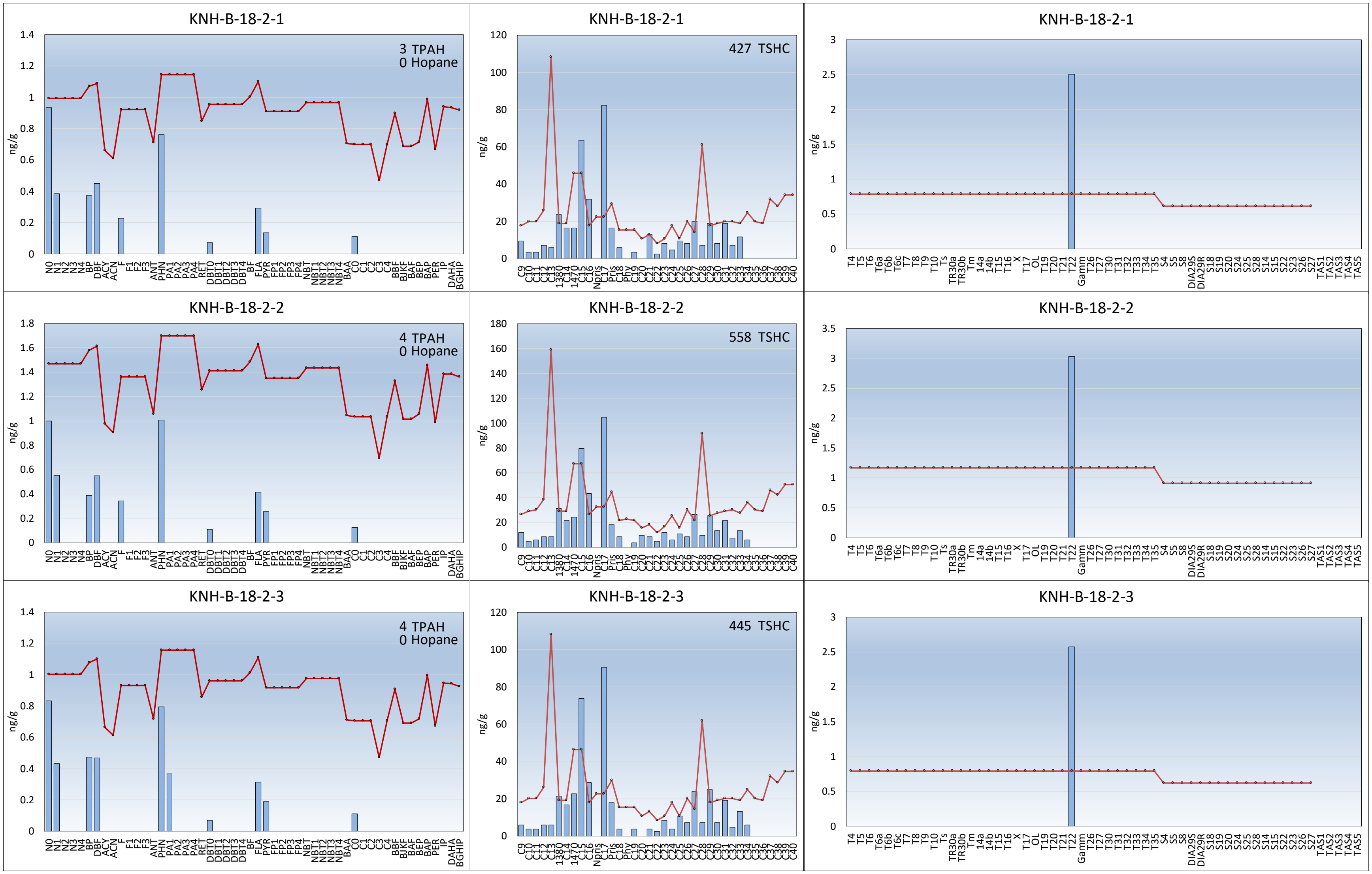

The dotted red line represents the sample-specific MDL for PAH, SHC, and biomarkers.

2018 SHB Tissues (PAH, SHC, and Biomarkers)

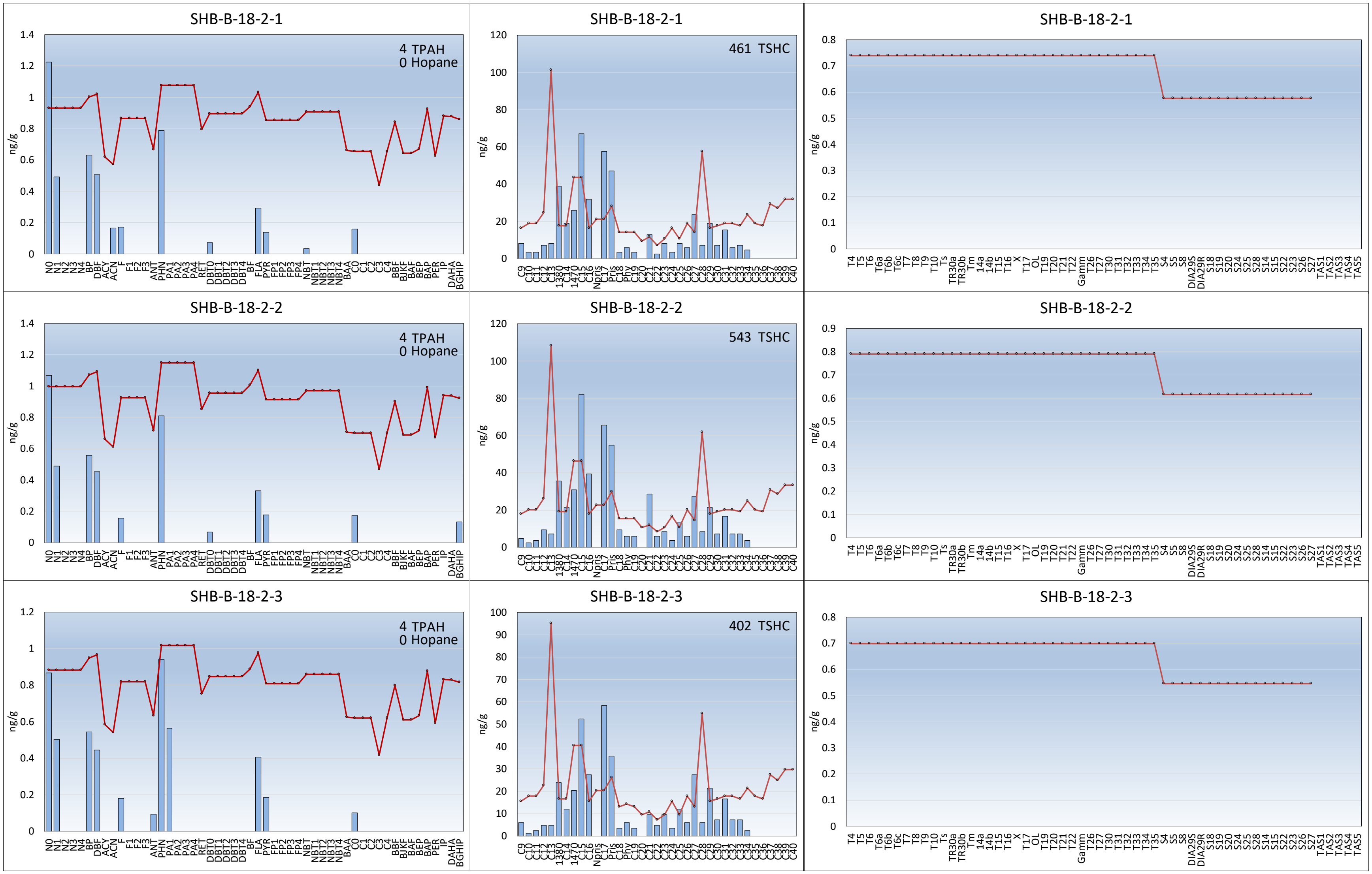

The dotted red line represents the sample-specific MDL for PAH, SHC, and biomarkers.

2018 AIB Tissues (PAH, SHC, and Biomarkers)

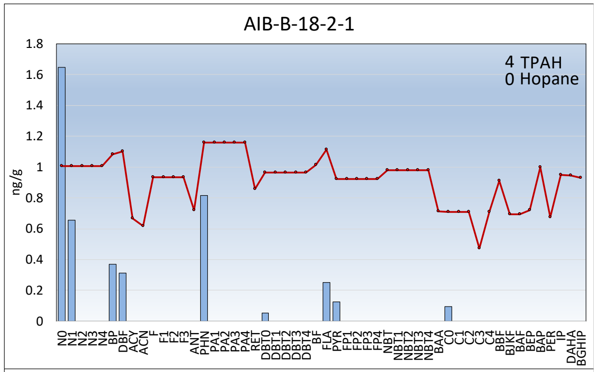

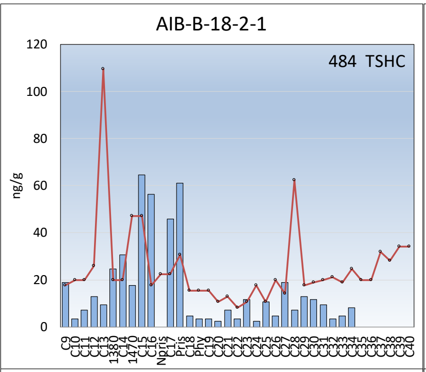

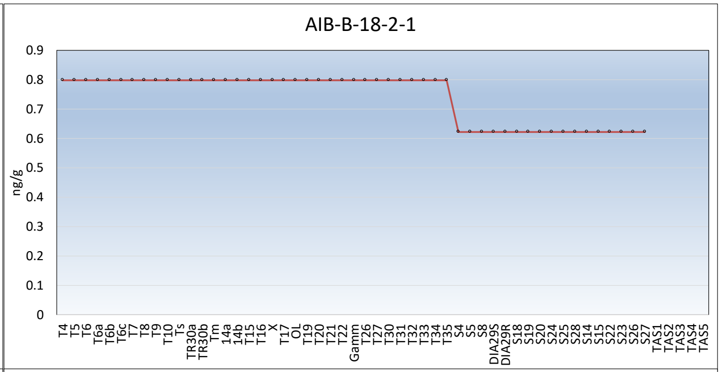

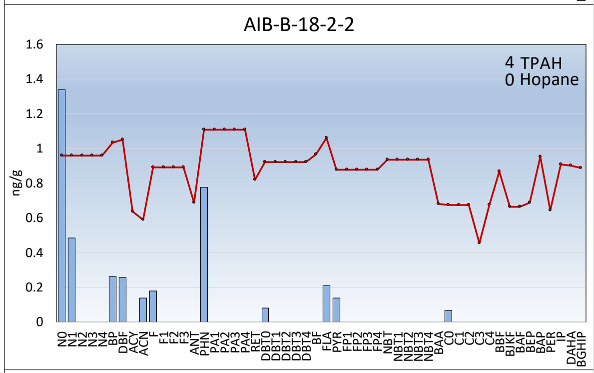

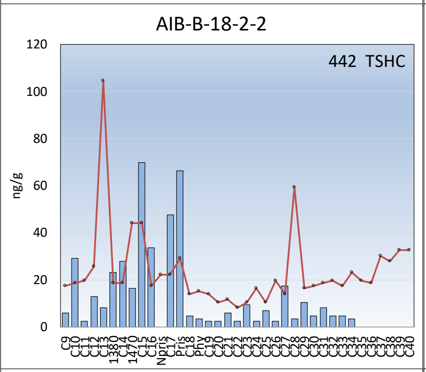

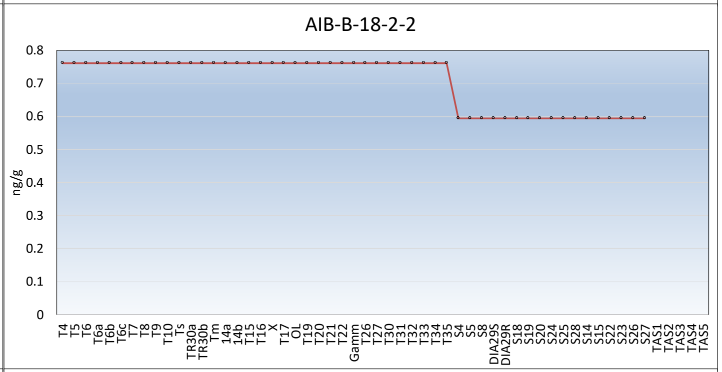

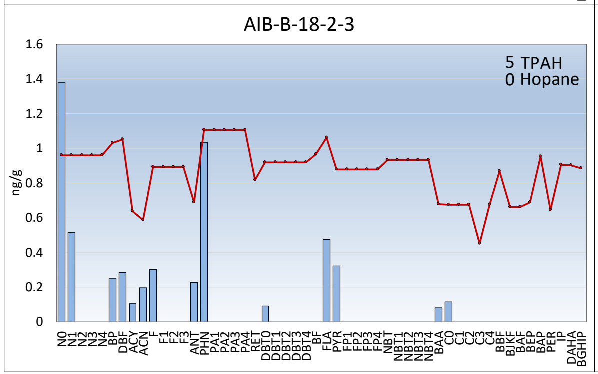

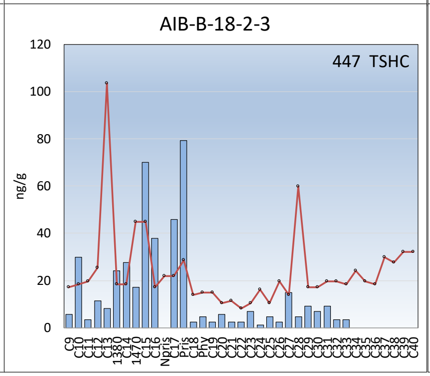

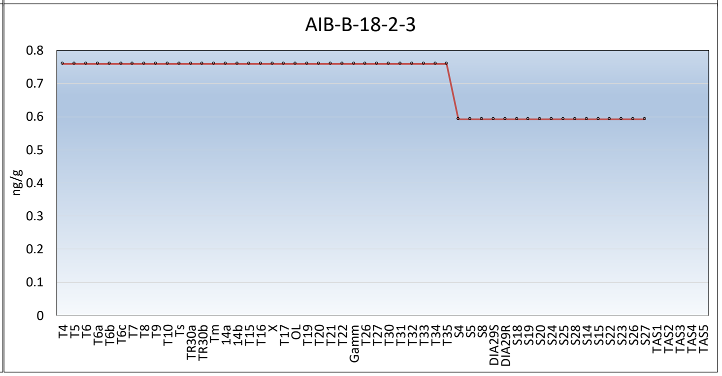

The dotted red line represents the sample-specific MDL for PAH, SHC, and biomarkers.

2018 DII Tissues (PAH, SHC, and Biomarkers)

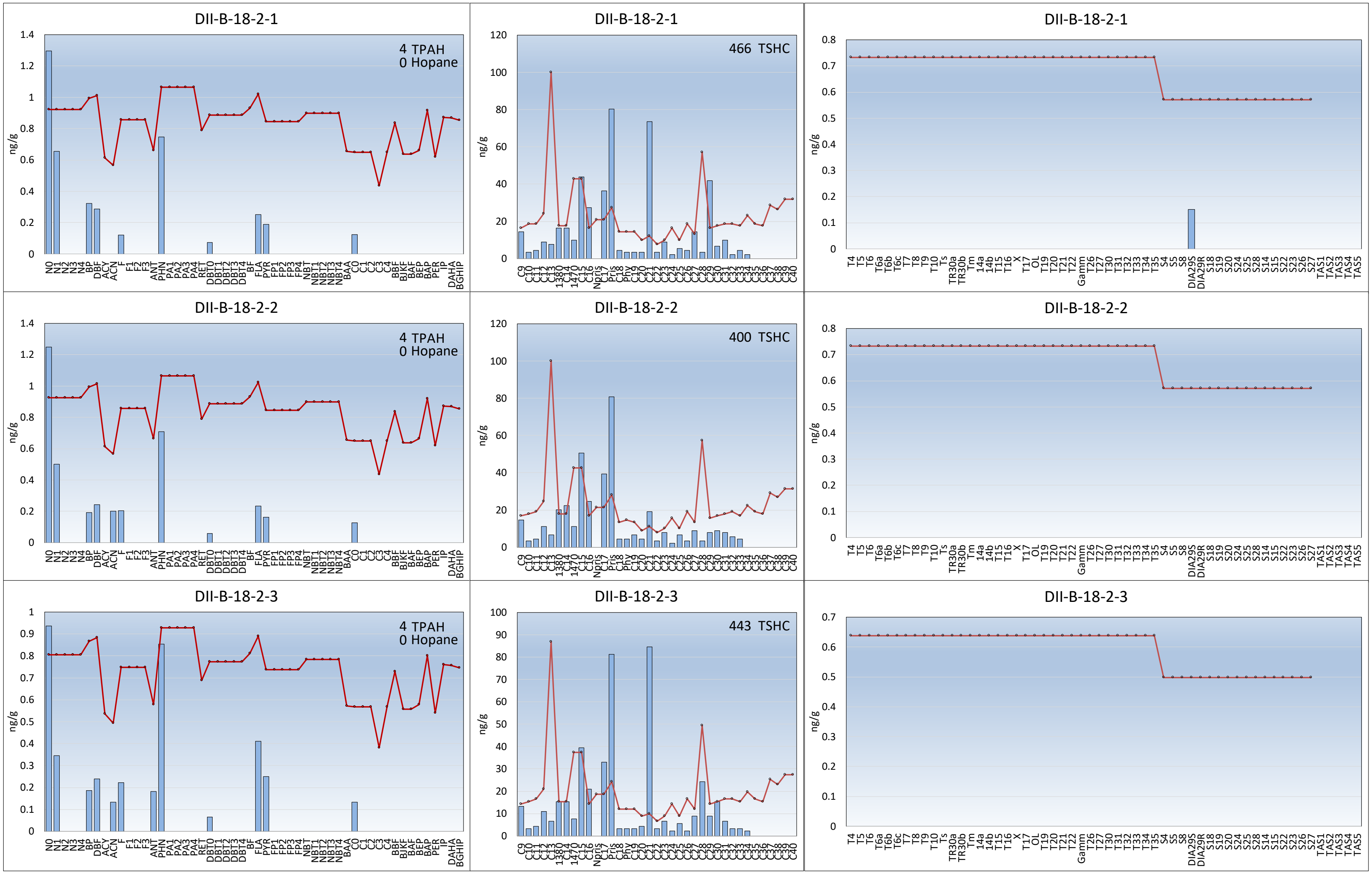

The dotted red line represents the sample-specific MDL for PAH, SHC, and biomarkers.

2018 SHH Tissues (PAH, SHC, and Biomarkers)

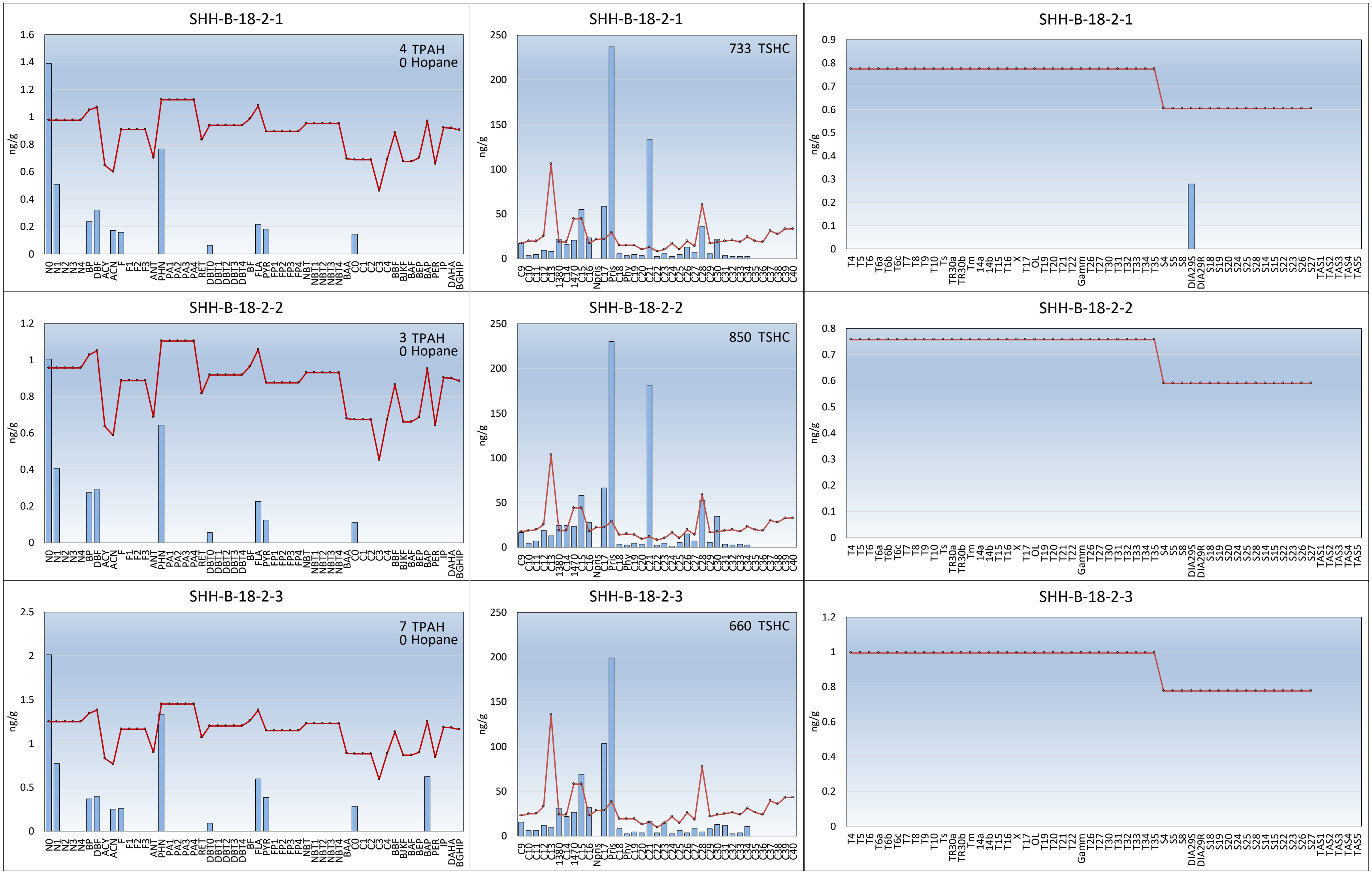

The dotted red line represents the sample-specific MDL for PAH, SHC, and biomarkers.

2018 SLB Tissues (PAH, SHC, and Biomarkers)

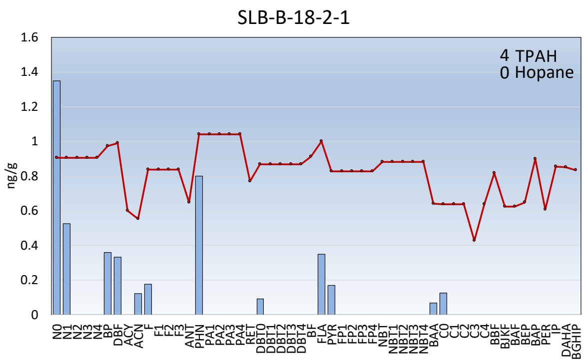

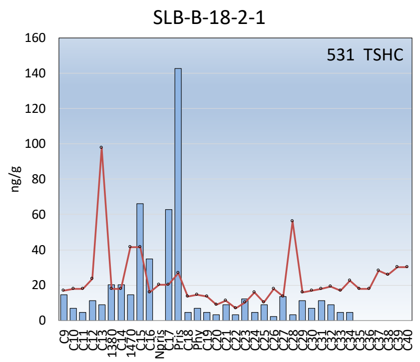

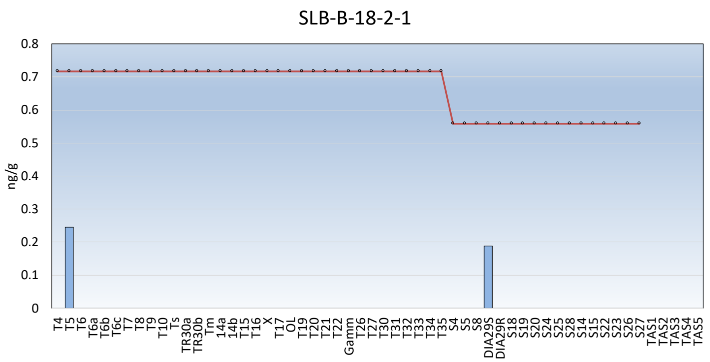

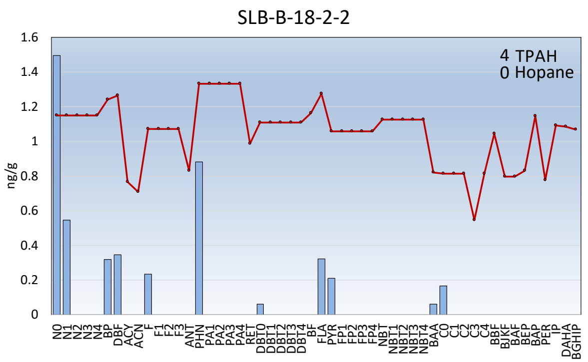

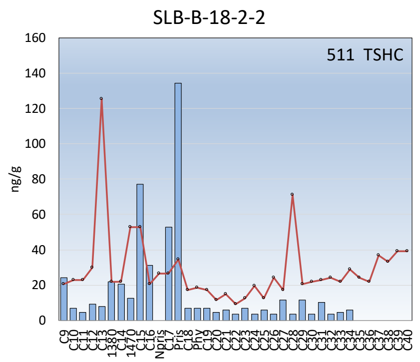

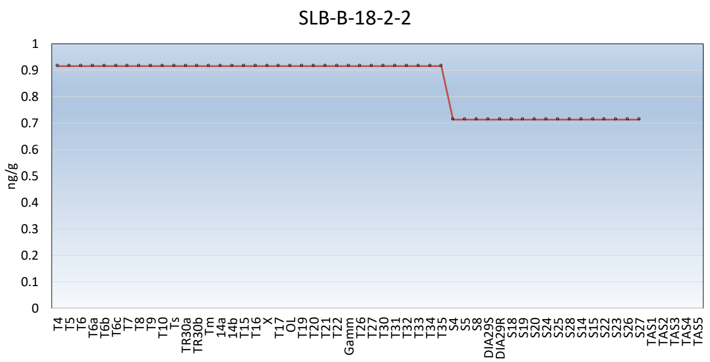

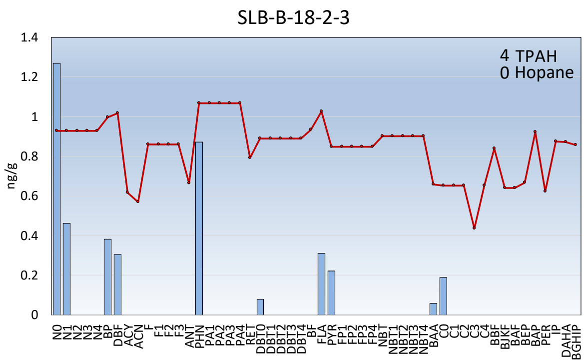

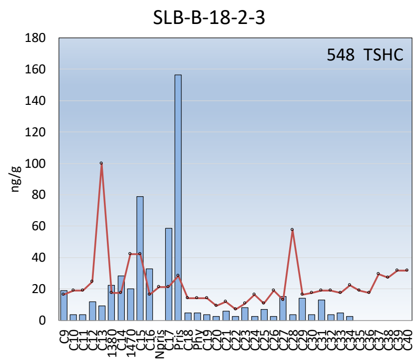

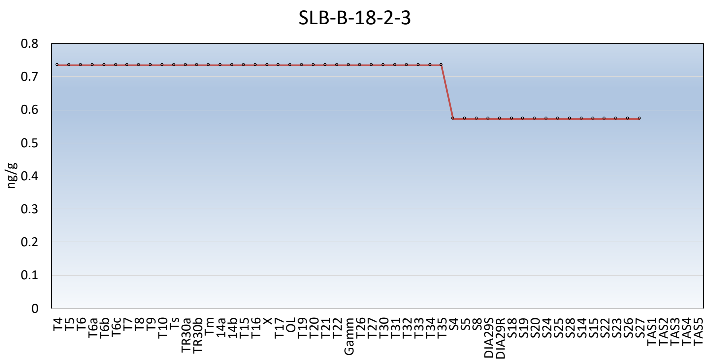

The dotted red line represents the sample-specific MDL for PAH, SHC, and biomarkers.

2018 WIB Tissues (PAH, SHC, and Biomarkers)

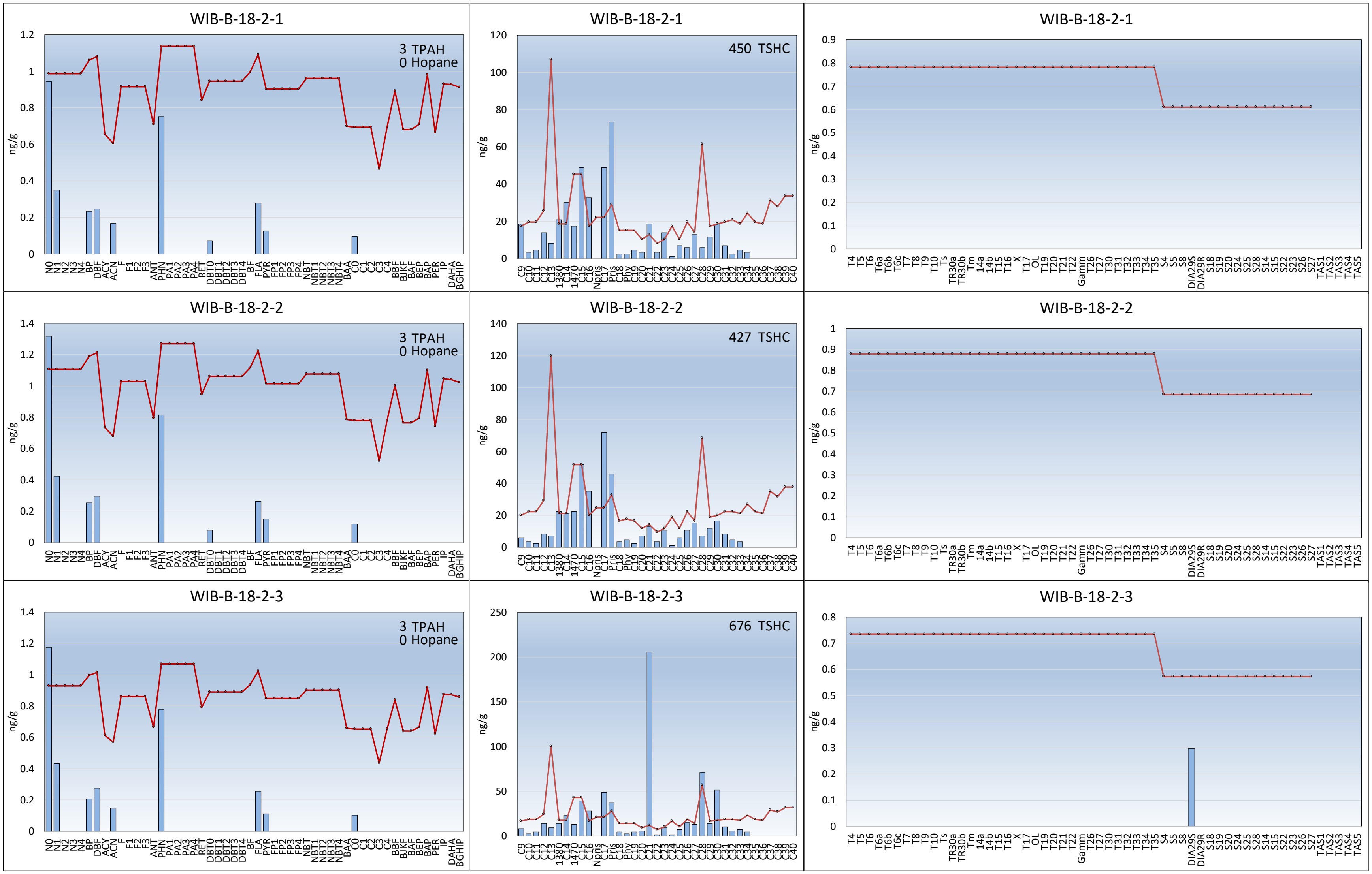

The dotted red line represents the sample-specific MDL for PAH, SHC, and biomarkers.

2018 ZAB Tissues (PAH, SHC, and Biomarkers)

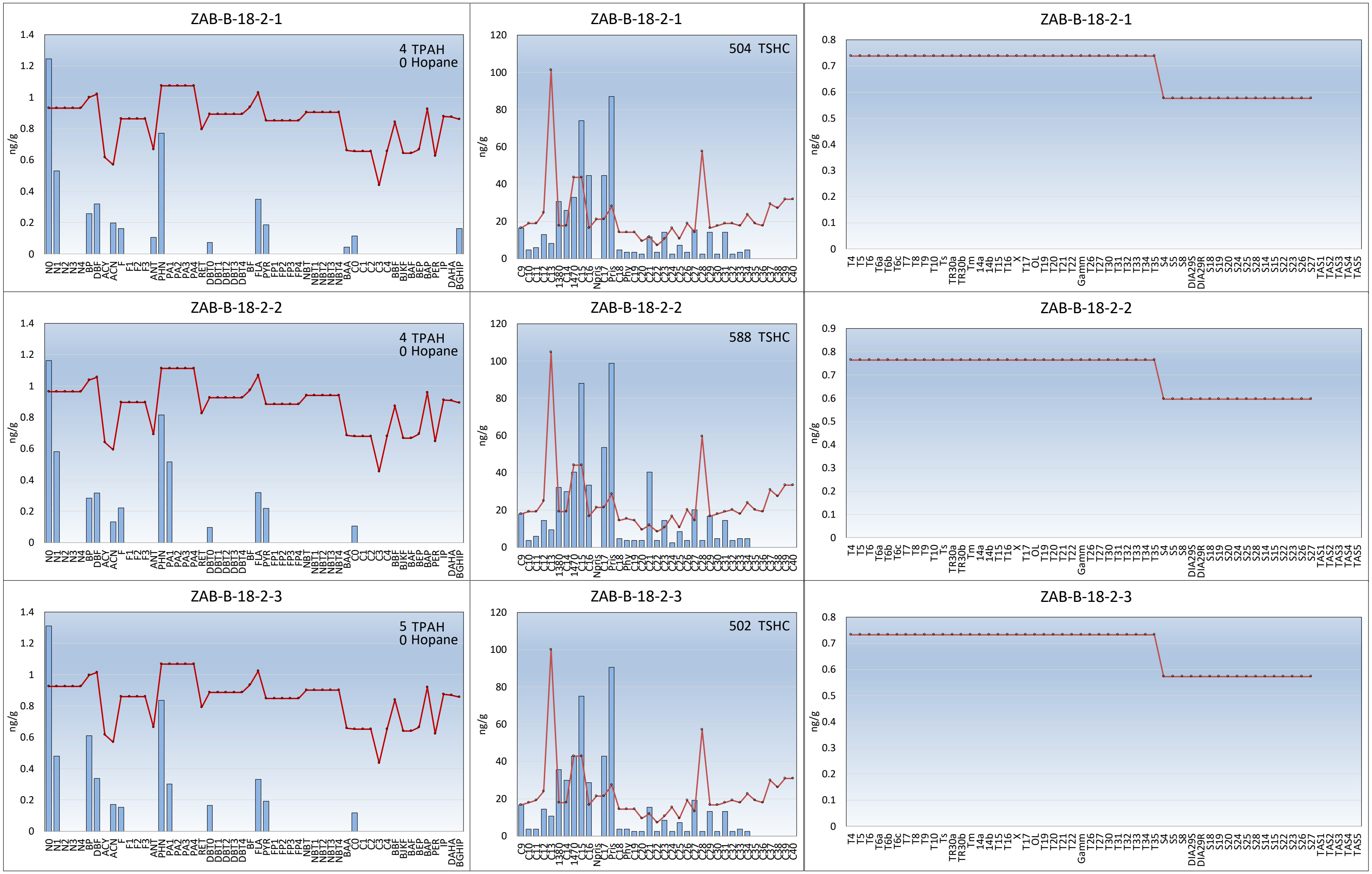

The dotted red line represents the sample-specific MDL for PAH, SHC, and biomarkers.

2018 Tissue Lab Method Blanks with MDL overlay

2018 Sediment Lab Method Blank with MDL overlay

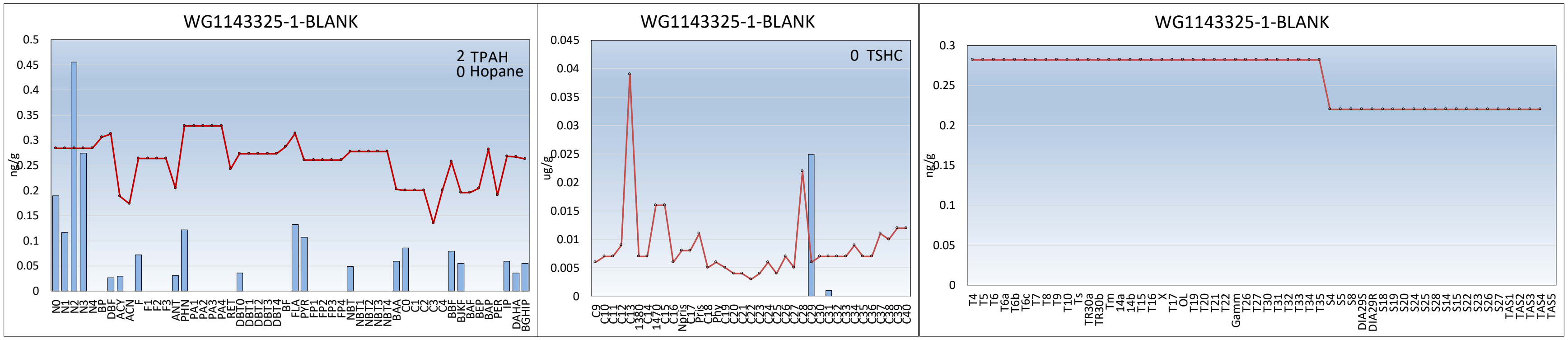

The dotted red line represents the sample-specific MDL for PAH, SHC, and biomarkers.

2018 PSD profiles for Jackson Point (JAC), Saw Island (SAW), Gold Creek (GOC), Disk Island (DSK), and Knowles Head (KNH). Note blue-colored analytes are scaled on the left x-axis; red-colored analytes on the order-of-magnitude lower scale on the right. Note: the site abbreviations reflect the data and names as received from OSU.

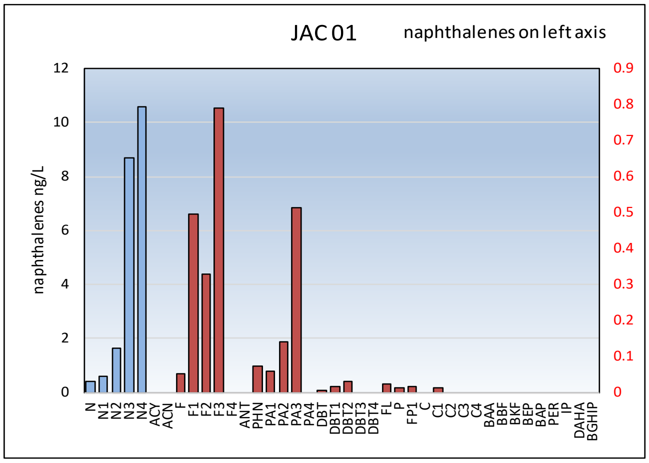

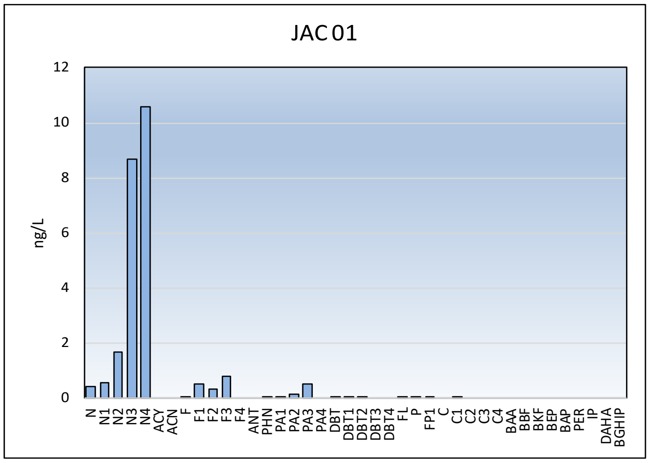

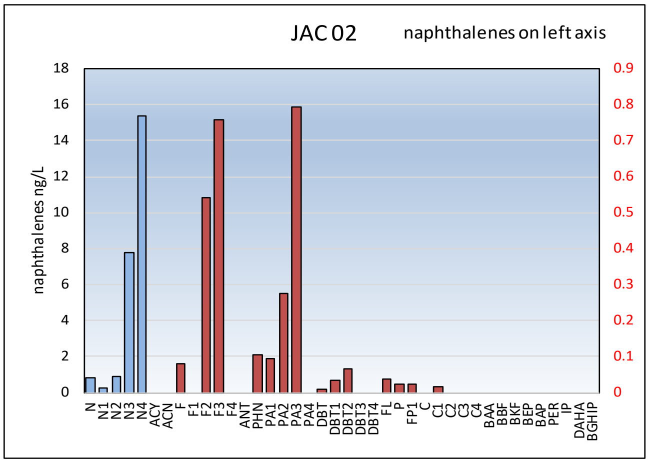

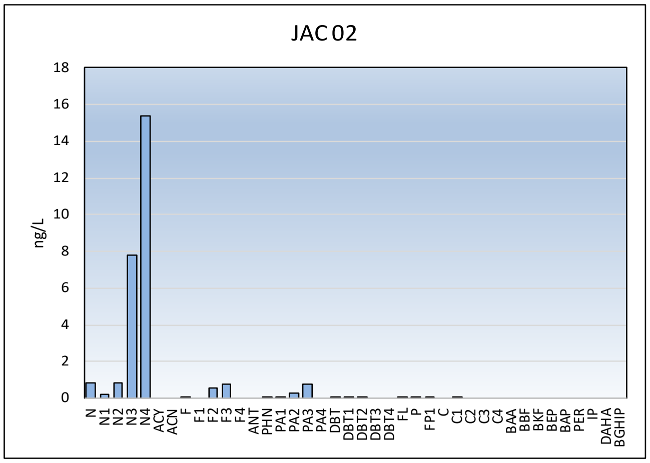

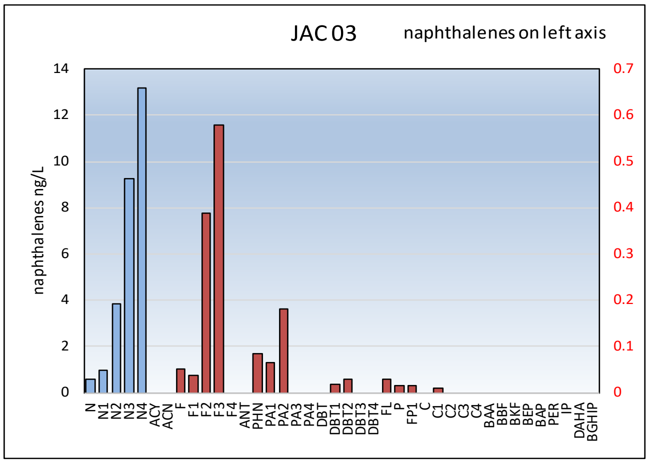

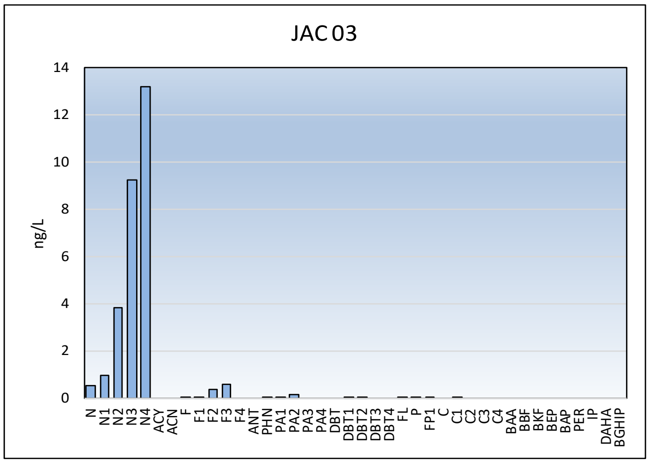

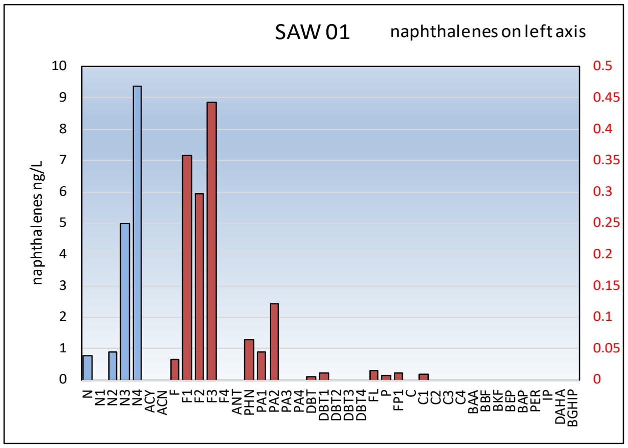
SAW 01
naphthalenes on left axis
naphthalenes ng/L
0
1
2
3
4
5
6
7
8
9
10
0
0.05
0.1
0.15
0.2
0.25
0.3
0.35
0.4
0.45
0.5
N N1 N2 N3 N4 ACY ACN F F1 F2 F3 F4 ANT PHN PA1 PA2 PA3 PA4 DBT DBT1 DBT2 DBT3 DBT4 FL P FP1 C C1 C2 C3 C4 BAA BBF BKF BEP BAP PER IP DAHA BGHIP

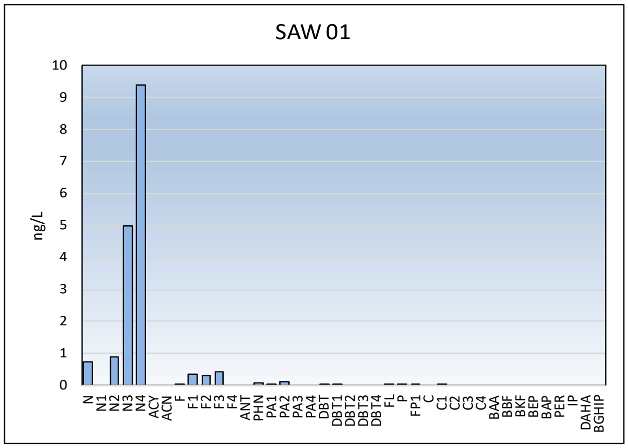
SAW 01
ng/L
0
1
2
3
4
5
6
7
8
9
10
N N1 N2 N3 N4 ACY ACN F F1 F2 F3 F4 ANT PHN PA1 PA2 PA3 PA4 DBT DBT1 DBT2 DBT3 DBT4 FL P FP1 C C1 C2 C3 C4 BAA BBF BKF BEP BAP PER IP DAHA BGHIP

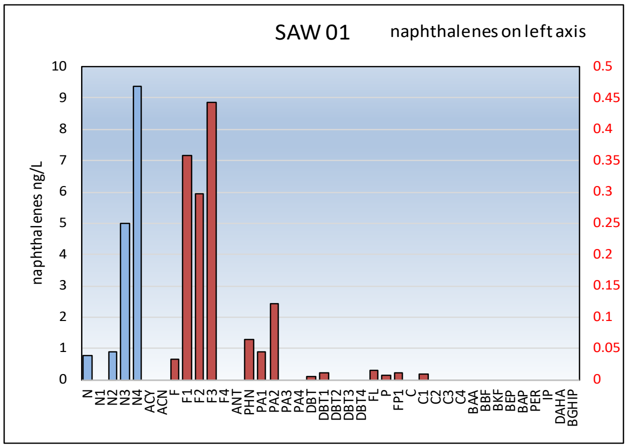
SAW 01
naphthalenes on left axis
naphthalenes ng/L
0
1
2
3
4
5
6
7
8
9
10
0
0.05
0.1
0.15
0.2
0.25
0.3
0.35
0.4
0.45
0.5
N N1 N2 N3 N4 ACY ACN F F1 F2 F3 F4 ANT PHN PA1 PA2 PA3 PA4 DBT DBT1 DBT2 DBT3 DBT4 FL P FP1 C C1 C2 C3 C4 BAA BBF BKF BEP BAP PER IP DAHA BGHIP

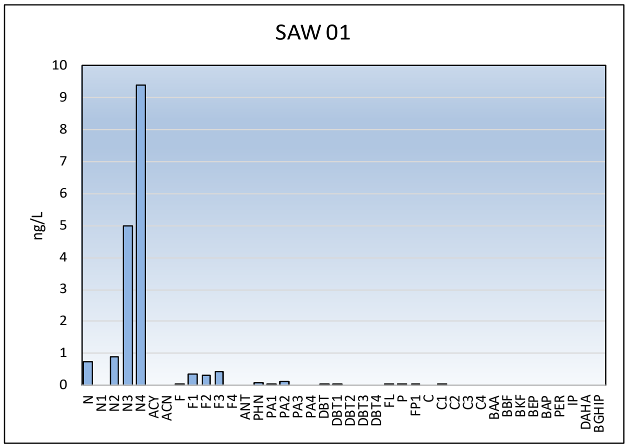
SAW 01
ng/L
0
1
2
3
4
5
6
7
8
9
10
N N1 N2 N3 N4 ACY ACN F F1 F2 F3 F4 ANT PHN PA1 PA2 PA3 PA4 DBT DBT1 DBT2 DBT3 DBT4 FL P FP1 C C1 C2 C3 C4 BAA BBF BKF BEP BAP PER IP DAHA BGHIP

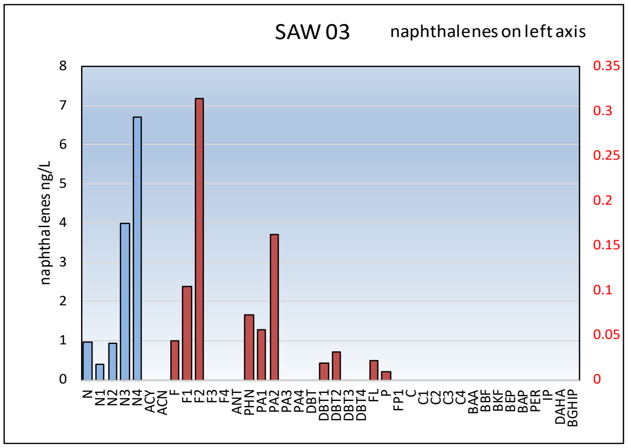
SAW 03
naphthalenes on left axis
naphthalenes ng/L
0
1
2
3
4
5
6
7
8
0
0.05
0.1
0.15
0.2
0.25
0.3
0.35
N N1 N2 N3 N4 ACY ACN F F1 F2 F3 F4 ANT PHN PA1 PA2 PA3 PA4 DBT DBT1 DBT2 DBT3 DBT4 FL P FP1 C C1 C2 C3 C4 BAA BBF BKF BEP BAP PER IP DAHA BGHIP

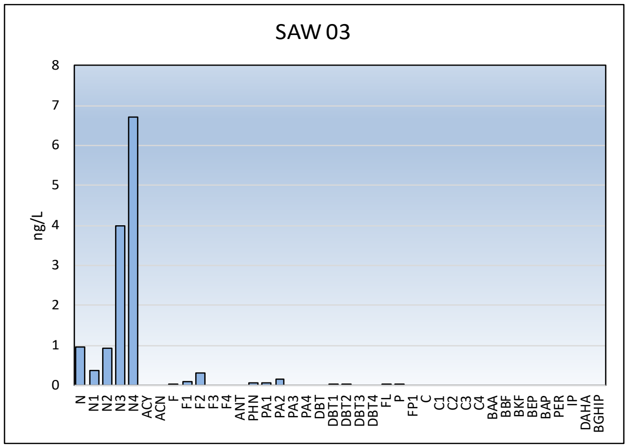
SAW 03
ng/L
0
1
2
3
4
5
6
7
8
N N1 N2 N3 N4 ACY ACN F F1 F2 F3 F4 ANT PHN PA1 PA2 PA3 PA4 DBT DBT1 DBT2 DBT3 DBT4 FL P FP1 C C1 C2 C3 C4 BAA BBF BKF BEP BAP PER IP DAHA BGHIP

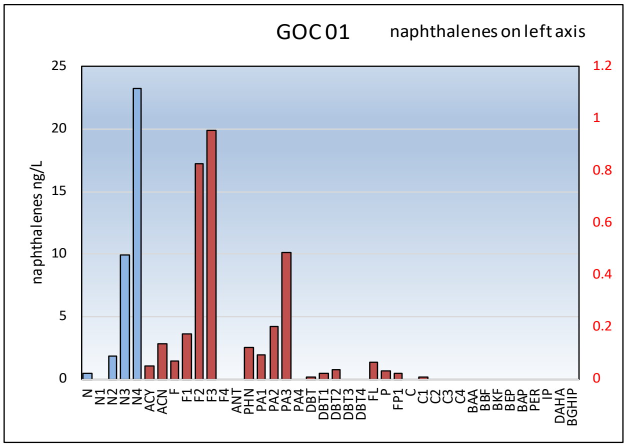
GOC 01
naphthalenes on left axis
naphthalenes ng/L
25
20
15
10
5
0
1.2
1
0.8
0.6
0.4
0.2
0
N N1 N2 N3 N4 ACY ACN F F1 F2 F3 F4 ANT PHN PA1 PA2 PA3 PA4 DBT DBT1 DBT2 DBT3 DBT4 FL P FP1 C C1 C2 C3 C4 BAA BBF BKF BEP BAP PER IP DAHA BGHIP

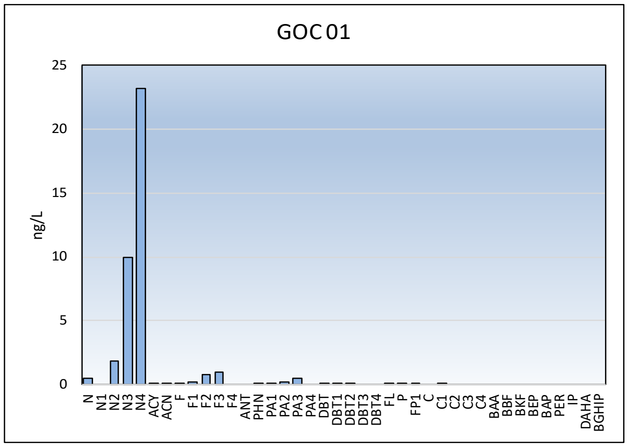
GOC 01
ng/L
25
20
15
10
5
0
N N1 N2 N3 N4 ACY ACN F F1 F2 F3 F4 ANT PHN PA1 PA2 PA3 PA4 DBT DBT1 DBT2 DBT3 DBT4 FL P FP1 C C1 C2 C3 C4 BAA BBF BKF BEP BAP PER IP DAHA BGHIP

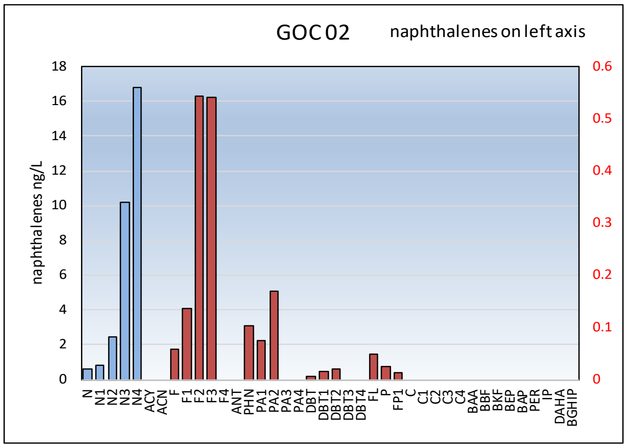
GOC 02
naphthalenes on left axis
naphthalenes ng/L
18
16
14
12
10
8
6
4
2
0
0.6
0.5
0.4
0.3
0.2
0.1
0
N N1 N2 N3 N4 ACY ACN F F1 F2 F3 F4 ANT PHN PA1 PA2 PA3 PA4 DBT DBT1 DBT2 DBT3 DBT4 FL P FP1 C C1 C2 C3 C4 BAA BBF BKF BEP BAP PER IP DAHA BGHIP

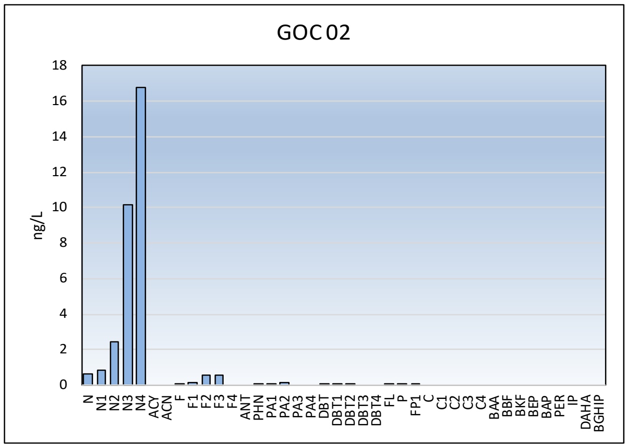
GOC 02
ng/L
18
16
14
12
10
8
6
4
2
0
N N1 N2 N3 N4 ACY ACN F F1 F2 F3 F4 ANT PHN PA1 PA2 PA3 PA4 DBT DBT1 DBT2 DBT3 DBT4 FL P FP1 C C1 C2 C3 C4 BAA BBF BKF BEP BAP PER IP DAHA BGHIP

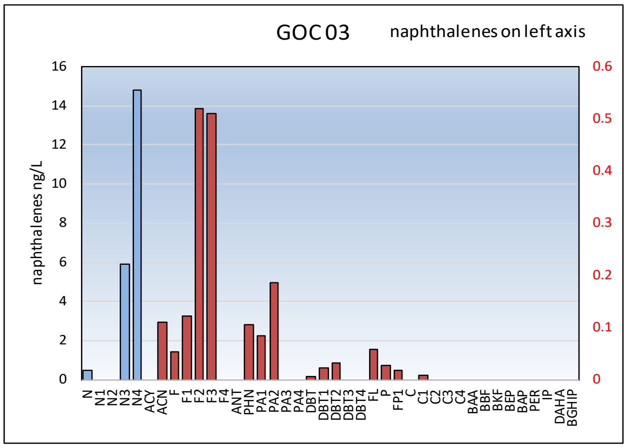
GOC 03
naphthalenes on left axis
naphthalenes ng/L
16
14
12
10
8
6
4
2
0
0.6
0.5
0.4
0.3
0.2
0.1
0
N N1 N2 N3 N4 ACY ACN F F1 F2 F3 F4 ANT PHN PA1 PA2 PA3 PA4 DBT DBT1 DBT2 DBT3 DBT4 FL P FP1 C C1 C2 C3 C4 BAA BBF BKF BEP BAP PER IP DAHA BGHIP

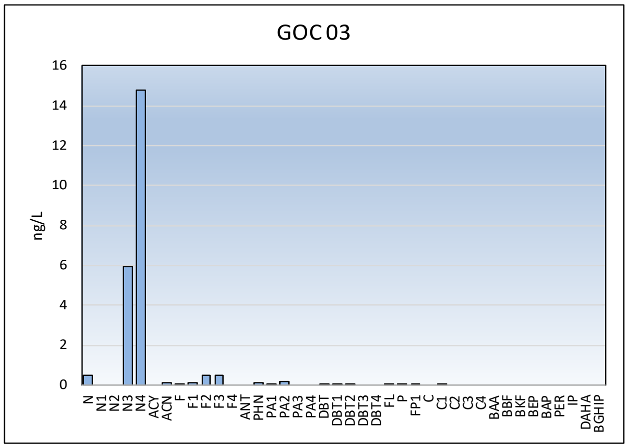
GOC 03
ng/L
16
14
12
10
8
6
4
2
0
N N1 N2 N3 N4 ACY ACN F F1 F2 F3 F4 ANT PHN PA1 PA2 PA3 PA4 DBT DBT1 DBT2 DBT3 DBT4 FL P FP1 C C1 C2 C3 C4 BAA BBF BKF BEP BAP PER IP DAHA BGHIP

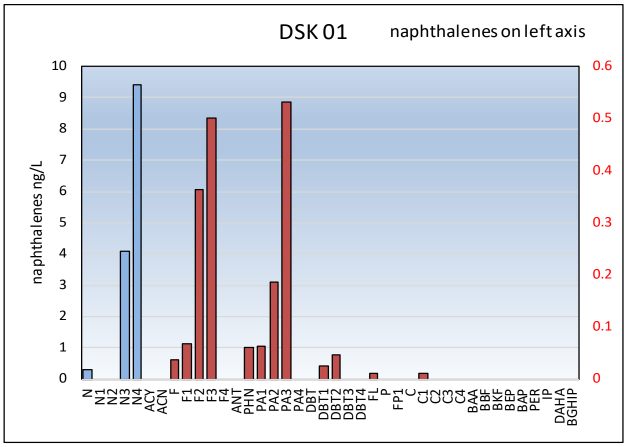
DSK 01
naphthalenes on left axis
naphthalenes ng/L
10 9 8 7 6 5 4 3 2 1 0
0.6 0.5 0.4 0.3 0.2 0.1 0
N N1 N2 N3 N4 ACY ACN F F1 F2 F3 F4 ANT PHN PA1 PA2 PA3 PA4 DBT DBT1 DBT2 DBT3 DBT4 FL P FP1 C C1 C2 C3 C4 BAA BBF BKF BEP BAP PER IP DAHA BGHIP

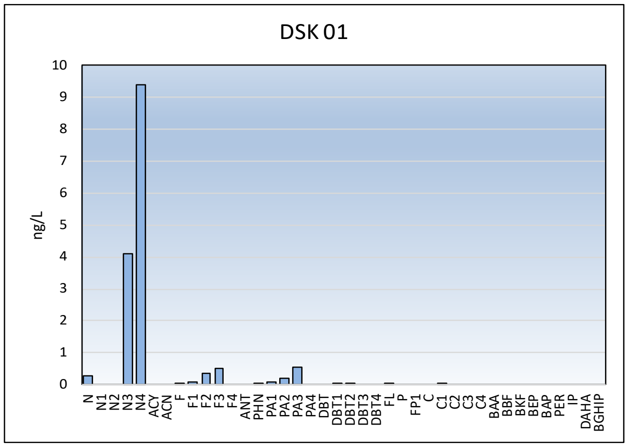
DSK 01
ng/L
10 9 8 7 6 5 4 3 2 1 0
N N1 N2 N3 N4 ACY ACN F F1 F2 F3 F4 ANT PHN PA1 PA2 PA3 PA4 DBT DBT1 DBT2 DBT3 DBT4 FL P FP1 C C1 C2 C3 C4 BAA BBF BKF BEP BAP PER IP DAHA BGHIP

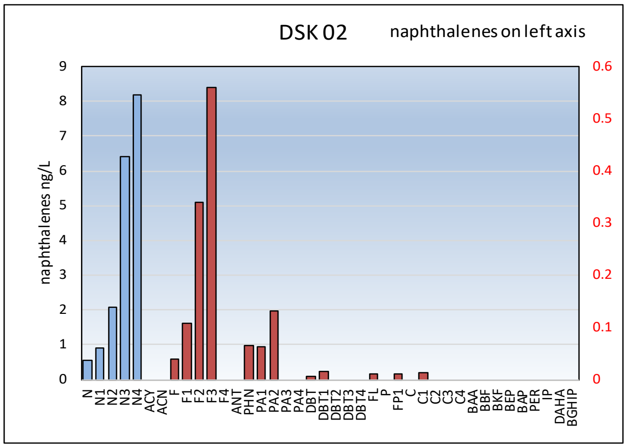
DSK 02
naphthalenes on left axis
naphthalenes ng/L
9 8 7 6 5 4 3 2 1 0
0.6 0.5 0.4 0.3 0.2 0.1 0
N N1 N2 N3 N4 ACY ACN F F1 F2 F3 F4 ANT PHN PA1 PA2 PA3 PA4 DBT DBT1 DBT2 DBT3 DBT4 FL P FP1 C C1 C2 C3 C4 BAA BBF BKF BEP BAP PER IP DAHA BGHIP

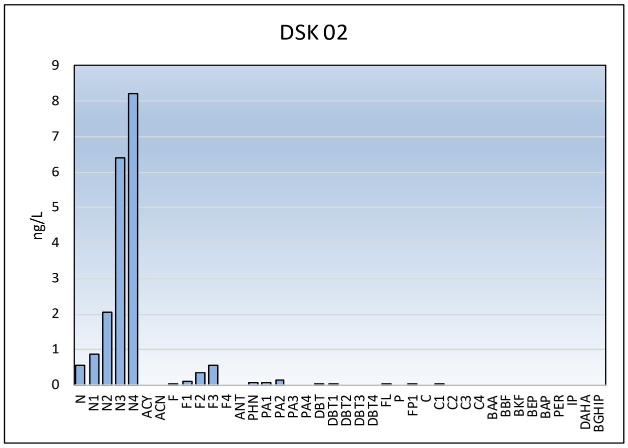
DSK 02
ng/L
9 8 7 6 5 4 3 2 1 0
N N1 N2 N3 N4 ACY ACN F F1 F2 F3 F4 ANT PHN PA1 PA2 PA3 PA4 DBT DBT1 DBT2 DBT3 DBT4 FL P FP1 C C1 C2 C3 C4 BAA BBF BKF BEP BAP PER IP DAHA BGHIP

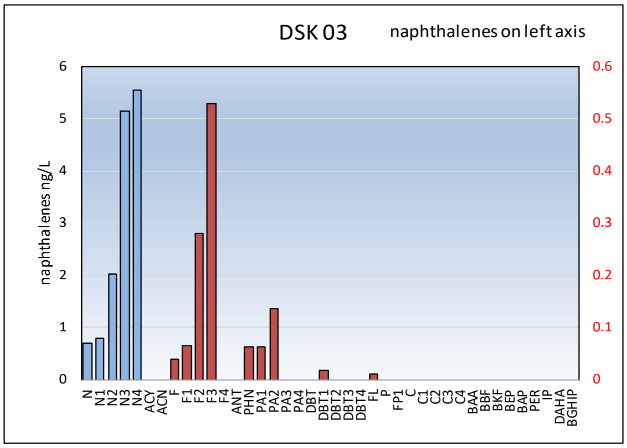
DSK 03
naphthalenes on left axis
naphthalenes ng/L
6 5 4 3 2 1 0
0.6 0.5 0.4 0.3 0.2 0.1 0
N N1 N2 N3 N4 ACY ACN F F1 F2 F3 F4 ANT PHN PA1 PA2 PA3 PA4 DBT DBT1 DBT2 DBT3 DBT4 FL P FP1 C C1 C2 C3 C4 BAA BBF BKF BEP BAP PER IP DAHA BGHIP

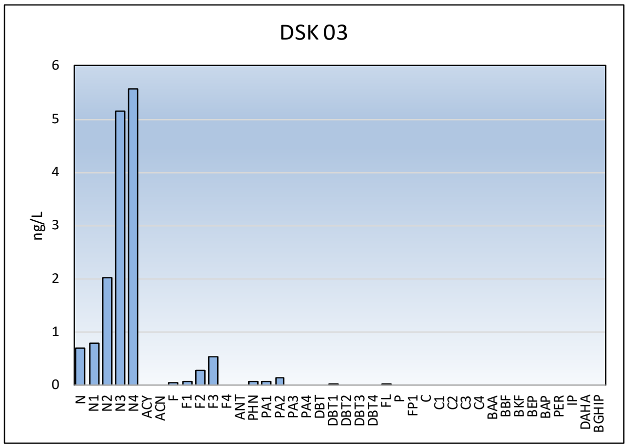
DSK 03
ng/L
6 5 4 3 2 1 0
N N1 N2 N3 N4 ACY ACN F F1 F2 F3 F4 ANT PHN PA1 PA2 PA3 PA4 DBT DBT1 DBT2 DBT3 DBT4 FL P FP1 C C1 C2 C3 C4 BAA BBF BKF BEP BAP PER IP DAHA BGHIP

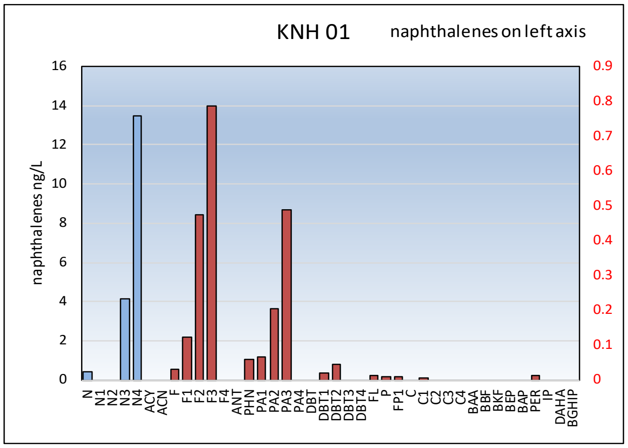
KNH 01
naphthalenes on left axis
naphthalenes ng/L
0 2 4 6 8 10 12 14 16
0 0.1 0.2 0.3 0.4 0.5 0.6 0.7 0.8 0.9
N N1 N2 N3 N4 ACY ACN F F1 F2 F3 F4 ANT PHN PA1 PA2 PA3 PA4 DBT DBT1 DBT2 DBT3 DBT4 FL P FP1 C C1 C2 C3 C4 BAA BBF BKF BEP BAP PER IP DAHA BGHIP

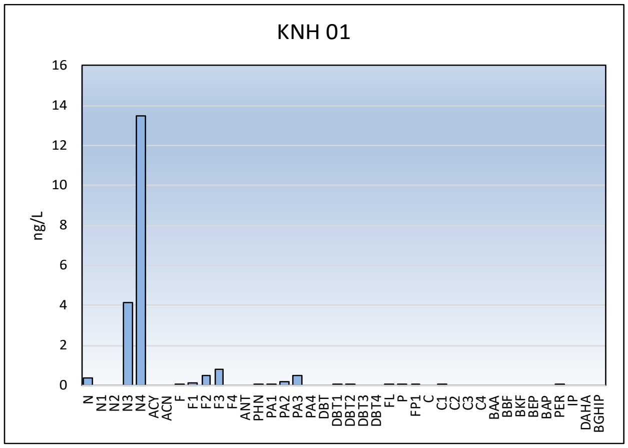
KNH 01
ng/L
0 2 4 6 8 10 12 14 16
N N1 N2 N3 N4 ACY ACN F F1 F2 F3 F4 ANT PHN PA1 PA2 PA3 PA4 DBT DBT1 DBT2 DBT3 DBT4 FL P FP1 C C1 C2 C3 C4 BAA BBF BKF BEP BAP PER IP DAHA BGHIP

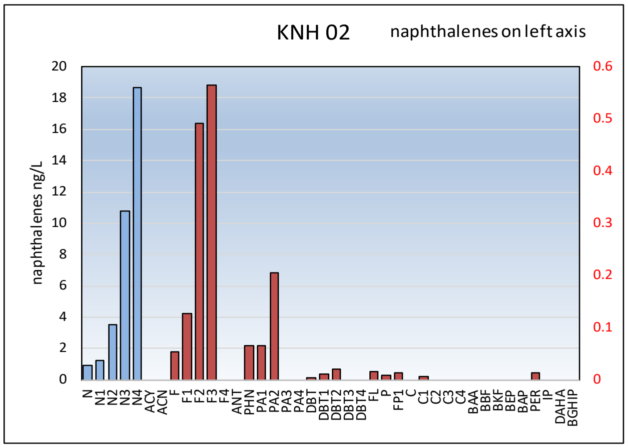
KNH 02
naphthalenes on left axis
naphthalenes ng/L
0 2 4 6 8 10 12 14 16 18 20
0 0.1 0.2 0.3 0.4 0.5 0.6
N N1 N2 N3 N4 ACY ACN F F1 F2 F3 F4 ANT PHN PA1 PA2 PA3 PA4 DBT DBT1 DBT2 DBT3 DBT4 FL P FP1 C C1 C2 C3 C4 BAA BBF BKF BEP BAP PER IP DAHA BGHIP

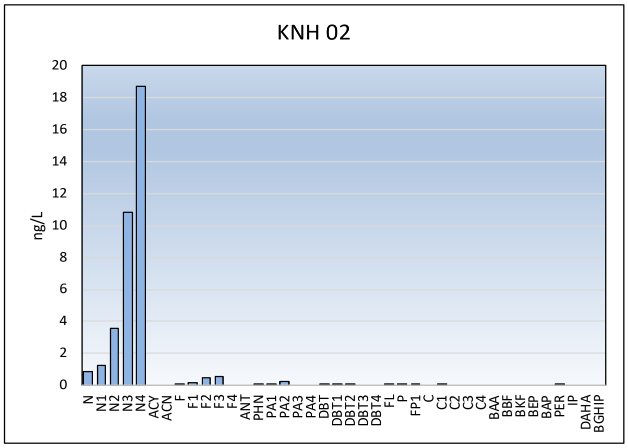
KNH 02
ng/L
0 2 4 6 8 10 12 14 16 18 20
N N1 N2 N3 N4 ACY ACN F F1 F2 F3 F4 ANT PHN PA1 PA2 PA3 PA4 DBT DBT1 DBT2 DBT3 DBT4 FL P FP1 C C1 C2 C3 C4 BAA BBF BKF BEP BAP PER IP DAHA BGHIP

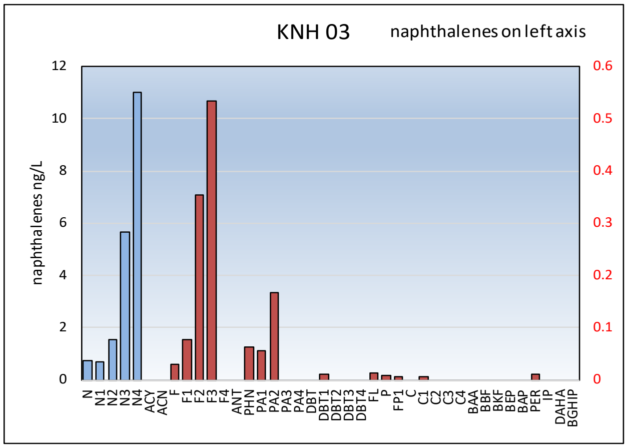
KNH 03
naphthalenes on left axis
naphthalenes ng/L
0 2 4 6 8 10 12
0 0.1 0.2 0.3 0.4 0.5 0.6
N N1 N2 N3 N4 ACY ACN F F1 F2 F3 F4 ANT PHN PA1 PA2 PA3 PA4 DBT DBT1 DBT2 DBT3 DBT4 FL P FP1 C C1 C2 C3 C4 BAA BBF BKF BEP BAP PER IP DAHA BGHIP

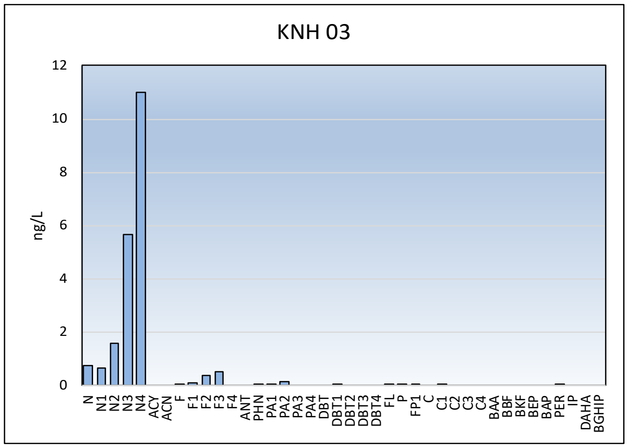
KNH 03
ng/L
0 2 4 6 8 10 12
N N1 N2 N3 N4 ACY ACN F F1 F2 F3 F4 ANT PHN PA1 PA2 PA3 PA4 DBT DBT1 DBT2 DBT3 DBT4 FL P FP1 C C1 C2 C3 C4 BAA BBF BKF BEP BAP PER IP DAHA BGHIP